COST Action CM1104

Reducible oxide chemistry, structure and functions

www.cost-redox.eu

4th and Final General Meeting

Universität Osnabrück

April 6th to 8th 2016

Local Organiser: Michael Reichling (Action Chair)

Meeting Program

Wednesday, April 6th 2016

10:00-12:30		**Registration**
12:30-13:30		**Lunch**
13:50-14:00		**Opening**

Session 1 Titania

14:00-14:20	X. Hu	Surface structures of ultrathin Ti_2O_3 films on Au(111)
14:20-14:40	A. Migani	Advanced modelling of electronic and optical properties of photocatalytic interfaces: water and alcohols on TiO_2(110)
14:40-15:00	R. Lazzari	Electron energy loss study of excess electrons in reducible TiO_2: dual behaviour or coexistence of trapped and free states? Bulk or surface defects?
15:00-15:20	F. Illas	Towards a first principles description of realistic models of TiO_2 nanoparticles
15:20-15:40	G. Thornton	Non-band-gap photoexcitation of hydroxylated TiO_2
15:40-16:20		**Coffee**

Session 2 Oxide films

16:20-16:40	J. I. Flege	Growth of (100) oriented ceria nanostructures on close packed transition metal surfaces
16:40-17:00	S. Surnev	WO_3 monolayer on Pd(100): an advanced model catalyst for reactivity studies
17:00-17:20	U. Diebold	Surface chemistry and homo-epitaxial growth of selected perovskite oxides
17:20-17:40	S. Shaikhutdinov	Metal supported ultrathin oxide films and SMSI effects
17:40-18:00	P. Luches	Modifications of structure and electronic properties in cerium oxide ultrathin epitaxial films on Pt(111) induced by thermal reduction
18:00-18:20	N. Nilius	Cuprous oxide films on Au(111): growth, surface termination and electronic properties
18:20-18:40	L. Deák	The impact of molybdenum oxides on the structure and reactivity of atomically thin Rh films and a comparison with the effect of titanium oxides
19:00-21:00		**Poster presentations**

Thursday, April 7th 2016

Session 3 Ceria and related structures

09:00-09:20	M. J. Wolf	Interaction of oxygen and water molecules with fluorine impurities at CeO_2(111)
09:20-09:40	M. V. Ganduglia-Pirovano	How unique is VO_x/ceria for enhanced oxidation Activity: The examples of MnO_x-ceria, CrO_x-ceria and Mg-doped VO_x-ceria
09:40-10:00	A. Bonivardi	Cerium-niobium mixed oxides for the water gas shift reaction
10:00-10:20	P. Broqvist	SCC-DFTB calcs. of complex metal-oxides: ZnO and CeO_2
10:20-10:40	K. Neyman	Modelling of ceria-based nanostructures inspired by CM1104
10:40-11:20		**Coffee**

Session 4 Atom/molecule-surface interaction

11:20-11:40	J. Paier	Methanol adsorption on monocrystalline ceria surfaces
11:40-12:00	R. Pérez	Gold adsorption and diffusion on reduced CeO_2(111)
12:00-12:20	H. Aleksandrov	Simulations of IR vibrational frequencies of CO adsorbed on ceria platinum species: a DFT study
12:20-12:40	J. Lauritsen	Water dissociation and H diffusion is water-assisted on CoO_x/Au(111)
12:40-13:00	G. Rupprechter	Model catalysts for reforming reactions: water interaction with ultrathin films of zirconium oxide
13:00-14:00		**Lunch**

Session 5 Hafnia and perovskites

14:00-14:20	A. Stesmans	Paramagnetic oxide traps in Sc_2O_3-passivated (100)Ge/HfO_2 stacks
14:20-14:40	V. Afanas'ev	Annealing-induced electron traps in atomic-layer deposited HfO_2 layers
14:40-15:00	A. Shluger	Intrinsic electron and hole trapping in amorphous hafnia
15:00-15:20	E. Kotomin	Ab initio calculations of neutral and charged oxygen vacancies in $BaZrO_3$ perovskite crystals
15:20-16:00		**Coffee**

Session 6 Fundamental aspects and Photocatalysis

16:00-16:20	Y. Mastrikov	Water interaction with perfect and F-doped Co_3O_4(100)
16:20-16:40	C. Noguera	Structural transitions induced by polarity in ultra-thin films and nanoribbons
16:40-17:00	A. Braun	Chemistry and dynamics of the proton phonon coupling in proton conducting ceramic electrolytes
17:00-17:20	O. Diwald	Annealing induced oxygen vacancy formation in nanoparticle systems of reducible metal oxides
17:20-17:40	H. Grönbeck	Importance of attractive pair interactions in reactions on metal oxide surfaces
17:40-18:00	J. Conesa	The Fe:NiOOH Co-catalyst for O_2 generation: el. structure and band offset with the $BiVO_4$ vis. light active photocatalyst

18:30-19:00 **Management Committee Meeting** (MC members only)

20:00 **Conference dinner** (advance registration is required)

Friday, April 8th

Session 7 Dopants and defects

09:00-09:20	J. Gryboś	Morphology, surface structure relaxation and defects of ZrO_2 nanocrystals explored by DFT modelling and HR TEM
09:20-09:40	H. Jónsson	Self-interaction corrected density functional calculations of localized electron hole formed by Li dopant in MgO
09:40-10:00	E. Giamello	Is nitrogen doping of tin oxide a way to create a p-type semicond. oxide? A multi-technique investigation of N-SnO_2

Session 8 Catalysis

10:00-10:20	C. Rameshan	Methane dry reforming studied on inv. Pt/ZrO_2 model catalyst

10:20-11:00 **Coffee**

11:00-11:20	Y. Lykhach	Metal-oxide interactions in Pt/CeO_2 catalysts
11:20-11:40	M. Calatayud	Promoting catalytic activity by doping: a theoretical approach to ceria-gallia mixed materials
11:40-12:00	G. Vayssilov	Identification of intermediates for NO conversion on ceria
12:00-12:20	J. Carey	H_2S decomposition on bare and doped (0001) surface of Cr_2O_3: Doping changes the thermodynamic selectivity towards H_2O formation
12:20-12:40	A. Martínez-Arias	XPS characterization of active interfacial copper in ceria-supported copper catalysts for pref. oxidation of CO

12:40-12:50 **Closure**

13:00 **Lunch**

Oral presentation abstracts

Surface Structures of Ultrathin Ti_2O_3 Films on Au(111)

Xiao Hu[1], Chen Wu[1, 2], Lewys Jones[1], Jacek Goniakowski[3, 4], Claudine Noguera[3, 4] and Martin R. Castell[1]

[1] *Department of Materials, University of Oxford, Parks Road, Oxford, OX1 3PH, UK*
[2] *School of Materials Science and Engineering, Zhejiang University, Hangzhou 310027, China*
[3] *CNRS, Institut des Nanosciences de Paris, UMR 7588, 4 place Jussieu, 75005 Paris, France*
[4] *UPMC Univ Paris 06, INSP, UMR 7588, 4 place Jussieu, 75252 Paris CEDEX, France*

email: xiao.hu@materials.ox.ac.uk

Titanium oxides are materials used in photocatalysis [1] and gas sensing [2]. Most of the studies are based on the two common TiO_2 polymorphous – rutile and anatase. However, new titanium oxide structures can be created in ultrathin film forms that are very different from the bulk crystal terminations. There is increasing interest in this field because these novel structures may be associated with enhanced properties.

We have carried out growth of TiO_x ultrathin films on (22 × √3)-reconstructed Au(111) substrates through Ti deposition and post-deposition oxidation and annealing. In the growth of the thin films three different structures were observed: a (2 × 2)-reconstructed Ti_2O_3 structure resembling a honeycomb pattern, a TiO pinwheel shape and triangular shaped TiO_x islands [3,4]. The (2 x 2) honeycomb structure has two crystallographically unique domain boundaries (DBs) along the <1-10> directions, and also two unique DBs along the <11-2> directions. Along the <11-2> directions the preferred boundary structure is to have alternating rings of 4 and 8 Ti atoms. Along the <1-10> directions there are two commonly observed DBs with either double 5-fold and single 8-fold rings or with alternating 5-fold and 7-fold rings. Scanning tunnelling microscopy (STM) images of these three DBs are shown in figure 1. Density functional theory (DFT) calculations were used to model the DB structures and to calculate their formation energies. Two DBs that are crystallographically unique, but are not observed by STM over long repeat periods, were also modelled.

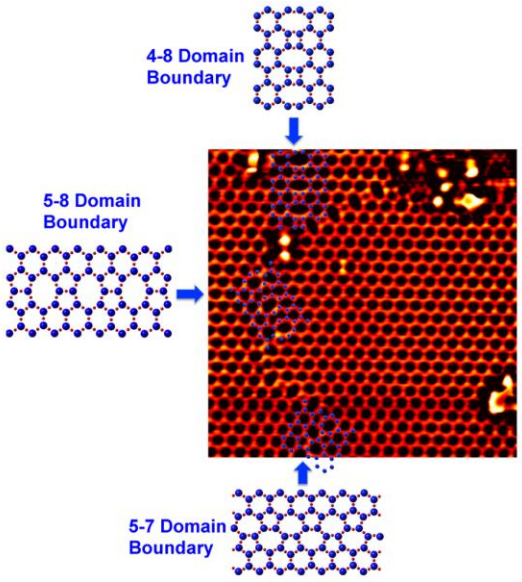

Figure 1: STM image of Ti_2O_3 honeycomb thin films with 4-8, 5-8 & 5-7 DBs (image size: 14 × 14 nm^2, V_s = 0.9 V, I_t = 0.22 nA). Ti atoms are draw as big blue balls; O atoms are small red balls.

References:

[1] J. Chen, F. Qiu, W. Xu, S. Cao and H. Zhu, Appl. Catal. A-Gen. **495**, 131 (2015).
[2] J. Bai and B. Zhou, Chem. Rev. **114**, 10131 (2014).
[3] C. Wu, M. S. J. Marshall and M. R. Castell, J. Phys. Chem. C **115**, 8643 (2011).
[4] D. Ragazzon, A. Schaefer, M. H. Farstad, L. E. Walle, P. Palmgren, A. Borg, P. Uvdal and A. Sandell, Surf. Sci. **617**, 211 (2013).

Advanced Modelling of Electronic and Optical Properties of Photocatalytic Interfaces: Water and Alcohols on TiO_2(110).

Annapaola Migani[1]
[1]Catalan Institute of Nanoscience and Nanotechnology (ICN2), CSIC and The Barcelona Institute of Science and Technology, Campus UAB, Bellaterra, E-08193 Barcelona, Spain
annapaola.migani@icn2.cat

Heterogeneous photocatalysis is a very important area of research because of its potential for applications in energy and environmental technologies. CH_3OH and H_2O on single-crystal rutile TiO_2(110) interfaces represent model systems for ultra-high vacuum (UHV) surface science studies aimed at revealing the basic principle of heterogeneous photocatalysis [1]. Despite this dedicated experimental work there are many obscure parts in our atomistic understanding of the mechanism of photocatalytic processes. This requires an accurate description of both the electronic structure of the CH_3OH and H_2O on TiO_2(110) interfaces in the ground-state prior to light irradiation, optical absorption spectra and excitons' energy and spatial distribution across the entire photochemical coordinate. Here, I show that such an accurate description can be accomplished by means of state-of-the-art computational approaches such as many–body quasiparticle *GW* (specifically G_0W_0) and the Bethe-Salpeter equation (BSE) based on density functional theory (DFT) calculations employing PBE or HSE06 exchange and correlation functionals in a periodic framework. In particular I will show that G_0W_0 calculations successfully reproduce the interfacial level alignment of occupied molecular and Ti 3d levels obtained from ultraviolet photoemission spectroscopy (UPS) [2]. Given this accuracy, they serve to verify the adsorption structure of the molecular overlayer assigned experimentally or can be used to make new assignments. Finally, I will focus on the mechanism of light-induced dissociation of CH_3OH and H_2O on TiO_2(110) and in particular I will discuss the charge separation of hole and electron carriers that constitute excitons with singlet and triplet spin multiplicity, obtained from HSE06 BSE and DFT calculations for these dissociation processes [3]. These calculations contribute to improve our understanding of the photocatalysis model, by identifying the moment at which the charge carriers's separation takes place, and show that it does not occur before migration of the charge carriers to the surface prior to the photocatalytic process, but during its course.

[1] Friend, C.M. Perspectives on Heterogeneous Photochemistry. Chemical record (New York, N.Y.) 2014.
[2] A. Migani et al., J. Chem. Theory Comput. **11**, 239 (2015).
[3] A. Migani et al., in preparation.

Electron energy loss study of excess electrons in reducible TiO_2: dual behaviour or coexistence of trapped and free states? Bulk or surface defects?

Jinfeng Li, Jacques Jupille and **Rémi Lazzari**
Sorbonne Université, UPMC/CNRS, Institut des NanoSciences de Paris, 4 Place Jussieu 75005 Paris, France
e-mail: lazzari@insp.jussieu.fr

Stoichiometry defects play a tremendous role in the surface chemistry of titanium oxide [1,2]. Reduced rutile is indubitably a n-type semiconductor in terms of electrical transport but electron-based spectroscopies and scanning tunnelling microscopy show the existence of a defect-related gap state lying 0.8-1eV below the Fermi level [1,2]. Its nature *i.e.* surface oxygen vacancies [2,3] versus sub-surface interstitial titaniums [4] is still highly debated in the literature as well the actual (de)localisation of the associated excess electrons [4,5,6].
In our work, electron energy loss spectroscopy in low and high resolution modes was used to probe band gap state and phonon excitations in TiO_2(110) as a function of oxygen exposure at 100 and 300K. By comparing surfaces, from reduced to fully oxidized obtained by various means including electron bombardment, and by using EELS depth sensitivity in out-of-specular detection, a contribution from sub-surface defects is clearly evidenced. A method to prepare defect-free surfaces (as observed by EELS) is even proposed. Using dielectric modelling of spectra including phonons, carriers, gap state and interband transitions and multiple excitations, it was shown that "free-like" carriers characterized by their plasmon excitation coexists with band gap states. While the latter give rise to an obvious peak in the band gap, the former induce a temperature dependent broadening of the quasi-elastic peak and a sizeable screening and upward frequency shift of phonons compared to stoichiometric samples. Through data fitting, both surface and bulk carrier densities and dampings could be quantified as well their profile. A very different dynamics of the healing of the associated signals upon O_2 exposure was also observed. The implication of such findings in terms polaronic nature of excess electron will be discussed.

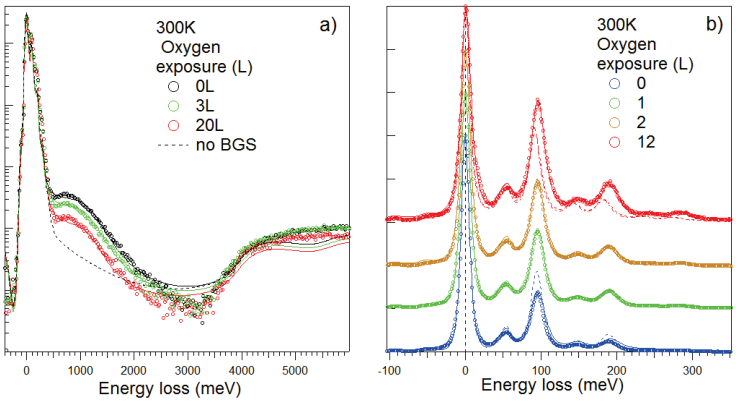

Figure 1: Evolution upon oxygen exposure of a) EELS b) HREELS spectra of reduced TiO_2(110). Data (circle) have been fitted (full lines) within dielectric theory including plasmon excitations. Simulation without free-like carriers and band-gap state appear as dotted lines.

[1] U. Diebold, Surf. Sci. Rep. 48 (2003) 43; C. Pang *et al.*, Chem. Rev. 113 (2013) 3887
[2] C. Yim *et al.*, Phys. Rev. Lett. 104 (2010) 036806
[3] P. Kruger *et al.*, Phys. Rev. Lett 100 (2008) 055501
[4] S Wendt *et al.*, Science 320 (2008) 1755
[5] M. Setvin *et al.*, Phys. Rev. Lett. 113 (2014) 086402
[6] A. Janotti *et al.*, Phys. Stat. Solidi RRL 7 (2013) 199

Towards a first principles description of realistic models of TiO_2 nanoparticles

Oriol Lamiel-García,[1] Kyoung Chul Ko,[2] Stefan T. Bromley,[3] Jin Yong Lee,[2] Francesc Illas[1]

1) *Departament de Química Física & Institut de Química Teòrica i Computacional (IQTCUB), Universitat de Barcelona, c/ Martí i Franquès 1,08028 Barcelona, Spain*

2) *Department of Chemistry, Sungkyunkwan University, Suwon 440-746, Korea*

3) *Institució Catalana de Recerca i Estudis Avançats (ICREA), 08010 Barcelona, Spain*

Under UV irradiation, titanium dioxide (TiO_2) anatase-like nanoparticles decompose water into hydrogen and oxygen. This photocatalytic reaction is of huge technological relevance since it provides a simple, clean and almost endless fuel. The problem is, however, that only a fraction of sunlight arrives to the Earth surface in the form of UV radiation, this precludes the direct use of this material and claims for suitable modifications in the resulting electronic structure so that the same chemical reaction could be triggered by sunlight in the visible range. To this end it is necessary to understand the properties of this material and, hence, be able to produce suitable modifications. Most of the effort has been focused on the electronic structure of bulk TiO_2 anatase and derived materials or on extended surfaces. In the present work we go one step further by considering more realistic models. To this end, the atomic and electronic structure of $(TiO_2)_n$ nanoparticles of increasing size (n= 10, 84, 165, 286, 455) reaching up tp 4-6 nm have been obtained by means of density functional theory within the PBE exchange-correlations functional and the electronic structure refined by the PBE0 functional. Results provide useful information about the convergence of properties towards bulk and of the dependence of electronic structure with particle size thus opening the way study for the study of chemically modified nanoparticles with possible photocatalytic activity towards water splitting in the visible.

Non-Band-gap Photoexcitation of Hydroxylated TiO_2

Y. Zhang, D.T. Payne, C.L. Pang, H.H. Fielding, G. Thornton

London Centre for Nanotechnology, University College London,
20 Gordon Street, London WC1H 0AJ, UK
(Corresponding author: G. Thornton, e-mail g.thornton@ucl.ac.uk)

This TiO_2 is a prototypical light-harvesting semiconductor showing promising potential in the application of photocatalysis. Nevertheless, it has proven difficult to establish the detailed processes involved in photocatalysis, partly because the excited states involved are difficult to study. Here, we present evidence for the existence of hydroxyl-induced states in the conduction band region that may also play a role in photocatalysis. In the two-photon photoemission (2PPE) experiment on rutile TiO_2(110), an electron in the well-known defect states about 0.8 eV below E_F is excited into an intermediate state by absorbing a photon, from which it is further excited above the vacuum level by a second photon. By varying the photon energy from about 3 to 4 eV, we observe a pronounced resonant enhancement of the 2PPE intensity when the photon energy is about 3.5 eV as shown in the Figure (a). It indicates an intermediate state at about 2.7 eV above E_F marked by the green peak in the Figures. Further investigations show that this state is induced by the hydroxyls on the TiO_2 surface with a lifetime shorter than 15 fs. The intensity of the resonance can be greatly enhanced by the adsorption of molecular water at 100 K. The energy of the hydroxyl-induced state is found to be 2 eV lower and less-influenced by the water adsorption than that expected for a hydroxylated TiO_2(110) surface.

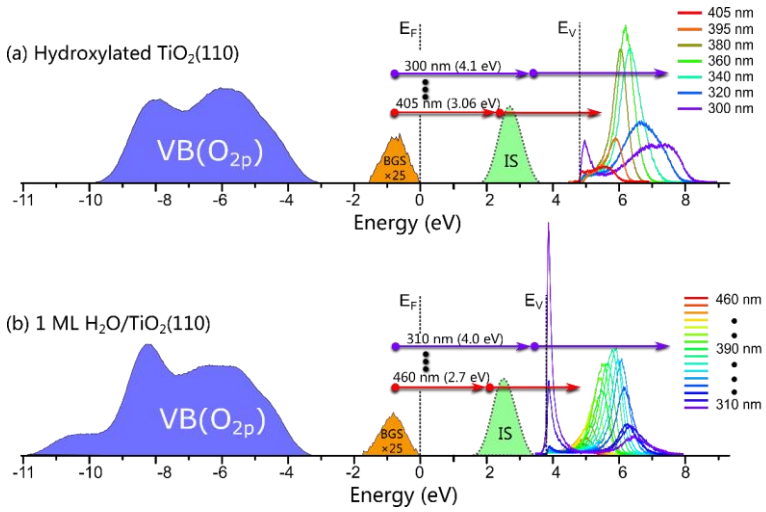

Figure 1. Schematic of 2PPE transitions.

1. Y. Zhang, D.T. Payne, C.L. Pang, H.H. Fielding, G. Thornton, J. Phys. Chem. Lett. 6 (2015) 3391-3395.

Growth of (100) oriented ceria nanostructures on close-packed transition metal surfaces

Jan Ingo Flege, Jan Höcker, Tomáš Duchoň[1], Kateřina Veltruská[1], Vladimír Matolín[1], S. Gangopadhyay[2], Jerzy T. Sadowski[3], Sanjaya D. Senanayake[4], and Jens Falta

Institute of Solid State Physics, University of Bremen, Bremen, Germany
[1]Charles University in Prague, Faculty of Mathematics and Physics, Prague, Czech Republic
[2]Department of Physics, BITS Pilani, Pilani, Rajasthan, India
[3]Center for Functional Nanomaterials, Brookhaven National Laboratory, Upton, United States
[4]Chemistry Department, Brookhaven National Laboratory, Upton, United States
flege@ifp.uni-bremen.de

The epitaxial growth of cerium oxide on transition metal surfaces has become a very popular approach to create model catalyst architectures as, e.g., nanoparticles or ultrathin films for the investigation of its peculiar chemical properties. Typically, the emerging ceria adopts the (111) surface orientation, which is usually considered most stable from a thermodynamical point of view. Intriguingly, also more open surface orientations are found in the case of, e.g., cuboidal nanoparticles, which may exclusively be terminated by (100) surfaces. Furthermore, these surfaces have been shown to exhibit very different chemical behavior from the more prominent (111) orientation [1]. However, for a selective study of the individual catalytic properties of the different ceria surfaces employing the powerful tools of surface science their controlled preparation under near-ultrahigh-vacuum conditions is highly desirable.

Here, a novel and simple method is presented for the preparation of a well-defined $CeO_2(100)$ model system on Cu(111) based on the adjustment of the Ce/O ratio during growth[2]. The method yields micrometer-sized, several nanometers high, single-phase $CeO_2(100)$ islands with controllable size and surface termination that can be benchmarked against the known (111) nanostructured islands on Cu(111). Furthermore, we demonstrate the ability to adjust the Ce to O stoichiometry from $CeO_2(100)$ (100% Ce^{4+}) to c-$Ce_2O_3(100)$ (100% Ce^{3+}), which can be readily recognized by characteristic surface reconstructions observed by low-energy electron diffraction. The discovery of the highly stable $CeO_x(100)$ phase on a hexagonally close packed metal surface represents an unexpected growth mechanism of ceria on Cu(111), which will be contrasted with the formation of ceria(100) nanoparticles on Ru(0001) upon thermal annealing [3] or epitaxial growth at temperatures above 1100 K [4].

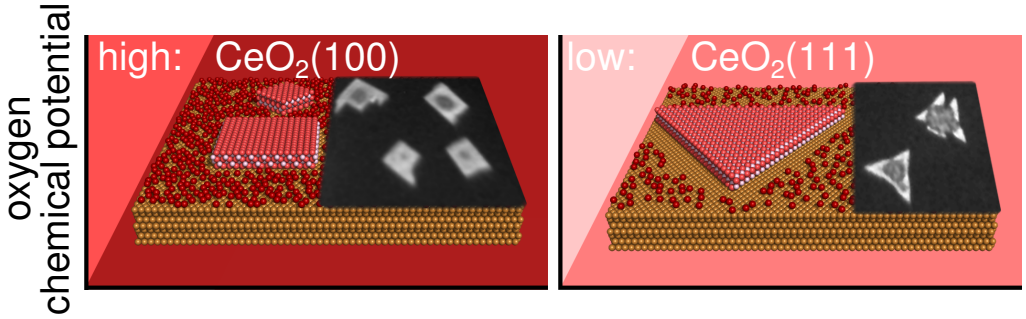

[1] G. Vilé et al., Angew. Chem. Int. Ed. **53**, 1 (2014).
[2] J. Höcker et al., J. Phys. Chem. C, *in press*. DOI: 10.1021/acs.jpcc.5b11066.
[3] Y. Pan et al., Adv. Mater. Interfaces **1**, 1400404 (2014).
[4] J. I. Flege et al., *submitted*.

WO_3 Monolayer on Pd(100): An Advanced Model Catalyst for Reactivity Studies

N. Doudin, M. Blatnik, D. Kuhness, F.P. Netzer, and S. Surnev

Surface and Interface Physics, Institute of Physics, Karl-Franzens University Graz
A-8010 Graz, Austria

Tungsten oxide (WO_3) is a key material in several applications including smart windows technology, photo-electrochemical water splitting, gas sensors and heterogeneous catalysis. In particular, tungsten oxides are important acid-base and redox catalysts, and they show excellent activity for many catalytic reactions, such as alcohol dehydrogenation, alkane hydrogenation and metathesis [1]. WO_3 has been produced in single crystal form or as supported thin films with the bulk crystal structure. The latter is strongly temperature dependent, displaying a series of polymorphs, based on an idealized cubic ReO_3 corner–sharing WO_6 octahedral framework. Recently, the formation of an ordered two-dimensional (2D) tungsten oxide layer on Pt(111) has been reported, where however W atoms show a mixture of 5+ and 6+ oxidation states [2]. In principle, 2D oxide films may be regarded as so-called "oxide monolayer catalysts", since they may exhibit higher catalytic activities for selective oxidation reactions than their bulk counterparts [3].

Here we report on the preparation of a well-ordered 2D WO_3 layer on a Pd(100) surface and the characterization of its geometric, electronic and vibrational structure by a combination of STM, LEED, XPS and HREELS. The WO_3 monolayer wets completely the Pd(100) surface (Fig. 1a) and features a surface network consisting of small (~ 4 nm) square-shaped domains, separated by narrow (~ 0.5 nm) trenches. The latter are identified as anti-phase domain boundaries, as evidenced by atomically-resolved STM images (see inset of Fig. 1a) and the characteristic spot splitting around the (±1/2, ±1/2) LEED positions (Fig. 1b). The STM image shows that each domain exhibits a square surface structure with a lattice constant of 0.39 nm, which corresponds to a c(2x2) superstructure. Another important feature is the presence of few dark depressions inside the domains, which we attribute to missing terminal O atoms (see model in Fig. 1d), in corroboration with HREELS results and high-resolution W 4f core-level spectra (Fig. 1c). The latter consist of three $4f_{7/2}$ - $4f_{5/2}$ doublet components, due to W atoms at different surface locations: within the defect-free areas (major component at 34.4 eV), with missing terminal oxygens (minor component at 33.3 eV), and at the domain boundaries (35.2 eV). The proposed structure model of the WO_3 monolayer is shown in Fig. 1d and consists of a layer of O atoms adsorbed in fourfold hollow Pd positions, followed by a c(2x2) layer of W atoms, which are connected at the top to terminal O atoms via strong W=O bonds, as suggested by our HREELS results. It can be viewed in a way as a 2D analogue of a cubic WO_3(001) crystal, featuring a similar lattice constant (0.39 nm vs. 0.38 nm) and polyhedral linkage, but with a modified W-O coordination sphere due to the contact with the Pd(100) surface. We consider this 2D WO_3 layer on Pd(100) as a well-defined monolayer model catalyst, which can be potentially suitable for reactivity studies.

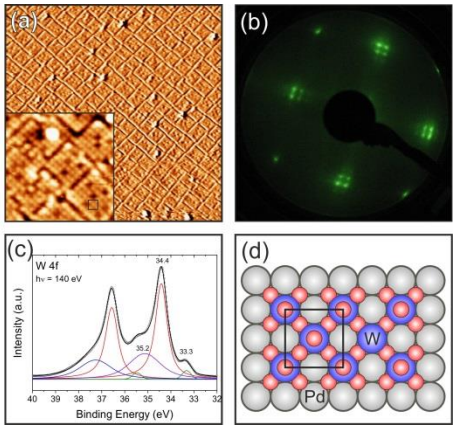

Fig. 1: (a) STM image (65nm x 65nm) of the WO_3 monolayer on Pd(100). The inset displays a high-resolution STM image (8.5nm x 8.5nm) of the 2D WO_3 phase (the c(2x2) unit cell is indicated); (b) LEED pattern, showing the spot splitting due to anti-phase domain boundaries; (c) High-resolution W 4f spectrum of the WO_3 monolayer, decomposed into three different components, as discussed in the text; (d) Proposed structure model of the 2D WO_3 layer on Pd(100), the c(2x2) unit cell is indicated (Pd: gray; W: blue; O: red).

[1] D. Gazzoli et al, J. Phys. Chem. B 101 (1997) 11129
[2] Z. Li, et al, J. Phys. Chem. C 115 (2011) 5773
[3] G. Deo, et al, Crit. Rev. Surf. Chem. 4 (1994) 141

This work has been supported by the FWF Project P26633-N20 and by the EU COST Action CM1104.

Surface Chemistry and Homo-epitaxial Growth of Selected Perovskite Oxides

Ulrike Diebold, Michele Riva, Stefan Gerhold, Daniel Halwidl, and Michael Schmid
[1]Institute of Applied Physics, TU Wien, Vienna, Austria
diebold@iap.tuwien.ac.at

Ternary oxides with the perovskite structure exhibit an intriguingly rich variety in their physical and chemical properties. The surfaces of these promising materials are equally complex and generally poorly understood. Here we report an overview of surface studies of two perovskite oxides, the prototypical $SrTiO_3$ in (110) orientation and Sr_3RuO_7, the n=2 member of the Ruddlesden-Popper series.
The surface of the layered compound, Sr_3RuO_7, is structurally quite simple: cleaving in UHV yields a SrO-terminated layer, which is essentially defect-free, except for impurities in the bulk material [1]. The surface is very reactive towards components of the residual gas, however. CO, CO_2, and H_2O adsorb readily and form adsorption complexes [2, 3]. $SrTiO_3$(110) is polar and exhibits a series of reconstructions that can be controlled by adjusting the chemical potential of its constituents, i.e. by evaporating appropriate amounts of Sr and Ti and annealing in O_2. The (nx1) reconstructions consist of a monolayer of titania with tetrathedrally-coordinated Ti atoms that are arranged in corner-sharing rings [4]. When the Ti chemical potential is increased, the surface switches over to a (2xm) symmetry with a titania layer that is composed of Ti in octahedral coordination. These stoichiometry-dependent, facile structural changes have a profound effect on surface reactivity, and on the homoepitaxial growth of $SrTiO_3$ during pulsed laser deposition [5].

[1] B. Stöger, et al, Phys. Rev. B 90 (2014) 165438.
[2] B. Stöger, et al., Phys Rev Lett 113 (2014) 116101
[3] D. Halwidl et al. Nature Mater. (2015) doi:10.1038/nmat4512
[4] Z. Wang et al., Phys. Rev. Lett. Phys Rev Lett 111 (2013) 056101.
[5] S. Gerhold et al., submitted

Metal Supported Ultrathin Oxide Films and SMSI Effects

Shamil Shaikhutdinov
Department of Chemical Physics, Fritz Haber Institute, Faradayweg 4-6, 14195 Berlin
shaikhutdinov@fhi-berlin.mpg.de

Thin oxide films grown on metal single-crystal substrates have been successfully used as suitable oxide supports for modeling highly dispersed metal catalysts at the atomic scale. Recent studies from different groups worldwide showed that ultrathin transition metal oxide (TMO) films themselves may exhibit interesting properties, which are not observed on thick films or bulky counterparts.

In this talk, we will address some general aspects and trends observed in our laboratories with respect to reactivity of ultrathin TMO films in oxidation reactions, primarily in CO oxidation. [1-5] In particular, support effects and film thickness effects will be discussed. Where appropriate, the experimental results will be corroborated by theoretical calculations performed within this Action.

We believe that structure and reactivity of ultrathin films may have strong link to the so called Strong Metal/Support Interaction effects in catalysis, which often manifest itself by encapsulation of metal nanoparticles by oxide overlayer of the TMO support. Few examples will be discussed to demonstrate that such encapsulation may, indeed, have promotional effects on reactivity, in full agreement with studies performed on extended two-dimensional films.

[1] Q. Pan et al. ChemCatChem **7**, 2620 (2015)
[2] K. Zhang et al. ChemCatChem **7**, 3725 (2015)
[3] M. Willinger et al., Angew. Chem. Intern. Ed. **53**, 5998 (2014)
[4] Q. Pan et al. Catal. Lett. **144**, 648 (2014)
[5] Y. Martynova et al., ChemCatChem **5**, 2162 (2013)

Modifications of structure and electronic properties in cerium oxide ultrathin epitaxial films on Pt(111) induced by thermal reduction

G. Gasperi[1,2], L. Amidani[3], F. Benedetti[1,2], J. S. Pelli Cresi,[1,2], F. Boscherini[4], P. Glatzel[3], S. Valeri[1,2], **P. Luches[1]**

[1]Istituto Nanoscienze, Consiglio Nazionale delle Ricerche, Modena, Italy
[2]Dipartimento di Scienze Fisiche Matematiche e Informatiche, Università degli Studi di Modena e Reggio Emilia, Modena, Italy
[3] ESRF, F-38043 Grenoble, France
[4] Dipartimento di Fisica e Astronomia, Università di Bologna, Bologna, Italy

e-mail: paola.luches@unimore.it

In order to improve the understanding of reducibility in oxides, it is very important to describe the modifications of the atomic scale structure and of the electronic configuration of the material when oxygen vacancies are formed.
The results of our studies, performed by X-ray absorption based techniques, elucidate the evolution of the structure and of the electronic properties of cerium oxide epitaxial films during reduction and re-oxidation induced by thermal cycles in vacuum and oxygen atmosphere, respectively. In particular, the modifications of the electronic structure are followed by high-resolution fluorescence detected X-ray absorption near edge spectroscopy (HERFD-XANES) and resonant inelastic x-ray scattering (RIXS) at the Ce L_3-edge, while the structural evolution is investigated by extended x-ray absorption fine structure (EXAFS) measurements at the same Ce absorption edge.
The measurements were performed at ID26 and BM08 beamlines of the ESRF on well controlled cerium oxide films of different thickness grown on Pt(111) by reactive molecular beam epitaxy.
The results demonstrate a higher extent of reduction in films of subnanometric thickness compared to thicker films, possibly due to the influence of the platinum substrate on the surface oxygen vacancy formation energy. The analysis of HERDF-XANES and RIXS data shows that, in general, the electronic structure of the 4f levels and 5d bands of the Ce^{3+} sites formed at the early stages of reduction is comparable with the one of Ce^{3+} sites in highly reduced samples. However, at low thickness and at a specific degree of reduction a phase with a different electronic structure was identified. After full reduction the Ce-O distance in ultrathin films, measured by EXAFS, is compressed by 2-3%, suggesting the possible formation of an A-type Ce_2O_3 phase.

CUPROUS OXIDE FILMS ON AU(111): GROWTH, SURFACE TERMINATION AND ELECTRONIC PROPERTIES

Hanna Fedderwitz,[1] Boris Gross,[1] Niklas Nilius,[1] Claudine Noguera,[2] Jacek Goniakowski[2]

[1] Carl von Ossietzky Universität, Institut für Physik, 26111 Oldenburg, Germany
[2] CNRS-Sorbonne, UPMC Univ. Paris 06, UMR 7588, INSP, F-75005 Paris, France

A band gap that perfectly overlaps with the solar spectrum and an intrinsically p-type conductance behavior renders cuprous oxide (Cu_2O) a fascinating material for photocatalytic and photovoltaic applications. In order to explore its structural, electronic and optical properties, we have prepared thin-film model systems by vapor-depositing Cu onto an Au(111) surface at different oxygen pressures and temperatures [1]. Whereas CuO-like films are formed at high-pressure conditions ($p_{O2} > 10^0$ mbar), Cu_2O layers with good structural quality are grown at ~10^{-5} mbar. LEED and STM measurements performed on the Cu_2O films reveal a (111)-type surface, exposing a hexagonal lattice with 6Å periodicity. Detailed insight into the film structure comes from DFT HSE calculations that find the stoichiometric Cu_2O termination to be thermodynamically preferred at the experimental conditions [2]. The observed STM contrast is assigned to the low-coordinated Cu atoms that also induce an unoccupied gap state with strong Cu 5s character. This surface state is indeed found with STM conductance spectroscopy at 0.9 eV above E_{Fermi}, confirming the proposed structure model. On this basis, also point and line defects in the Cu_2O surface and their role in strain compensation are discussed.

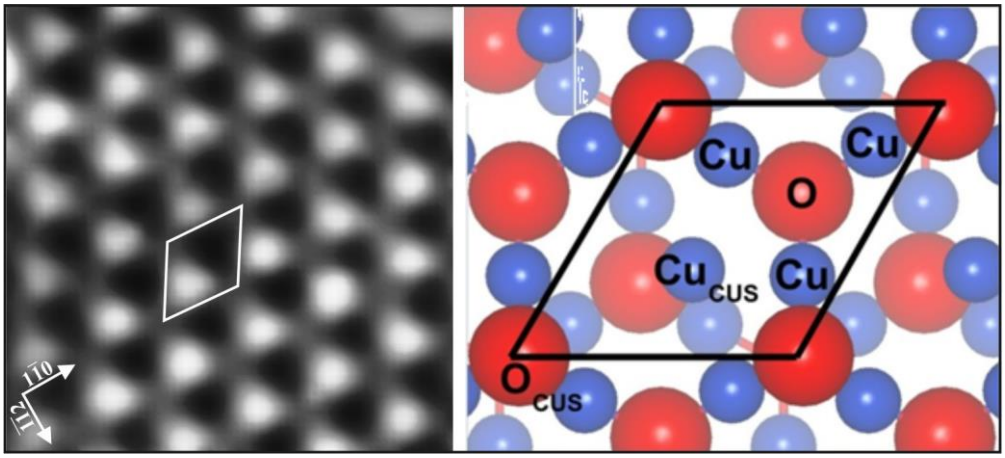

Figure: STM topographic image (3.3 × 3.3 nm^2) and corresponding structure model of $Cu_2O(111)$.

[1] H. Sträter, H. Fedderwitz, B. Gross, N. Nilius, *J. Phys. Chem. C 119 (2015)* 5975–5981
[2] N. Nilius, H. Fedderwitz, B. Groß, J. Goniakowski, C. Noguera, *PCCP 18 (2016)* 6729-6733

The impact of molybdenum oxides on the structure and reactivity of atomically thin Rh films and a comparison with the effect of titanium oxides

L. Deák[1], I. Szenti[2], R. Gubó[2], L. Óvári[1], A. Berkó[1] and Z. Kónya[1,2]
[1] MTA-SZTE, Reaction Kinetics and Surface Chemistry Research Group, H-6720 Szeged
[2] University of Szeged, Department of Applied and Enviromental Chemistry, Hungary
sir@chem.u-szeged.hu

A considerable promotional effect of reducible oxides, like MoO_X and TiO_X on the reactivity rhodium and even on that of the rather inert Au(111) surface has been reported [1-3] which initiated our investigations. The effects of molybdenum oxide and titanium oxide supports and overlayers on the structural and chemical properties of rhodium nanoparticles and highly defective continuous Rh films produced by Ar^+-ion sputtering has been addressed and compared to each other. The Mo and Rh films formed by PVD on a nearly stoichiometric TiO_2(110) single crystal were characterized by AES, XPS, LEIS, STM, TPD and work function (WF) measurements under UHV conditions. MoO_X and TiO_X encapsulation layers were produced on ultrathin Rh films by appropriate heat treatments. MoO_X overlayers were also formed by means of oxidation of Mo deposits.

The molybdenum oxide supports were prepared via the oxidation of 0.15-20.0 ML thick Mo deposits by the titania support and in O_2 gas at 650 and 1000 K. The WF values of oxidized Mo films were higher than that of TiO_2(110) by 0.3, 1.2 and 1.9 eV, attributable to the formation of mixed MoO_X-TiO_X, MoO_2 and MoO_3 surface layers, respectively. Rh was found to grow in a layer-by-layer fashion on the oxidized Mo films at 0.15-2.7 ML Mo coverage, corresponding to a considerably enhanced dispersion of rhodium as compared with that on the clean TiO_2(110). The encapsulation and surface reactivity of Rh layers supported by molybdenum oxides as a function of pre-annealing temperature was followed by carbon monoxide adsorption-desorption cycles. The molecular CO desorption (T_p=560 K) from a 0.4 ML thick Rh film formed on the MoO_3 support was strongly suppressed at 300 K, indicating the encapsulation of rhodium with MoO_X species of low surface free energy. The release of CO from rhodium particles supported by both MoO_3 and MoO_2 layers was eliminated due to pre-annealing at 600 K, related to the extended decoration of rhodium particles by MoO_X moiety as compared to that by TiO_x on the TiO_2(110) supported Rh at the same temperature. The encapsulation of the rhodium films by MoO_X proceeded above 600 K on both supports, and annealing to 1000 K resulted in nearly equal WF values, indicating the formation of MoO_X overlayers of similar surface composition close to MoO_2. AES depth profiles revealed that the 0.4 ML thick Rh deposits covered by MoO_X at 1000 K preserved their island structure.

Beside molecular CO desorption, both MoO_X and TiO_X covered Rh surfaces showed recombinative CO desorption states, the amount of which being proportional to the extent of CO dissociation. The decomposition of CO occurred in both cases only above a threshold Rh coverage and according to the oxide-metal boundary effect established for inverse catalyst systems, went through maximum at intermediate oxide coverages. Under the influence of MoO_X overlayer the desorption peak temperature for associative CO desorption has been decreased substantially as related to that for TiOx covered Rh, indicating the enhanced promotional effect of MoO_X.

[1] E.E. Lowenthal, L.F. Allard, M. Te, H.C. Foley, J. Mol. Catal. A-Chem., **100**, 129 (1995).
[2] K. Hayek, M. Fuchs, B. Klötzer, W. Reichl, G. Rupprechter, Top. Catal. **13,** 55, (2000).
[3] J. A. Rodriguez, S. Ma, P. Liu, J. Hrbek, J. Evans, M. Pérez, Science **318,** 1757 (2007).

Interaction of Oxygen and Water Molecules with Fluorine Impurities at CeO_2(111)

Matthew J. Wolf[1], Jolla Kullgren[1], Peter Broqvist[1] and Kersti Hermansson[1]
[1]Department of Chemistry–Ångström, Uppsala University, Sweden

In experiments on commercially produced single crystalline samples of ceria, quantities of F impurities on the order of 7–10% in the near-surface region were detected [1]. The origin of such a large impurity concentration is not known, but fluorine was also found to migrate into ceria films grown on CaF_2 substrates upon annealing, suggesting that it is readily incorporated into the ceria lattice [2]. The substitution of F for O reduces the amount of available lattice oxygen, and might therefore be expected to decrease the redox activity of ceria. However, nanoparticles doped with 10% F were found to exhibit *enhanced* catalytic activity in an oxidative reaction [3]. This somewhat counterintuitive behaviour motivates further study of the influence of F on the surface chemistry of ceria. As some initial steps in this direction, we studied the interaction of such defects at the (111) facet with O_2 and H_2O, using DFT+*U* calculations.

For both molecules, we considered their interaction with F impurities at the surface, and compared it with the O vacancy. We find that F ions act as a "counterweight" in redox cycles involving these molecules, reducing the energy difference between the reduced and oxidised states of the surface, as their location changes between being *in* the surface, and *on* the surface. Thus, although the amount of lattice oxygen is decreased by the presence of F, it potentially facilitates the release of oxygen, thereby enhancing the oxidative activity. Furthermore, we find that extraction of F to the gas phase either in the form of F_2 or HF is energetically unfavourable, and therefore it is stable at the surface.

[1] H. H. Pieper *et al*., Phys. Chem. Chem. Phys. **14** (2012) 15361
[2] J. Zarraga-Colina *et al*., J. Phys. Chem. B 109 (2005) p10978
[3] S. Ahmad *et al*., Inorg. Chem. **53** (2014) p2030

How unique is VO_x/ceria for enhanced oxidation Activity: The examples of MnO_x-ceria, CrO_x-ceria and Mg-doped VO_x-ceria

M. Nolan[1], **M. V. Ganduglia-Pirovano**[2]

[1]Tyndall National Institute, University College Cork, Lee Maltings, Cork, Ireland
[2]Instituto de Catálisis y Petroleoquímica, CSIC, 28049 Madrid, Spain
vgp@icp.csic.es

Ceria is an important component of catalysts for oxidation reactions that proceed through the Mars-van Krevelen mechanism, promoting activity. A paradigm example of this is the VO_x-CeO_2 system for oxidative dehydrogenation reactions, see, e.g., Refs. [1–4], where vanadium oxide species are supported on ceria and a special synergy between them is behind the enhanced activity: reduction of the catalyst is promoted by ceria undergoing reduction. This leads to favourable oxygen vacancy formation and hydrogen adsorption energies –useful descriptors for the oxidation activity of VO_x-CeO_2 catalysts. The question arises on the uniqueness of vanadia modifier leading to enhance activity and the possibility to rationally design improved ceria-supported transition metal oxide catalysts (MO_x/ceria) for oxidation reactions.

To this end, we investigate MnO_n- and CrO_n-CeO_2(111) (n=0–4) as examples of MO_x/ceria systems. We show, combining density functional theory calculations and statistical thermodynamics that similarly to the vanadia modifier, the stable species in each case is MnO_2- and CrO_2-CeO_2. Both show favourable energetics for oxygen vacancy formation and hydrogen adsorption, indicating that VO_2-CeO_2 is not the only system of this type that can have an enhanced activity for oxidation reactions. However, the mechanism involved in each case is different: CrO_2-CeO_2 shows similar properties to VO_2-CeO_2 with ceria reduction upon oxygen removal stabilising the 5+ oxidation state of Cr. In contrast, with MnO_2-CeO_2, Mn is preferentially reduced. Finally, a model system of VO_2-Mg:CeO_2 is explored that shows a synergy between VO_2 modification and Mg doping. These results shed light on the factors involved in active oxidation catalysts based on supported metal oxides on ceria that should be taken into consideration in a rational design of such catalysts [5].

[1] I. E. Wachs, Catal. Today 100, 79 (2005)
[2] A. Dinse, B. Frank, C. Hess, D. Habel and R. Schomäcker, J. Mol. Catal. A: Chem. 289, 28 (2008)
[3] M. V. Ganduglia-Pirovano, C. Popa, J. Sauer, H. Abbott, A. Uhl, M. Baron, D. Stacchiola, O. Bondarchuk, S. Shaikhutdinov, and H. J. Freund, J. Am. Chem. Soc. **132**, 2345 (2010)
[4] T. Kropp, J. Paier and J. Sauer, J. Am. Chem. Soc. **136**, 14616 (2014)
[5] M. Nolan and M. V. Ganduglia-Pirovano, Applied Catalysis B (submitted)

Cerium-niobium mixed oxides for the water gas shift reaction

S. Hernández[1], S. Collins[1], J. Carrasco[2], M. V. Ganduglia-Pirovano[3], J. Delgado[4] and **A. Bonivardi**[1]
[1] INTEC (UNL and CONICET), Güemes 3450, 3000 Santa Fe, Argentina
[2] CIC Energigune, Albert Einstein 48, 01510 Miñano, Alava, Spain
[3] Instituto de Catálisis y Petroleoquímica (CSIC), Canto Blanco, Madrid, 28049, Spain
[4] Universidad de Cádiz, Puerto Real, E11510, Spain

CeO_2, as a support, has proved to enhance the global rate for the water gas shift (WGS) reaction. It has been claimed that this behavior relies on the redox property of ceria that results in an increase of the rate of re-oxidation by water in the catalytic cycle, as compare to others non-redox supports (e.g., alumina) [1]. However, some of us have previously shown that although oxygen vacancies can react faster with water on gallium-promoted ceria catalysts, this is not the rate-determining step in the WGS reaction mechanism since an inverse correlation was found between the catalytic activity and the Ce^{3+} concentration [2].
Recent results for Pt/Nb_2O_5-CeO_2 catalysts show that niobia clearly improved the activity of Pt/ceria based catalyst for the WGS reaction. Moreover, the turnover rate per Ce^{3+} (sub)surface sites (measured by c-MES-DRIFTS under operando conditions) suggests that those sites should be part of the catalytic site. We report here, the results of the characterization of the ceria-niobia supports by XEDS (STEM-HAADF mode, Fig. 1), XPS, TPR-H2 (IR, MS) and TPR-CO (IR), which show that well-dispersed niobia on ceria increased the reducibility of CeO_2, but not of niobia. Theoretical calculations by DFT also show that ceria always stabilizes Nb^{5+} ions, even for the supported NbO_2, by removing an additional electron of the Nb 3d states which then occupies Ce 4f states. Low energy is demanded for the additional reduction by oxygen vacancy formation, which in turns increases the Ce^{3+} amount (Fig. 2). The combined approach of theoretical and experimental results proved that the ability of ceria for the stabilization of reduced states is favored by niobium oxide species in 5+ oxidation state.

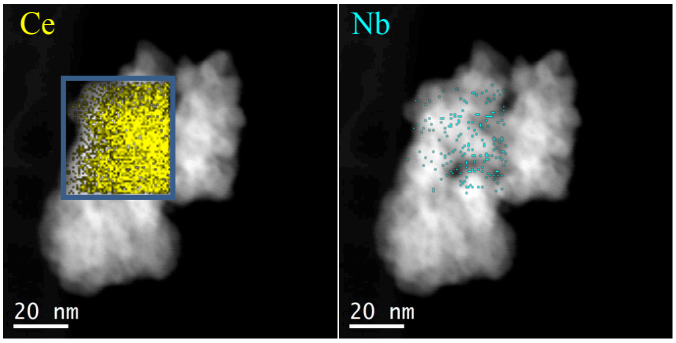

Figure 1. XEDS nano-structural analysis in STEM-HAADF mode (by HREM).

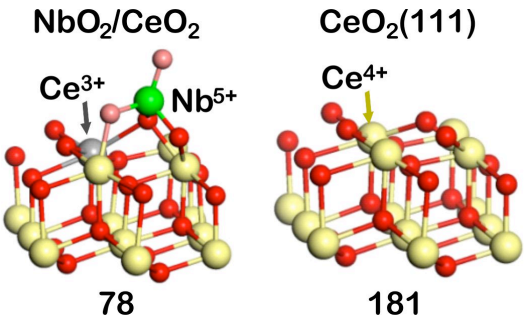

Figure 2. Energy of oxygen vacancy formation (in KJ/mol).

[1] J. Graciani, J. Fernández Sanz, Catal. Today, **240**, 214 (2015).
[2] J. Vecchietti et al., ACS Catalysis, **4**, 2088 (2014).

SCC-DFTB calculations of complex metal-oxides: ZnO and CeO_2

Jolla Kullgren, Kersti Hermansson, and **Peter Broqvist**

Department of Chemistry – The Ångström Laboratory, Uppsala University, Sweden

peter.broqvist@kemi.uu.se

First principles modeling, using e.g. the density functional theory (DFT), has become a valuable tool in materials research. However, today's computer resources limit the size and time scales that can be studied with such techniques, thereby hindering the full utilization of computational chemistry for large-scale systems in practice. Thus, new developments of reliable approximate and/or parameterized methods are needed. One promising approximate method, conceptually similar to the DFT, is the self-consistent charge density functional based tight binding method (SCC-DFTB). SCC-DFTB calculations are at least two orders of magnitude faster than a standard DFT calculation using semi-local functionals. However, to obtain accuracy comparable to DFT requires a proper parameterization, a task that has proven to be a challenge for complex oxides.

In this talk, I will present our SCC-DFTB parameterization efforts for two technologically important oxides: ZnO and CeO_2. These oxides are prototypical semiconducting oxides, where one is non-reducible (ZnO) and the other reducible (CeO_2). I will discuss the strategies we have developed for the parameterization and the special complication with reducible oxides.

Finally, I will demonstrate the applicability of the generated parameters and show results from validation by comparing to data obtained from DFT calculations. In the case of ZnO, I will present water adsorption on the most stable surfaces, surface reconstructions of the polar ZnO(0001) surface, and phonon properties of ZnO bulk and surfaces. For CeO_2, I will show results for oxygen vacancy formation in various ceria structures of different dimensionality, ranging from 0D (nano) to 3D (bulk).

Modelling of ceria-based nanostructures inspired by the Action CM1104

Konstantin M. Neyman[1,2], Alberto Figueroba[1], Sergey M. Kozlov[1]

[1] Dep. de Química Física and IQTCUB, Universitat de Barcelona, 08028 Barcelona, Spain
[2] Institució Catalana de Recerca i Estudis Avançats (ICREA), 08010 Barcelona, Spain
e-mail: konstantin.neyman@icrea.cat

We overview the most recent results of our density functional modelling of ceria-based nanostructures relevant for catalysis and energy technologies. Most of these studies have been inspired in the course of the COST Action by several participating groups and performed jointly with these experimentally and theoretically working teams.
Among the topics to be highlighted in the presentation are:

- Self-assembled ceria nanoparticles and oxygen vacancy formation energies therein [1].
- Most energetically stable structures of thin Ce_2O_3 films [2].
- Electron transfer from platinum particles deposited on ceria to the support [3].
- Reactivity of atomically dispersed Pt^{2+} species in fuel cell catalysts towards H_2 [4,5].
- Stability of transition metal species atomically dispersed at surfaces of nanostructured ceria as prospective single-metal catalysts [6].

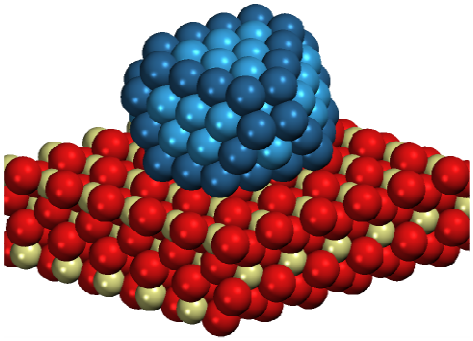

Figure. Model Pt_{122} nanoparticle supported on $CeO_2(111)$.

References:

[1] M. A. Sk, S. M. Kozlov, K. H. Lim, A. Migani, K. M. Neyman, Oxygen vacancies in self-assemblies of ceria nanoparticles. J. Mater. Chem. A **2**, 18329 (2014).
[2] S. M. Kozlov, I. Demiroglu, K. M. Neyman, S. T. Bromley, Reduced ceria nanofilms from structure prediction. Nanoscale **7**, 4361 (2015).
[3] Y. Lykhach, S. M. Kozlov, T. Skála, A. Tovt, V. Stetsovych, N. Tsud, F. Dvořák, V. Johánek, A. Neitzel, J. Mysliveček, S. Fabris, V. Matolín, K. M. Neyman, J. Libuda, Counting electrons on supported nanoparticles. Nature Materials **15**, 284 (2016).
[4] Y. Lykhach, A. Figueroba, M. Farnesi Camellone, A. Neitzel, T. Skála, F.R. Negreiros, M. Vorokhta, N. Tsud, K.C. Prince, S. Fabris, K.M. Neyman, V. Matolín, J. Libuda, Reactivity of atomically dispersed Pt^{2+} species towards H_2: Model Pt-CeO_2 fuel cell catalyst. Phys. Chem. Chem. Phys. **18** (2016), doi: 10.1039/c6cp00627b.
[5] R. Fiala, A. Figueroba, A. Bruix, M. Václavů, A. Rednyk, I. Khalakhan, M. Vorokhta, J. Lavková, V. Potin, I. Matolínová, F. Illas, K.M. Neyman, V. Matolín, High efficiency Pt^{2+}-CeO_x novel thin film catalyst as anode for proton exchange membrane fuel cells. Appl. Catal. B: Environ. (2016), doi: 10.1016/j.apcatb.2016.02.036.
[6] A. Figueroba, G. Kovács, A. Bruix, K.M. Neyman, Towards stable single-atom catalysts: Strong binding of atomically dispersed transition metals on the surface of nanostructured ceria. Catal. Sci. Technol. **6** (2016), in press.

Methanol adsorption on monocrystalline ceria surfaces

Thomas Kropp, Leonid Komissarov, Christopher Penschke, Robin Moerer, **Joachim Paier**, Joachim Sauer, Chengwu Yang[1], Fabian Bebensee[1], Alexei Nefedov[1], Christof Wöll[1]

Humboldt-Universität zu Berlin, Unter den Linden 6, 10099 Berlin, Germany
[1]Karlsruher Institut für Technologie, 76021 Karlsruhe, Germany
joachim.paier@chemie.hu-berlin.de, christof.woell@kit.edu

We have studied the adsorption of methanol on the (110) and (111) surfaces of bulk ceria (CeO_2) single crystals using infrared reflection-absorption spectroscopy (IRRAS) [1]. To assign the experimentally observed features, density functional theory (DFT) has been applied. For ceria (110), only a single intense band at 1108 cm^{-1} is observed, which is assigned to a monodentate methoxy species. For the fully oxidized ceria (111) surface, a more complex spectrum has been obtained: the small band at 1108 cm^{-1} is attributed to methanol adsorption at a small amount of (110) facets exposed at step edges in the (111) surface. The strong bands at 1085 and 1060 cm^{-1} are assigned to a methanol monolayer that consists of H-bonded methoxide as well as molecularly adsorbed methanol species. These assignments are derived from molecular dynamics simulations for several adsorption structures with low and high methanol coverage. Surface defects were also considered. Our results reveal that a simple relation between the redshift in the methoxy CO stretching mode and the number of cerium cations coordinated to the methoxide oxygen atom (as often used in previous work [2-7]) does not apply.

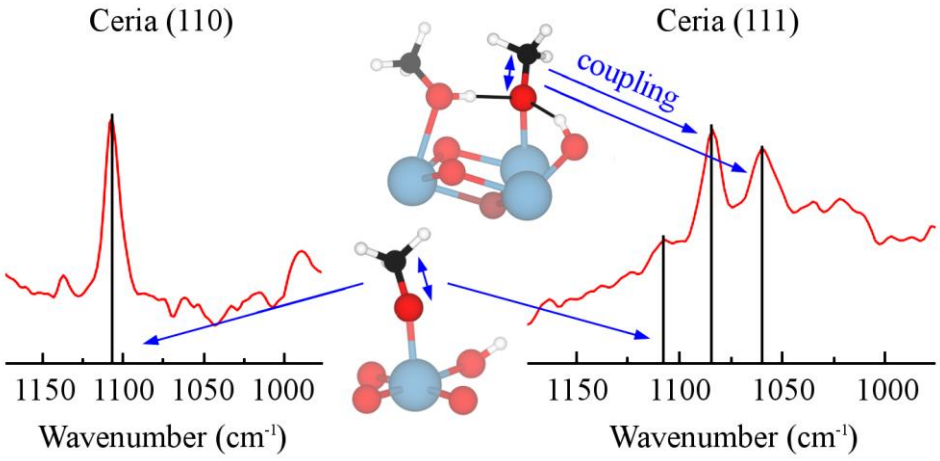

[1] C. Yang, F. Bebensee, A. Nefedov, C. Wöll, T. Kropp, L. Komissarov, C. Penschke, R. Moerer, J. Paier, J. Sauer, J. Catal., **336**, 116, (2016).
[2] C. Li, K. Domen, K.-i. Maruya, T. Onishi, J. Catal. **125**, 445, (1990).
[3] A. Badri, C. Binet, J.C. Lavalley, J. Chem. Soc.-Faraday Trans. **93**, 1159, (1997).
[4] Z. Wu, M. Li, D.R. Mullins, S.H. Overbury, ACS Catalysis **2**, 2224 (2012).
[5] A. Siokou, R.M. Nix, J. Phys. Chem. B **103**, 6984, (1999).
[6] H.L. Abbott, A. Uhl, M. Baron, Y. Lei, R.J. Meyer, D.J. Stacchiola, O. Bondarchuk, S. Shaikhutdinov, H.J. Freund, J. Catal. **272**, 82, (2010).
[7] J. Uhlrich, B. Yang, S. Shaikhutdinov, Top. Catal. **57**, 1229, (2014).

Gold adsorption and diffusion on reduced CeO_2(111)

R. Pérez[1], P. G. Lustemberg[2], Y. Pan[3], K. Kośmider[1], V. Brázdová[4,5], G. Thorton[5,6], M. V. Ganduglia-Pirovano[7], N. Nilius[8]

[1]Dept. Física Teórica de la Materia Condensada, UAM and IFIMAC, 28049 Madrid, Spain
[2] Instituto de Física Rosario (IFIR, CONICET-UNR) and UNR, 2000 Rosario, Argentina
[3]Paul-Drude-Institut für Festkörperelektronik, 10117 Berlin, Germany
[4]Thomas Young Centre and Dept. of Physics and Astronomy, UCL, London WC1E 6BT, UK
[5]London Centre for Nanotechnology, London WC1H 0AH, UK
[6]Dept. of Chemistry, UCL, London WC1H 0AJ, UK
[7]Instituto de Catálisis y Petroleoquímica, CSIC, 28049 Madrid, Spain
[8]Institute of Physics, Carl von Ossietzky University, 26111 Oldenburg, Germany
ruben.perez@uam.es

Surface oxygen defects are believed to govern the adsorption characteristics of reducible oxides such as CeO_2. We address the adsorption and diffusion of Au atoms on CeO_2(111) and challenge this perception on the basis of a combined scanning tunneling microscopy and DFT (PBE)+*U* study.

Surface oxygen vacancies are clearly thermodynamically preferred for Au adsorption, but incoming Au atoms at moderate temperature are found to occupy mostly regular bridge surface sites, and *not* the vacant site. The observation is explained with the strong polaronic nature of the Au-ceria system, which imprints a dominant diabatic character to the diffusive motion of Au atoms. Au adatoms, moving from a terrace to an oxygen vacant site, would change their oxidation state from Au^+ to Au^0 to Au^-. The associated diabatic barriers for the $Au^+ \rightarrow Au^0$ step of 0.6 to 1.0 eV are insurmountable, and the vacant sites remain unoccupied.

Moreover, for a reduced surface with subsurface oxygen vacancies, Ce^{3+} sites were suggested to be the preferred location for the binding of Au^- species [1], based on DFT calculations with a (2×2) unit cell (Θ_{def}=1/4) and the HSE06 hybrid functional. Using the same computational set-up, we find that a hollow site centered at a subsurface oxygen atom, where the 4f → 6s charge transfer occurs from a Ce^{3+} ion in a deeper layer, is energetically more favorable by 0.36 (0.34) eV with HSE06 (PBE+*U*) than on-top of a Ce^{3+} ion in the outermost cerium layer [2]. The preference is explained in terms of the reduction of both lattice strain and Coulomb repulsion. We note that *neither* the hollow *nor* the Ce^{3+} sites are stable in the isolated defect or dilute limit [*e.g.*, Θ_{def}=1/16, (4×4)], reflecting the impact of lattice strain in reduced ceria on the Au adsorption behavior.

These results underline the importance of polaronic lattice distortions and charge-transfer processes for adsorption and diffusion phenomena on reducible oxides.

[1] Y. Pan, N. Nilius, H.-J. Freund, J. Paier, C.Penschke, and J.Sauer, Phys. Rev. Lett. **111**, 206101 (2013)
[2] K. Kośmider, V. Brázdová, M. V. Ganduglia-Pirovano, and R. Pérez, J. Phys. Chem. C **120**, 927 (2016)

Simulations of IR vibrational frequencies of CO adsorbed on isolated and supported on ceria platinum species: a density functional study

Hristiyan A. Aleksandrov[1,2], Konstantin M. Neyman[2,3], Georgi N. Vayssilov[1]

[1] Faculty of Chemistry and Pharmacy, University of Sofia, 1126 Sofia, Bulgaria
[2] IQTCUB, Universitat de Barcelona, C/Martí i Franquès 1, 08028 Barcelona, Spain
[3] Institució Catalana de Recerca i Estudis Avançats (ICREA), 08010 Barcelona, Spain

e-mails: haa@chem.uni-sofia.bg, konstantin.neyman@icrea.cat, gnv@chem.uni-sofia.bg

Our periodic density functional calculations of various Pt-containing models helped to confirm and clarify assignments of various bands detected experimentally when CO is adsorbed on Pt/CeO_2 samples [1,2]. The calculations also predicted where the IR bands of CO molecules with certain coordination environment are to be found. For instance, bridged coordinated CO on Pt is expected to have a band at 1840-1885 cm^{-1}, while linearly adsorbed CO to Pt^0 have an IR feature at 2018-2077 cm^{-1}, depending on the coordination number of Pt atoms. As a trend the lower the CN is, the lower the C-O vibrational frequency, ν(C-O), is. Another factor which can influence the position of the IR band is the flexibility of the Pt surface. More flexible surfaces bind CO stronger and this provokes a C-O vibration shift to lower frequencies.

The ν(C-O) values are in the range 2010-2032 cm^{-1} for CO molecules adsorbed on isolated Pt atoms supported on stoichiometric or reduced ceria. At oxidative conditions, the C-O vibration is shifted to notably higher frequencies, 2043-2077 cm^{-1} and 2095-2121 cm^{-1}, for CO adsorption on Pt^{2+} and Pt^{4+}, respectively. We also found that Pt^{2+} species form very stable square planar dicarbonyl complexes. In this case the C-O vibrational frequencies are in the regions: 2066-2086 (antisymmetric) and 2115-2142 (symmetric) cm^{-1}.

At reductive or moderate oxidative conditions the most stable sites for mononuclear Pt species are at small (100) facets, while at strongly oxidative conditions the most stable positions are at (111) facets [3]. When CO is adsorbed, the preferred adsorption sites are interchanged: at reductive conditions preferred positions of the PtCO complexes are at (111) facets, while at oxidative conditions preferred positions of the PtOCO complexes are at the small (100) facets.

Spillover of one O atom from ceria support to the small Pt clusters does not change notably the adsorption energy of the CO and its vibrational frequency, but when oxygen coverage increases the adsorption energy of CO is reduced and the CO vibration is shifted to higher frequencies.

Acknowledgments: The authors are grateful for the support from the European Commission (FP7 projects BeyondEverest and ChipCAT 310191), Spanish MINECO (grant CTQ2012-34969), COST Action CM1104, and the Bulgarian Supercomputer Center for provided computational resources and assistance.

References

[1]. M. Happel, J. Mysliveček, V. Johánek, F. Dvořák, O. Stetsovych, Y. Lykhach, V. Matolín, J. Libuda, J. Catal., **289**, 118-126, (2012).

[2]. P. Bazin, O. Saur, J. C. Lavalley, M. Daturi and G. Blanchard, Phys. Chem. Chem. Phys., **7**, 187-194, (2005).

[3]. H. A. Aleksandrov, K. M. Neyman, G. N. Vayssilov, Phys. Chem. Chem. Phys., **17**, 14551-14560, (2015).

Water Dissociation and H diffusion is Water-Assisted on CoO_x/Au(111)

Jakob Fester[1], Maximillian. G. Melchor[2], Alex Walton[1], Michal Bajdich[2], Aleksandra Vojvodic[2], **Jeppe V. Lauritsen[1]**
[1]*Interdisciplinary Nanoscience Center Aarhus University, Aarhus, 8000, Denmark*
[2] *SUNCAT Center for Interface Science and Catalysis, SLAC National Accelerator Laboratory, 2575 San Hill Road, Menlo Park, California 94025, United States.*
email: jvang@inano.au.dk

Cobalt oxides are among the best performers as future alternative electro-catalysts for the water splitting reaction, with attractive properties in terms of stability, efficiency, abundance and low cost. However, fundamental understanding of the catalytic properties of cobalt oxides is still limited. To elucidate the fundamental structure, composition and surface chemistry of a CoO_x based catalysts, we characterize here the surface of a model catalyst consisting of CoO nanoislands and provide an atomic-scale investigation water dissociation reactions on the CoO/Au(111).

We find that the oxygen pressure has a profound effect on the CoO structure, accompanied by changes in the cobalt oxidation states. The structure at low pressure is a rock-salt Co-O bilayer exposing the (111) plane with cobalt in the +2 oxidation state. However, this can be converted into a more oxygen rich stoichiometry with cobalt in the +3 state, accomplished by intercalation of an additional oxygen layer in the island/gold interface. Both structures exhibit a high activity towards water dissociation at room temperature, leading to hydroxylation of up to 50% of the island basal plane oxygen atoms as observed in-situ by both dynamic STM movies recorded during H_2O dosing and by corresponding analysis of the hydroxyl component in the O1s core-level XPS spectrum. The reactivity towards water dissociation is measured as function of island edge concentration, revealing the CoOx edges to host the most active sites. Atom-resolved STM images furthermore show how hydroxyls first form in the dissociation process on the edges and subsequently migrate to the basal plane oxygen sites, serving as a hydrogen reservoir. By density functional theory the water dissociation mechanism is explained and is shown that an additional water molecule, remarkably, acts to promote *all* the elementary steps of water dissociation on the Co edge sites.

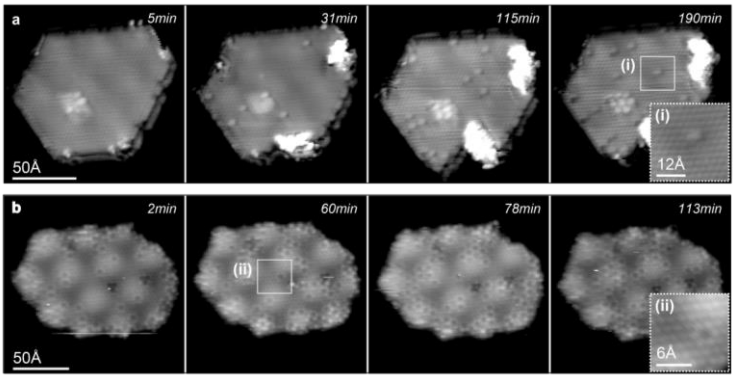

[1] A. S. Walton, J. Fester, M. Bajdich, et al., ACS Nano 9, 2445 (2015).

Model catalysts for reforming reactions: water interaction with ultrathin films of zirconium oxide

Hao Li [1], Wernfried Mayr-Schmölzer [2], Joong-Il Jake Choi [2], Christoph Rameshan [1], Florian Mittendorfer, [2]Michael Schmid [2], Josef Redinger [2], and Günther Rupprechter [1*]
[1] Institute of Materials Chemistry, Technische Universität Wien, A-1060 Wien, Austria
[2] Institute of Applied Physics, Technische Universität Wien, A-1040 Wien, Austria
e-mail: guenther.rupprechter@tuwien.ac.at

It is well accepted that surface science based planar model catalysts are well-suited for fundamental studies of surfaces processes, despite the inherent differences between model and technological catalysts [1-3]. Methodological advances also allow to examine active functioning model catalysts, at (near) atmospheric pressure and at elevated temperature. Frequently applied methods encompass polarization-modulation infrared reflection absorption spectroscopy (PM-IRAS), sum frequency generation (SFG) laser spectroscopy and near atmospheric pressure X-ray photoelectron spectroscopy (NAP-XPS). In the current contribution this approach is utilized to examine Ni-ZrO_2 „cermet“ anodes that are employed in Solid Oxide Fuel Cells (SOFCs) for CH_4 reforming to H_2 and/or H_2 oxidation.

In order to model SOFC anodes well-ordered ultrathin films of ZrO_2 were grown in UHV by oxidation and annealing of $Pt_3Zr(0001)$ single crystals [4]. Ni was deposited by physical vapor deposition. Low Energy Electron Diffraction (LEED), Scanning Tunneling Microscopy (STM), high resolution X-ray Photoelectron Spectroscopy (XPS) and Density Functional Theory (DFT) indicated the formation of a well-structured ZrO_2 trilayer film, corresponding to the (111) facet of cubic ZrO_2. Whereas the interaction of the ZrO_2 film with CO or CO_2 was very weak (desorption temperatures of 155 and 117 K, respectively), its interaction with water was very strong (desorption temperature of 485 K). NAP-XPS (O1s and Zr3d) and PM-IRAS were thus applied to examine water adsorption/dissociation and hydroxylation of the O-Zr-O film. Backed by DFT, three channels of water adsorption (molecular vs. dissociative, reversible vs. non-reversible) could be identified. Creation of defects by ion bombardment strongly enhanced water dissociation.

Once hydroxylated the ZrO_2 film exhibited exceptional activity for reaction with CO_2 (whereas the non-hydroxylated film did not). IRAS, using formic acid (HCOOH) and formaldehyde (HCHO) as reference, was used to identify the functional groups of the species formed. Ni nanoparticles grown on the ZrO_2 trilayer were examinded by PM-IRAS and XPS.

Support by the Austrian Science Fund (FWF SFB-F45 FOXSI) is gratefully acknowledged.

[1] G. Rupprechter, Advances in Catalysis, 51 (2007) 133-263.
[2] K. Föttinger, G. Rupprechter, Accounts of Chemical Research, 47 (2014) 3071−3079.
[3] Y. Suchorski, G. Rupprechter, Surface Science, 643 (2016) 52-58.
[4] H. Li, J.J. Choi, W. Mayr-Schmölzer, C. Weilach, C. Rameshan, F. Mittendorfer, J. Redinger, M. Schmid, G. Rupprechter, Journal of Physical Chemistry C, 119 (2015) 2462–2470.

Intrinsic electron and hole trapping in amorphous hafnium oxide

Moloud Kaviani[1], Valery V. Afanas'ev[2], Jack Strand[3], and **Alexander Shluger**[1,3]
[1]WPI-Advanced Institute for Materials Research, Tohoku University, Sendai, Japan
[2]Department of Physics, University of Leuven, Leuven, Belgium
[3]Department of Physics and Astronomy, University College London, London, UK
a.shluger@ucl.ac.uk

Recent experimental evidence suggests that in some amorphous oxides intrinsic electron localisation occurs in deep states, where the effect of local disorder is amplified by polaronic relaxation of amorphous network [1-3]. In particular, the experimental results using the exhaustive photo-depopulation spectroscopy demonstrate the existence of deep electron trapping states in amorphous hafnium oxide (a-HfO_2) structures [4] which are not associated with oxygen deficiency. To investigate whether these states can be caused by intrinsic charge trapping, we modelled the behaviour of extra electrons and holes in stoichiometric a-HfO_2 structures.

Amorphous hafnia models including up to 324 atoms were generated using classical force-fields and their geometries optimised using density functional theory (DFT). They have densities in the range of 9.2-9.9 g/cm^3, averaging at 9.6 g/cm^3. The electronic structures of these models with extra electrons and holes were calculated using DFT with the hybrid functional HSE06. In all models, an extra electron or hole is initially partially delocalized, but the structure relaxation demonstrates that they can trap spontaneously at particular precursor sites in deep states in the band gap. For trapped electrons, these states are located at ~2.0 eV below the bottom of CB, ranging from 1.0 to 2.7 eV, in good agreement with the experimental data [4]. This energy depends on the a-HfO_2 density and on local environment. Extra electrons are localized typically on two or three Hf ions associated with longer Hf-O bonds or under-coordinated Hf atoms in the structures and induce strong polaronic distortion of the surrounding network. The same trap can accommodate two electrons creating a deeper state at ~3.0 eV below the bottom of the conduction band. Holes are typically localized on two under-coordinated O ions and have trapping energies of about 1.0 eV. Our results broaden the concept of intrinsic polaron trapping to disordered oxides.

[1] A.-M. El-Sayed, M. B. Watkins, V. V. Afanas'ev and A. L. Shluger, Phys. Rev. B **89**(12), 125201, (2014).
[2] A.-M. El-Sayed, K. Tanimura and A. L. Shluger, J. Phys.: Condens. Matter, **27**(6), 265501, (2015).
[3]. H.-H. Nahm and Y.-S. Kim, NPG Asia Materials **6**, el43 (2014).
[4]. F. Cerbu, O. Madia, V. Afanasiev, et al., ECS Transactions, **64** (8), 17-22 (2014).

Paramagnetic oxide traps in Sc_2O_3-passivated (100)Ge/HfO_2 stacks

A. Stesmans[1], S. Iacovo[1], D. Cott[2], A. Thean[2], H. Arimura[2], S. Sioncke[2], and V. V. Afanas'ev[1]
[1]*Department of Physics and Astronomy, University of Leuven, 3001 Leuven, Belgium*
[2]*Imec, Kapeldreef 75, 3001 Leuven, Belgium*
Andre.stesmans@fys.kuleuven;be

Passivation of Ge/insulator interfaces in n-channel field effect transistors remains a challenge. Whereas a reasonably low density of interface states (10^{11} $cm^{-2}eV^{-1}$ range) can be achieved using GeO_2-based passivation schemes [1,2], the low dielectric constant (κ) of the Ge-oxide interlayer (IL) prevents downscaling of the dielectric stack to the 0.5-0.6 nm equivalent oxide thickness (EOT) target. Introduction of passivation schemes using sesquioxides of group III metals (La, Y, Sc) seem to provide a promising path to mitigate this problem by increasing κ of the IL [2] and improving its stability [3]. However, as a common drawback, these passivating oxides exhibit considerable charge instability, indicative of a high oxide trap density.

Here, the usefulness of employing the rare-earth Sc_2O_3 high-κ (~16) dielectric in passivating Ge surfaces for metal-oxide-semiconductor device application is studied in terms of occurring inherent paramagnetic point defects, operating as detrimental charge traps.

To assess their atomic nature, low temperature K-band electron spin resonance (ESR) experiments have been carried out in combination with electrical probing, including capacitance-voltage, internal photoemission and photoconductance observations, on (100)Ge/(GeO_2)/Sc_2O_3/HfO_2 stacks grown by atomic layer deposition subjected to various processing steps.

As illustrated in Fig. 1, in stacks with Ge directly contacted with Sc_2O_3, without an additional O-supply processing step, ESR reveals the presence of a prominent signal of powder pattern shape, centred at g=2.0017(2). It is ascribed to O-deficiency centers located in the Sc_2O_3-based dielectric, which from attendant electrical analysis are concluded to be at the origin of substantial electron trapping (~6×10^{12} cm^{-2}) in near-interfacial layers.

It is concluded that in Sc_2O_3-passivated (100)Ge/Sc_2O_3/HfO_2 stacks, O-deficiency caused by oxidation of Ge (O-scavenging) emerges as key culprit in defect generation in high-κ layers on top. Remedying this requires a sufficient supply of O_2 during critical manufacturing steps.

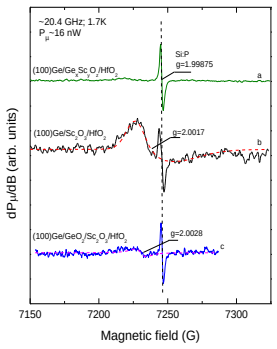

Fig. 1: Low-P_μ first derivative-absorption K-band ESR spectra dP_μ/dB (where P_μ is the applied microwave power) observed at 1.7K for the applied magnetic field **B** at angle 0-30° with the [100] interface normal on three types of p-(100)Ge/high-κ insulator (Sc_2O_3/HfO_2) stacks. The signal at g=1.99875 stems from a co-mounted Si:P marker sample, also used for field axis alignment of the spectra. The dashed curves represent computer simulations. The spectra have been normalized to equal sample area and Si:P marker intensity.

[1] F. Bellenger et al., J. Electrochem. Soc. **155,** G33**,** (2008); A. Toriumi et al., Microelectron. Eng. **86** (2009) 1571.
[2] C. X. Li and P. T. Lai, Appl. Phys. Lett. **95**, 022910 (2009).
[3] I. Z. Mitrovic et al., J. Appl. Phys. **115**, 114102 (2014)

Annealing-induced electron traps in atomic-layer deposited HfO_2 layers

V. V. Afanas'ev, F. Cerbu, O Madia, J. A. Kittl, M. Houssa, A. Stesmans
Department of Physics and Astronomy, KULeuven, Belgium
valeri.afanasiev@fys.kuleuven.be

HfO_2-based insulators used in logic and memory microelectronic devices are known to cause significant reliability problems associated with charge trapping in the oxide layer if annealed at high temperature. Development of oxygen deficiency leading to generation of traps during anneal in an O-free environment is usually kept responsible for the degradation. However, little is still known about properties of the O-deficiency related traps. Here, using analysis of photo-depopulation of electron states in HfO_2 films grown by atomic layer deposition (ALD), we will show how annealing affects the energy distribution of electrons trapped in HfO_2. Deep acceptor states energetically distributed at around $E_t \approx 2.0$ eV and $E_t \approx 3.0$ eV below the oxide conduction band are found to be the dominant electron traps. Comparison of the trapped electron energy distributions in HfO_2 layers prepared using different precursors or subjected to anneal suggests that these centers are intrinsic in origin. While the former traps are dominant in the as-deposited HfO_2 layers and those annealed at moderate temperatures (<800 ºC), annealing at higher temperature leads to generation of deeper traps as can be seen from the photo-(dis)charging spectra and spectral charge density (SCD) distributions directly reflecting the energy distribution of gap states and shown in Fig. 1. In addition, high-temperature annealing leads to higher density of positive charge in when the photon energy exceeds 5 eV and approaches the bandgap width of HfO_2 (5.6 eV for monoclinic phase). The absence of any measurable density of donor states in the upper half of the HfO_2 bandgap indicates that the common assumption implicating O vacancies cannot explain the observed charging behavior of HfO_2. Furthermore, energy levels of the revealed acceptor states are also inconsistent with theoretically evaluated energy levels of oxygen vacancies in monoclinic or amorphous HfO_2, suggesting that alternative models of trapping sites should be considered.

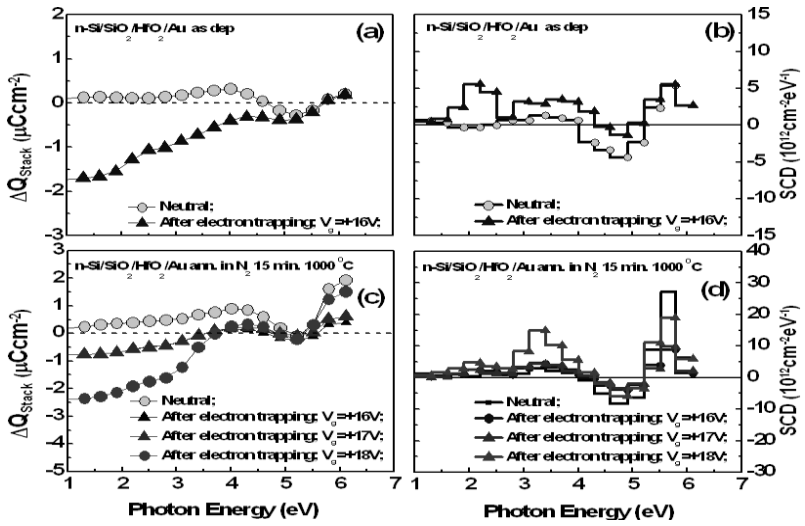

Fig. 1. Illumination-induced charge variation (a, c) and the inferred SCD spectra (b,d) as measured on $Si/SiO_2/HfO_2$ samples with 20-nm HfO_2 layers deposited using a chlorine-free ALD process and subjected to the 15 min post-deposition anneal in N_2 at 1000 °C. The results of measurements on the electron-injected samples are shown for several charging voltages.

Ab initio calculations of neutral and charged oxygen vacancies in $BaZrO_3$ perovskite crystals

E.A. Kotomin[1,2], Tor S. Bjørheim[3], D. Gryaznov[1], M. Arrigoni[2], J. Maier[2]

[1]*Institute for Solid State Physics, University of Latvia, Kengaraga str. 8, Latvia*
[2]*Max Planck Institute for Solid State Research, Heisenbergstr. 1, Stuttgart, Germany*
[3]*Centre for Materials Science and Nanotechnology, University of Oslo, Norway*

ABO_3 perovskites are widely used in solid oxide fuel cells (SOFCs) as cathodes, anodes and electrolyte materials. To enhance the kinetics of ion transport processes, high operational temperatures (800-1000°C) are usually employed. In the last few years, research has been focused to develop materials with lower operating temperatures (intermediate temperature range 600-800°C, low temperature range <600°C), as high operating temperatures are responsible for degradation phenomena and thermal stress that shorten the device life. Deposition of electrolyte thin films can successfully improve SOFCs performances in the intermediate temperature range.

In recent years, high-temperature proton conducting (HTPCs) ABO_3 perovskites have attracted considerable attention for their possible application as electrolyte materials in the intermediate temperature range, due to their lower activation energies of ionic transport compared to oxygen-ion conducting electrolytes. Yttrium doped $BaZrO_3$ (BZY) is considered as one of the most promising HTPCs, with optimal chemical stability under high temperature operational conditions and high partial proton conductivity. Oxygen vacancies therein play a major role in proton uptake and transport.

First principles calculations are routinely applied for the study of atomic, electronic and thermodynamic properties of oxides thin films and surfaces, and for point defects as well. However, despite the promising $BaZrO_3$ applications as a HTPC material, there is a lack of comprehension on the behavior of oxygen vacancies in its films and on surfaces from the microscopic point of view.

In this contribution, we explore possible confinement effects on the atomic and electronic structure, and phonon properties of neutral ($V_O^{\times}$) and fully charged ($V_O^{\bullet\bullet}$) oxygen vacancies in $BaZrO_3$(001) ultra-thin films [1,2] and compare these properties with vacancies in the bulk [3]. First principles phonon calculations were performed as a function of film thickness (varied between 3 to 7-atomic planes) using two complementary computer codes: VASP and CRYSTAL. The calculations reveal that for both types of vacancies the confinement effect is surprisingly short-range: for films containing 5 planes or more, the oxygen vacancy properties are predicted to be similar to those observed in the bulk material.

[1] M. Arrigoni et al, Phys. Stat. Solidi **B 252,** 139 (2015).
[2] M. Arrigoni et al, 2016, submitted
[3] T.Bjorheim et al, Phys. Chem. Chem. Phys. **17**, 20765 (2015).

Water interaction with perfect and fluorine-doped Co_3O_4(100) surfaces

Yu.A. Mastrikov[1], G.A. Kaptagay[2], T.M. Inerbaev[2], E.A. Kotomin[1], A.T. Akilbekov[2]

[1]*Institute of Solid State Physics, University of Latvia, Kengaraga str. 8, Riga, Latvia*
[2]*L.N. Gumilyov EurAsian National University, Mirzoyan str. 2, Astana, Kazakhstan*

The increasing consumption of energy in the world has stimulated an intensive research of different sources of renewable energy. This includes research on the electrochemical splitting of water, in order to increase the efficiency of the oxygen evolution reaction (OER) by means of reducing overpotential. The interaction of water with transition metal oxide surfaces plays an important role in catalysis, surface chemistry, gas sensors, photo- and electrochemistry. One of the promising materials for water splitting is spinel-type tricobalt tetra oxide, Co_3O_4.

Recently, Norskov et al. combined DFT+*U* calculations and atomistic thermodynamics in theoretical study of the OER activity on Co_3O_4 surfaces as a function of applied potential and pH [1]. Catalyst performance could be, in principle, improved using different promoters, e.g. via cation (Al) [2] or anion (F) [3] doping. It is expected that this is related to an increase of concentration of Co^{2+} surface catalytically active centers. Motivated by the latter experiments, in the present study we employed the GGA+*U* approach for analysis of the catalytic activity of different Co-sites on the perfect and F-doped Co_3O_4(100) surface in H_2O adsorption [4].

Using accurate DFT+*U* calculations, we have shown that water can be dissociatively adsorbed on the tetrahedrally coordinated Co^{2+} ions on the Co_3O_4 (100) surface. From the computed Gibbs free-energy changes along the OER, we found that the F-doped $Co_{0.5}$-terminated Co_3O_4(100) surface is catalytically active. We found also that at the Co^{O}_{5c} site on F-doped surface theoretical overpotential on the Co_3O_4(100) surface was considerably reduced. Due to the large overpotential, the OER efficiency on the pure Co_3O_4 substrate is expected to be low and F doping does improve it. This implies that F-doped Co_3O_4 is active for electrochemical oxidation of water, in full agreement with experimental observations [3]. In the forthcoming paper we discuss also cation, Cs doping effects.

[1] M.Garcia-Mota, Jens K. Norskov et al., J. Phys. Chem. C **116** (2012) 21077–21082.
[2] X.L.Xu, J.Q.Li, J. Surface Science **605** (2011) 1962-1968.
[3] A.Gasparotto et al, J.Amer.Chem.Soc.**133** (2011) 19362-19367.
[4] G.A. Kaptagay, Yu.A. Mastrikov, E.A. Kotomin et al., Solid State Ionics **277** (2015) 77-87.

Structural transitions induced by polarity in ultra-thin films and nanoribbons

C. Noguera*, J. Goniakowski*, L. Giordano**, A. M. Llois[1], F. Güller[1]

**Institut des NanoSciences de Paris, Paris, France*
***Dipartimento di Scienza dei Materiali, Universita di Milano-Bicocca, Via R. Cozzi, 53, 20125 Milano, Italy*
[1] Centro At´omico Constituyentes, GIyANN, CNEA, Av. Gral. Paz 1499, San Martın, Buenos Aires, Argentina

The properties of low dimensional nano-objects are strongly dependent upon their thickness/width, their stoichiometry, and their environment. It is, for example, well known that, below the so-called scalable regime, cluster structures may be totally different from the bulk one due to the increased energy weight of low coordinated atoms (e.g., surface versus bulk atoms). The same is true in ultrathin films or 2D nano-objects, especially when polarity effects are involved. In this communication, we will put in perspective the polarity-driven mechanism responsible for the structural transitions which take place in oxide thin films at low thickness and in dichalcogenide nanoribbons of small width.

With the help of first principles simulations, we have predicted [1] that, in order to avoid the energy cost of surface polarity, films of MgO(111) adopt a hexagonal Boron Nitride structural ground state under a critical thickness, made of a stacking of graphene-like monolayers, rather than the rocksalt structure. Similar findings concern ZnO(0001) films and more generally polar films of all oxides crystallizing in the wurtzite or rocksalt structure.

Going down in dimensionality and relying on first-principles simulations, we demonstrate that, in MoS_2, WS_2 , and $MoSe_2$ monolayer-thick nanoribbons with zigzag edges, the 1T phase, which is metastable in the full monolayer, is the actual (low temperature) ground state when the ribbon width is small. Above a critical width, a transition towards the expected 1H phase takes place, accompanied by a metal to semiconducting transition in the electronic properties. We assign this ground state modification at small width to the general effect of edge polarity. The same argument explains why there is no similar transition for ZrS2 whose infinite monolayer ground state is 1T, and why it is unlikely to occur in (non-polar) armchair nanoribbons.

[1] J. Goniakowski, C. Noguera, L. Giordano, Phys. Rev. Letters **93** (2004) 215702
[2] F. Güller, A. M. Llois, J. Goniakowski, and C. Noguera, "Prediction of structural and metal-to-semiconductor phase transitions in nanoscale MoS_2, WS_2, and other transition metal dichalcogenide zigzag ribbons", Phys. Rev. B **91** (2015) 075407

Chemistry and dynamics of the proton phonon coupling in proton conducting ceramic electrolytes

Artur Braun

Empa. Swiss Federal Laboratories for Materials Science and Technology
Überlandstrasse 129
CH – 8600 Dübendorf, Switzerland

Tel.: +41-58-765-4850
Fax: +41-58-765-6950
artur.braun@alumni.ethz.ch

Abstract

Super-protonic conductivity is a highly-wished-for functionality of solid electrolytes for intermediate temperature ceramic fuel cells and steam electrolyzers. Y-substituted barium cerate - conventional ceramics with ABO3-type perovskite structure, is a well-studied candidate for this purpose. We have investigated the functional oxygen vacancy filling of engineered oxygen deficient BCY by water molecules with electro-analytical methods and ambient pressure XPS [1], which enabled to sketch a detailed picture of the correlation of molecular and electronic structure changes, and the concomitant onset of proton conductivity at elevated temperatures. With this information we were able to design experiments, where the proton phonon coupling could be quantitatively investigated with high pressure-high temperature electrochemical impedance spectroscopy combined with quasi-elastic neutron scattering [2,3]. Supported with pressure dependent XRD and Raman scattering data [4,5] we were able to correlate the proton jumping parameters with the temperature and found that the proton jump times follow a Holstein polaron relation [6,7].

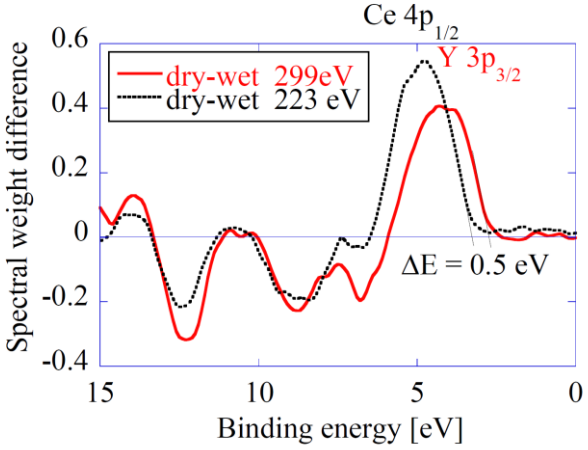

VB XPS difference spectra containing the spectral signature of oxygen defects in BaCeY-oxide, recorded in resonant condition for Y and Ce. The maxima of the pronounced difference peak at a binding energy of around 5 eV are shifted by about 0.5 eV, revealing that the gap state of oxygen vacancies next to Y is by 0.5 eV closer to the Fermi level than a gap state from an oxygen vacancy next to Ce.

[1] Q. Chen et al., Chem. Mater. 25 (23), 4690 (2013).
[2] Q. Chen et al., Solid State Ionics 252, 2 (2013).
[3] Q. Chen et al., High Pressure Research 32(4), 471 (2012).
[4] Q. Chen et al., J. Phys. Chem. C 115 (48), 24021 (2011).
[5] Q. Chen et al., J. Eur. Ceram. Soc. 31 (14), 2657 (2011).
[6] Q. Chen et al., Appl. Phys. Lett. 97, 041902 (2010)
[7] A. Braun et al., Appl. Phys. Lett., 95, 224103 (2009).

Annealing induced oxygen vacancy formation in nanoparticle systems of reducible metal oxides

Oliver Diwald[1], Daniel Thomele[1], Nicolas Siedl[2], Johannes Bernardi[3]
[1] Department of Chemistry and Physics of Materials, University of Salzburg, Salzburg, A
[2] Department of Chemical and Bioengineering, University Erlangen-Nürnberg, Erlangen, DE
[3] University Service Center for Transmission Electron Microscopy, TU Wien, Vienna, A
oliver.diwald@sbg.ac.at

Interfaces between nanoparticles of reducible metal oxides play a critical role for oxygen vacancy formation, stoichiometry changes and associated self-doping effects. With a combination of analytical techniques (electron paramagnetic resonance (EPR), FT-IR, UV-Vis-NIR absorption, XRD, and TEM) we addressed annealing induced oxygen vacancy formation on TiO_2 [1] and In_2O_3 [2,3] particle systems as candidates for printed electronics. In addition to optical property changes we identified a strong impact of particle contacts and grain boundaries on annealing induced stoichiometry changes and, thus, on the doping level of the processed nanostructures. Dielectric loss effects observed for nonstoichiometric In_2O_{3-x} nanoparticles inside the cavity of an EPR spectrometer system were used to determine trends in oxygen deficiency and n-type doping level for differently consolidated nanoparticle powders.[3] The observation of a clear correlation between reducibility on oxide nano-particles achieved by vacuum annealing and the amount of intergranular interface area underlines the multiple role of intergranular interfaces. Inside ensembles of semiconducting oxide nanoparticles, they not only provide diffusion paths for charge carriers, they also offer a handle to adjust the n-type doping level via heat treatment in reducing environments. Underlying mechanisms of process induced defect generation and annihilation will be discussed.

[1] Elser et al. J. Phys. Chem. C, 116 (2012) 2896
[2] Siedl et al. Langmuir, 29 (2013) 6077
[3] Thomele et al. J. Phys. Chem. C, (2016) DOI 10.1021/acs.jpcc.5b10648

Importance of attractive pair interactions in reactions on metal oxide surfaces

Maxime Van den Bossche, Brita Abrahamsson and **Henrik Grönbeck**
Department of Physics, Chalmers University of Technology, Göteborg, Sweden
ghj@chalmers.se

Metal oxides is a wide class of materials that are used in numerous applications where heterogeneous catalysis is but one example. Oxides are used in this field as supports for the active phase, storage materials and catalysts. Given the wide range of applications, it is important to explore general phenomena of oxide chemistry. In this contribution, we have used the density functional theory to investigate the reaction of small molecules such as H_2, O_2, CH_4, H_2O and NO_2 with oxide surface including wide as well as narrow band-gap materials. In particular, the effect of adsorbate pairing is investigated with emphasis on the performance of different approximations to the exchange-correlation functional and the effect on reaction kinetics.

The calculations are performed within the plane-wave – pseudopotential implementation of the density functional theory and a standard gradient corrected exchange-correlation functional is compared with the hybrid functional HSE06. Reaction kinetics is studied using first-principles micro-kinetic modeling. Oxide mediated attractive interactions between surface species are found to be a general phenomenon where the strength of the interaction and energetic stabilization is highly dependent on the functional. One example that will be discussed is NO/NO_2 adsorption on $BaTiO_3$, TiO_2, and BaO [1,2]. Simultaneous NO and NO_2 adsorption is favoured thanks to the formation of $[NO\text{-}O_s]$ - $[NO_2]$ pairs, where O_s is a surface anion. The pair formation is mediated by a charge transfer of one electron from the O_s site to NO_2.

One catalytic reaction where we show that reaction kinetics is strongly dependent on attractive adsorbate interactions is complete methane oxidation over PdO(101). Strong paring effects are observed between, for example, adsorbed methyl and atomic hydrogen which has pronounced effects on the reaction kinetics [3]. It is only when such interactions are taken into account that the micro-kinetic model can describe experimental observations.

[1] B. Abrahamsson, H. Grönbeck, J. Phys. Chem. C, **119**, 18495, (2015).
[2] M. Van den Bossche, B. Abrahamsson, H. Grönbeck, In preparation.
[3] M. Van den Bossche, H. Grönbeck, J. Am. Chem. Soc. **137**, 37, (2015).

Engineering the Nanostructure of Brookite Titania to Tune and Improve Its Photocatalytic Activity

M. Cargnello,[a,b] T. Montini,[c] S.Y. Smolin,[d] J.B. Priebe,[e] J.J. Delgado Jaén,[f] V.V. T. Doan-Nguyen,[g] I.S. McKay,[b] J. A. Schwalbe,[b] M.-M. Pohl,[e] T.R. Gordon,[a] Y.Lu,[g] J.B. Baxter,[d] A. Brückner,[e] P. C.B. Murray[a,g1] and Fornasiero,[c]

[a] Department of Chemistry, University of Pennsylvania, 19104 Philadelphia, Pennsylvania, United States., [b] Department of Chemical Engineering and SUNCAT Center for Interface Science and Catalysis, Stanford University, Stanford, CA 94305 (USA), [c] Department of Chemical and Pharmaceutical Sciences, ICCOM-CNR, Consortium INSTM, University of Trieste, 34127 Trieste, Italy, [d] Department of Chemical and Biological Engineering, Drexel University, 19104 Philadelphia, Pennsylvania, United States, [e] Leibniz-Institut für Katalyse e.V. an der Universität Rostock, 18059 Rostock (Germany), [f] Departamento de Ciencia de los Materiales e Ingeniería Metalúrgica y Química Inorgánica, Facultad de Ciencias, Universidad de Cádiz, Campus Río San Pedro, 11510 Puerto Real, Cádiz, Spain, [g] Deparment of Materials Science and Engineering, University of Pennsylvania, 19104 Philadelphia, Pennsylvania, United States.

Photocatalytic pathways could prove crucial to the sustainable production of fuels and feedstocks required for a carbon-neutral society. However, electron-hole recombination is a critical problem that has so far limited the efficiency of the most promising photocatalytic materials. Here, we show the efficacy of anisotropy in improving charge separation and thereby boosting the activity of a TiO_2 photocatalytic system. Specifically, we show that H_2 production in uniform, 1-dimensional brookite nanorods is highly enhanced by engineering their length. By using complimentary characterization techniques to separately probe excited electron and holes, we link the high observed reaction rates to the anisotropic nanorod structure, which favors efficient carrier utilization. Quantum efficiency values for hydrogen production from ethanol, glycerol, and glucose as high as 65, 35, and 6%, respectively, demonstrate the promise and generality of this approach for improving the photoactivity of semiconducting nanostructures for a wide range of reacting systems.

The Fe:NiOOH Co-catalyst for O_2 Generation: Electronic Structure and Band Offset with the $BiVO_4$ Visible Light Active Photocatalyst

J. C. Conesa
Inst. de Catálisis y Petroleoquímica, CSIC, Madrid, Spain (*jcconesa@icp.csic.es*)

Introduction

Fe-doped NiOOH, a highly active co-catalyst for O_2 evolution in photoelectrochemical water splitting [1], is not well understood since its structure, with H-bond linked layers, is normally highly disordered. Here this system, Fe-doped or not, is modelled with a hybrid DFT method, and its band alignment with a typical visible light active photocatalyst, $BiVO_4$, is studied.

Methods

VASP code was used for hybrid DFT calculations using a method that gives accurate bandgaps [2] and where the Fock exchange fraction is related to the optical dielectric constant. Band offsets were computed with periodic slab models using electrostatic potential as basis to which band edge positions were referenced [3].

Results & discussion

Several of the NiOOH sheet stackings and proton arrangements evaluated yield similar lowest energies, justifying the typical high disorder of this material. Centrosymmetric $NiO_n(OH)_{6-n}$ arrangements seem preferred to the average $NiO_3(OH)_3$ environment. Even n=0 gives some of such lowest energies; in that case disproportionation into Ni^{4+} and Ni^{2+} occurs. Bandgaps typically above 0.8 eV are found, the gap edges being formed mainly by Ni (3d) orbitals.

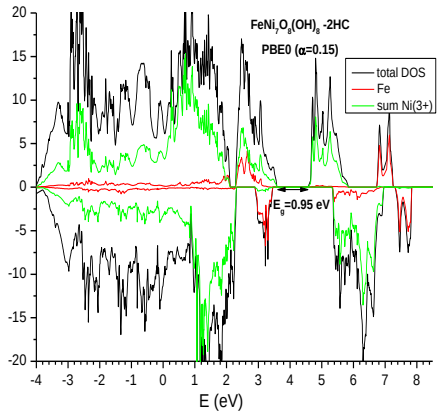

Fig.1 DOS curves for Fe-doped NiOOH, computed with hybrid DFT

Substitution of Ni by Fe leads to filled Fe(3d) levels near the valence band edge (Fig. 1). In some configurations a redox process $Ni^{3+} + Fe^{3+} \rightarrow Ni^{2+} + Fe^{4+}$ occurs, eventually with jump of protons from Fe to Ni coordination spheres. This justifies experimentally observed high conductivities and may be important for the photoelectrochemical O_2 formation mechanism from water.

The band alignment study (Fig. 2) indicates that holes generated at the $BiVO_4$ photocatalyst can be transferred easily to the NiOOH valence band, where they may oxidize surface OH to O_2.

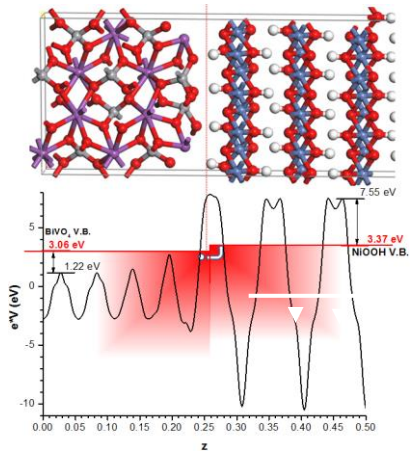

Fig. 2- Alignment of valence bands between $BiVO_4$ and NiOOH

References

[1] L. Trotochaud, S.L. Young, J.K. Ranney, S.W. Boettcher, *J. Am. Chem. Soc*. **136** (2014) 6744.
[2] E. Menéndez-Proupin, P. Palacios, P. Wahnón, J.C. Conesa, *Phys. Rev. B* **90** (2014) 045207 & references therein.
[3] J.C. Conesa, *J. Phys. Chem. C* **116** (2012) 18884.

Morphology, surface structure relaxation and defects of ZrO_2 nanocrystals explored by DFT modeling and HR TEM imaging.

Joanna Gryboś[1], Rafal Dunin – Borkowski[2], Zbigniew Sojka[1]
[1] Faculty of Chemistry, Jagiellonian University, Ingardena 3, 30-060 Krakow, Poland
[2] Ernst Ruska – Centre for Microscopy and Spectroscopy with Electrons, 52425 Jülich, Germany
e-mail: grybosjo@chemia.uj.edu.pl

New catalytic materials of enhanced activity and selectivity can be designed by exploiting the phenomenon that faceted polyhedral crystals expose well-defined crystallographic planes, depending on the synthesis method. Oxide nanocrystals due to their clear-cut structure and substantial surface area are excellent model systems for experimental and theoretical investigations into the surface related properties at atomic scale.

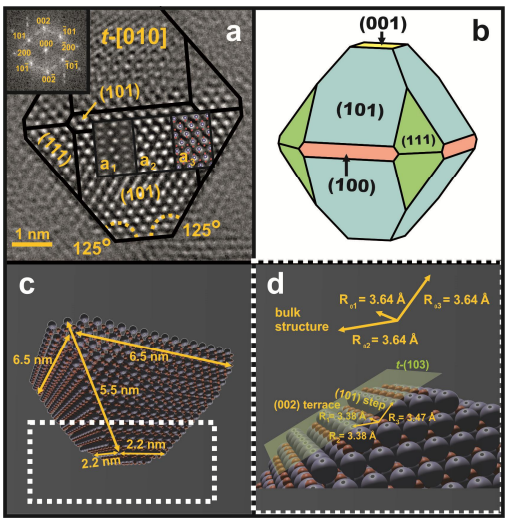

Fig. 1 Atomistic model of the *t*-ZrO_2 nanocrystal (c, d) retrieved from the HR TEM image (a) and the equilibrium Wulff shape (b) of the nanocrystal.

Within this contribution we present the analysis of the morphology, surface structure relaxation and defects of the euhedral *m*- and *t*-ZrO_2 nanocrystals obtained by combined HR TEM studies and periodic DFT/PW91 calculations. The equilibrium Wulff shape of the nanocrystals is constituted by the following facets: (-111) – 59%, (111) – 37%, (001) – 3%, (100) – 1% and (101) – 68%, (001) – 9%, (100) – 6%, (111) – 17%, for the monoclinic and tetragonal phase respectively. The equilibrium morphologies were further reshaped to match the corresponding shape projections on the HR TEM images. Such analysis of the morphology confirmed coexistence of the nanocrystals preserving the equilibrium shape and the nanocrystals with the shape modified due to the experimental conditions. More detailed morphology and structure analysis was performed for the aberration corrected HR TEM image of the *t*-ZrO_2 nanocrystal. High resolution image and the Wulff shape were used to construct the detailed atomistic model (Fig. 1) of the nanocrystal and to analyse the atomistic defects of its morphology (terraces, steps, etc.).

The exit wave function reconstructed from the focal series of the HR TEM images of the *m*-ZrO_2 nanocrystal oriented along the [110] axis was used for analysing the geometric relaxation process of the low index (100), (-111) and (111) facets of the *m*-ZrO_2 nanocrystal. The experimental results were compared with the results of the periodic DFT modelling. The phase image of the reconstructed exit-wave function contained the information about the positions of the zirconium columns. These data were further used for the statistical treatment: 2D Gaussian matching of the position of Zr^{4+} columns and retrieving the position of the corresponding planes by linear regression.

The analysis revealed that the (100) surface is the most rigid among the planes exposed by the investigated *m*-ZrO_2 nanocrystal. However, the retraction of the outermost planes (from 1 to 4) was observed (~12% and ~9%, respectively). In the case of the (-111) termination the retraction of the exposed plane (~20%) and the shortening of the distance between the successive planes (~12%) was observed. The similar oscillation behaviour was observed for the [111] direction. In this case, however, the relaxation effects are the strongest (the exposed plane is retracted by 50%), and produce a distinct pattern with the pitch of four planes: the first plane is retracted, the *d*-spacing between the second and the third plane is elongated and between the third and the fourth plane is shortened again. Such pattern corresponds well with the periodicity of the *m*-ZrO_2 structure along the [111] direction. The analysis revealed also that the extent of the relaxation effects (gauged by the amplitude of the *d*-spacing oscillations) is governed not only by the distance from the (111) surface, but also by the symmetry of the *m*-ZrO_2 structure (e.g., the relaxation of the 4th and 5th (28%) planes is stronger than the relaxation of the 2nd and 3rd (8%) or 3rd and 4th (2.%) planes).

Self-interaction corrected density functional calculations of localized electron hole formed by Li dopant in MgO

Marta Galynska, Elvar Jónsson, John J. Carey, Michael Nolan and Hannes Jónsson
Applied Physics Dpt., Aalto University, Espoo, Finland
Tyndall National Institute, Cork, Ireland
Faculty of Physical Sciences, University of Iceland, Reykjavík, Iceland
hj@hi.is

Abstract:
Theoretical calculations of the localized hole formed near a Li-atom dopant in MgO are presented. This system has become an important catalyst for methane activation and several experimental and theoretical studies have been carried out to determine the reaction mechanism. We find that commonly used DFT functionals such as generalized gradient approximation as well as commonly used hybrid functionals, such as HSE06, fail to stabilize the localized hole due to the self-interaction error inherent in Kohn-Sham density functionals. This is analogous to the well documented case of Al-atom dopant in SiO_2 [1,2,3]. We present results showing that variational, self-consistent calculations based on the Perdew-Zunger self-interaction correction [4] with complex optimal orbitals [5] can reproduce well experimental results showing localization of the hole on one O-atom as well as the energy of the defect state 2.1 eV above the valence band edge. Results obtained by varying the amount of exact exchange in the HSE functional form, and DFT+U will also be presented.

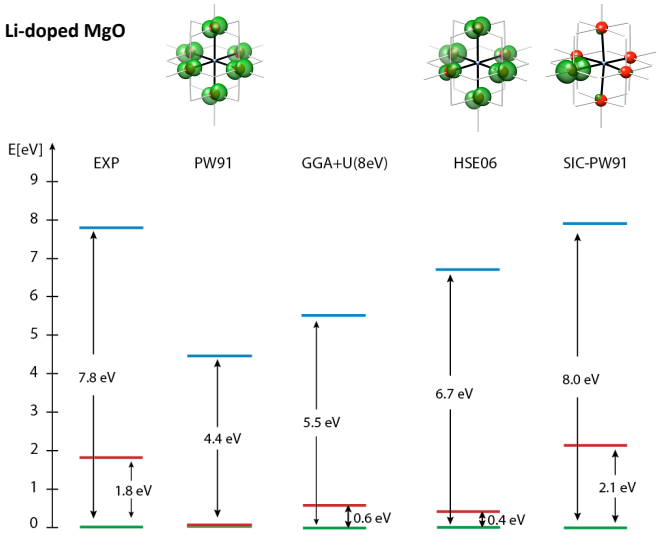

Above: Spin density (green), O-atoms (red). Below: Energy diagram comparing experimental estimates with GGA, HSE06, GGA+U and PZ-SIC calculated results.

References:

[1] G.Pacchioni, *J. Chem. Phys.***128**, 182505(2008); G.Pacchioni et al. *Phys. Rev. B***63**, 054102 (2000).
[2] J. Lægsgaard and K. Stokbro, Phys. Rev. Letters **86**, 2834 (2001).
[3] H. Gudmundsdóttir, E. Ö. Jónsson and H. Jónsson, New Journal of Physics **17**, 083006 (2015).
[4] J. P. Perdew and A. Zunger, *Phys. Rev. B* **23**, 5048 (1981).
[5] S. Klüpfel, P. J. Klüpfel and H. Jónsson, *Phys. Rev. A* 84, 050501 (2011); *J. Chem. Phys.* 137, 124102 (2012); S. Lehtola and H. Jónsson, *J. Chem. Theor. Comput.* 10, 5324 (2014).

Is nitrogen doping of tin oxide a way to create a p-type semiconducting oxide? A multi-technique investigation of N-SnO_2.

Stefano Livraghi[1], **Elio Giamello**[1] Stefano Agnoli[2], Gaetano Granozzi[2], Elisa Albanese[3], Gianfranco Pacchioni[3], Cristiana di Valentin[3].
[1]Dipartimento di Chimica, Università di Torino. Torino, Italy
[2]Dipartimento di Chimica, Università di Padova. Padova, Italy
[3]Dipartimento di Scienza dei Materiali, Università di Milano Bicocca, Milano, Italy

Tin oxide is a multifunctional semiconducting oxide which finds applications in several areas of modern material science including chemical sensors, ion batteries, solar cells. SnO_2 is also an extremely promising materials for next generation laser diodes and UV light emitting diodes. To prepare optoelectronic devices based on tin oxide, however, the fabrication of both n-type and p-type high quality thin films is mandatory. While in the former case the solution is straightforward as pristine tin oxide shows n-type conductivity (because of the presence of oxygen vacancies and excess electrons), the preparation of p-type SnO_2 remains a challenging task.
Since the pioneering work by Pantelides and coworkers [1] a possible issue to prepare p-type tin oxide was individuated in doping the oxide with nitrogen. This prediction, made on the basis of theoretical investigations and pointing to the formation of N-based acceptor levels (holes) in the band gap, has however found few experimental confirmations for several reasons including the difficulty in preparing thin films with appropriate concentration of the dopant.
We have recently developed a simple chemical synthesis of polycrystalline N-doped SnO_2 which allows the incorporation of appreciable amounts of nitrogen in the oxide. The present contribution reports s a wide multi-technique investigation (UV-Vis_NIR spectroscopy, XPS, UPS, EPR, DFT calculations) of this system allowing a new insight in its real electronic structure. Though the theoretical predictions on the role of N in determining the p-type character of the doped system are correct, new facts are put into evidence by the experiments. An important new evidence is that the presence of nitrogen accentuates the predisposition of the oxide to lose oxygen with consequent formation of excess electrons. This fact frustrates the role of low-lying N hole states resulting in the accentuation of the n-type character of the system.
A second evidence concerns the nature of the incorporated nitrogen that has been disclosed coupling Electron Paramagnetic Resonance and DFT modeling. Nitrogen takes the place of oxygen in the cassiterite structure forming both paramagnetic (N^{2-}) and diamagnetic (N^{3-}) nitride-type centers lying close to the valence band limit. The electron spin density id highly localized on the N center which is surrounded by three nearly equivalent tin ions [2]

[1] Y. Yan et al. Phys. Rev. Lett, **86**, 5723 (2001)
[2] S. Livragi et al. J. Phys. Chem.C **119**, 26895 (2015)

Metal-oxide interactions in Pt/CeO_2 catalysts and related phenomena

Y Lykhach[1], S. M. Kozlov[2], A. Bruix[2], G. N. Vayssilov[3], T. Skála[4], A. Tovt[4], N. Tsud[4], V. Stetsovych[4], F. Dvořák[4], V. Johánek[4], A. Neitzel[1], J. Mysliveček[4], I. Matolínová[4], M. Vorokhta[4], K. Ševčíková[4], R. Fiala[4], M. Václavů[4], K. C. Prince[5], S. Bruyère[6], V. Potin[6], A. Migani[2], T. Staudt[1], G. P. Petrova[3], F. Illas[2], S. Fabris[7], V. Matolín[4], K. M. Neyman[2], J. Libuda[1]

[1]Lehrstuhl für Physikalische Chemie II, FAU Erlangen-Nürnberg, 91058 Erlangen, Germany
[2]Departament de Química Física, QTCUB, Universitat de Barcelona, 08028 Barcelona, Spain
[3]Faculty of Chemistry, University of Sofia, 1126 Sofia, Bulgaria
[4]Charles University, Department of Surf. and Plasma Science, 18000 Prague, Czech Republic
[5]Sincrotrone Trieste, 34149 Basovizza, Trieste, Italy
[6]LICB, UMR 6303 CNRS-Université de Bourgogne, 21078 Dijon Cedex, France
[7]CNR-IOM DEMOCRITOS, IOM, CNR and SISSA, 34136, Trieste, Italy
yaroslava.lykhach@fau.de

Electronic interactions between metal nanoparticles and oxide supports control the functionality of nanomaterials. For three types of metal support interactions we demonstrate that these surprising phenomena can be understood at the atomic level [1-3]. Specifically, we consider (i) electronic metal support interactions, (ii) adsorbate spillover between the support and the supported particle and (iii) anchoring of metals on the oxide support (see Figure 1).
The electronic metal-support interaction associated with the charge transfer (CT) between supported nanoparticles and the oxide support (i) has never been quantified experimentally. In this work we measured this CT quantitatively on a well-defined platinum/ceria catalyst at particle sizes relevant for heterogeneous catalysis. The method is based on the estimation of the number of Ce^{3+} emerged due to the CT by means of resonant photoemission spectroscopy at utmost surface sensitivity. Combining this information with structural data from STM and XPS, we are able to "count" the number of electrons transferred per Pt particle and per Pt atom. The trends in the CT related to the particle size and density were rationalized by DF calculations. Using similar techniques we were able to explore the second interaction phenomenon (ii) associated with oxygen transfer from ceria to Pt, i.e. "reverse oxygen spillover". We show that the oxygen transfer requires the presence of nanostructured ceria in close contact with Pt and, thus, it is inherently a nanoscale effect. Finally, we employed strong metal-oxide interactions to anchor atomically dispersed Pt species on the surface of nanostructured CeO_2 film (iii). Using DF calculations and high-resolution transmission electron microscopy we identify a specific structural element on the support, a ceria "nanopocket", which binds Pt^{2+} so strongly that it withstands sintering and bulk diffusion.

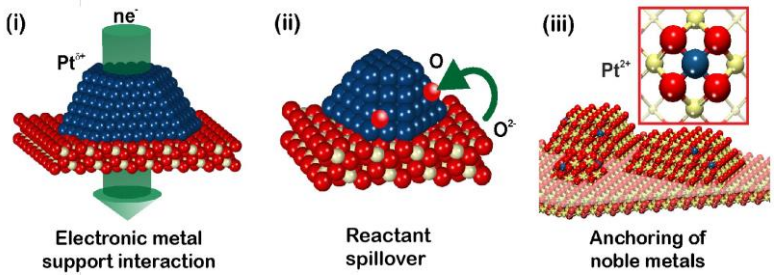

Figure 1. Three types of metal support interaction on Pt/CeO_2: (i) electronic metal support interaction; (ii) oxygen reverse spillover; (iii) anchoring of ionic Pt species on CeO_2.

[1] Y. Lykhach et al., Nat. Mater. **15**, 284 (2016).
[2] A. Bruix et al., Angew. Chem. Int. Ed. **53**, 10525 (2014).
[3] N. Vayssilov et al., Nat. Mater. **4**, 310 (2011).

Promoting catalytic activity by doping: a theoretical approach to ceria-gallia mixed materials.

M. Calatayud
Université Pierre et Marie Curie and CNRS, IUF, Paris, France

calatayu@lct.jussieu.fr

Abstract
The modification of ceria by doping with aliovalent cations like gallium is a promising way of tuning materials for key technological applications, in particular heterogeneous catalysis. Theoretical insights in the structural, electronic and surface properties of gallia-doped ceria systems will be presented and compared to recent experimental data [1-7] showing the actual interest of these materials for catalytic reactions such as WGS or selective hydrogenation reactions.

References
[1] J Vecchietti, et al. *Topics Catal.* **54** (2011) 201
[2] G Finos, S Collins, G Blanco, E del Rio, JM Cies, S Bernal, A Bonivardi. *Catal. Today* **180** (2012) 9
[3] S Collins, G Finos, R Alcantara, E del Rio, S Bernal, A Bonivardi. *Appl. Catal. A: General* **388** (2010) 202
[4] P Quaino, O Syzgantseva, L Siffert, F Tielens, C Minot, M Calatayud. *Chem. Phys. Lett.* **519-520** (2012) 69
[5] J. Vecchietti, S. Collins, W. Xu, L. Barrio, D. Stacchiola, M. Calatayud, F. Tielens, J. J. Delgado, A. Bonivardi J. Phys. Chem. C 117 (2013) 8822
[6] J. Vecchietti, A. Bonivardi, W. Xu, D. Stacchiola, J. J. Delgado, M. Calatayud, S. Collins ACS Catalysis **4**, (2014) 2088
[7] G. Vile, P. Dähler, J. Vecchietti, M. A. Baltanás, S. Collins, M. Calatayud, A. Bonivardi, J. Perez-Ramirez J. Catal. *Promoted ceria catalysts for alkyne semi-hydrogenation* 324 (2015) 69-78

Methane Dry Reforming studied on Inverse Pt/ZrO_2 Model Catalyst

Christoph Rameshan[1], Hao Li[1], Kresimir Anic[1], Verena Pramhaas[1], Matteo Roiaz[1], Raoul Blume[2], Michael Hävecker[2], Raffael Rameshan[2], Jan Knudsen[3], Axel Knop-Gericke[2], Günther Rupprechter[1]

1 Institute of Materials Chemistry, Technische Universität Wien, Vienna, Austria
2 Department of Inorganic Chemistry, Fritz-Haber-Institute of the Max Planck Society, Berlin, Germany
3 Department of Physics, MaxLab, Lund University, Lund, Sweden

Introduction

Being a carbon source, the utilization of carbon dioxide (CO_2) became attractive from both an environmental and economical perspective. However, CO_2 is a very stable molecule, thus to induce a reaction the activation of CO_2 by catalysts is required [1]. One way of activating CO_2 is dry reforming of methane (DRM), when CH_4 is reformed by CO_2 on Ni or Pt particles supported by zirconia (ZrO_2), $CH_4 + CO_2 \rightarrow 2\ CO + 2\ H_2$. During DRM, CO_2 is reduced to carbon monoxide (CO) via reaction precursors or intermediates, which can further oxidize the carbon formed via CH_4 dissociation. Such activation can occur on the ZrO_2 or on the interfacial sites [2]. As a support, technical ZrO_2 powder material can activate CO_2 by forming carbonate with basic anionic sites, or by forming formate with hydroxyl groups [2]. However, due to the possible different reaction pathways, microscopic mechanisms of the functions of ZrO_2 need to be further understood via a surface science approach. We therefore conducted a systematic study of the interaction between CO_2/CH_4 and ZrO_2 thin-films, inverse model systems with ZrO_2 particles supported on Pt single crystals and with the Pt support itself.

Experimental

ZrO_2 thin films were prepared on Pt_3Zr single crystals following the routine in ref. [3]. For the inverse system ZrO_2 particles were deposited on a Pt(111) single crystal by sputter deposition in $5x10^{-6}$ mbar O_2 at RT. Additionally, a clean Pt(111) single crystal was used as reference. After characterization DRM reactions were performed while measuring operando near atmospheric pressure XPS (NAP-XPS) in 0,2 mbar total pressure with the respective stoichiometric reaction mixture. The temperature was varied stepwise during reaction from RT to 600°C. Reaction educts and products were followed by mass spectrometry to obtain detailed structure activity correlations.

Results

Prior to actual dry reforming experiments the model catalyst surface was exposed only to either CH_4 or CO_2. Figure 1 shows Zr 3d (left) and C 1s (right) NAP-XPS

Identification of reaction intermediates for NO conversion on ceria

Mihail Y. Mihaylov,[1] Elena Z. Ivanova,[1] Hristiyan A. Aleksandrov,[2] Georgi N. Vayssilov,[2*] and Konstantin I. Hadjiivanov[1*]

[1] Institute of General and Inorganic Chemistry, Bulgarian Academy of Sciences, Sofia 1113, Bulgaria, e-mail: kih@svr.igic.bas.bg

[2] Faculty of Chemistry and Pharmacy, University of Sofia, 1126 Sofia, Bulgaria, e-mail: gnv@chem.uni-sofia.bg

Interaction of NO with ceria has been studied by density functional modeling and FTIR spectroscopy. The spectral studies using isotope labeled nitrogen monoxide revealed various bands corresponding to different types of nitrogen-containing species on ceria - nitrite species, hyponitrite species and nitrate species, as well as bands of new types of species on reduced ceria [1,2]. The conversion of the species with the temperature and the amount of NO was studied in order to estimate their stability. In order to clarify the structure of those species we modelled computationally such species on different positions on the facets and edges of a ceria nanoparticle. The calculations were performed with DFT+U approach using periodic code VASP. Ceria was modelled as $Ce_{21}O_{42}$ nanoparticle, used in previous studies. For all nitrogen-containing species the vibrational frequencies were calculated and compared to the experimentally measured value. This approach allowed assignment of the IR bands to specific structures of the surface species including different types of nitrates, nitrites, and hyponitrites, as well as new types of surface intermediates on reduced ceria - azides (N_3^-, 2044-2042 cm^{-1}) [1] and nitric oxide dianions (NO^{2-}, 1010-980 cm^{-1}) [2].

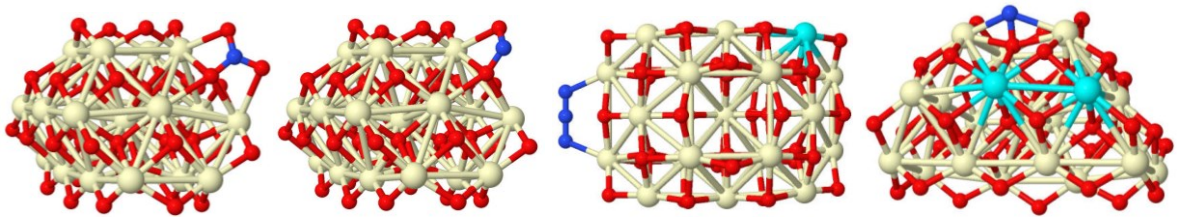

(a) (b) (c) (d)

Fig. 1. Selected model structures of nitrate (a), nitrite (b), azide (c), and NO dianion (d) species on ceria nanoparticle.

Acknowledgments: The authors are grateful for the support from the COST Action CM1104 and the Bulgarian Supercomputer Center for provided resources.

1. M.Y. Mihaylov, E.Z. Ivanova, H.A. Aleksandrov, P.St. Petkov, G.N. Vayssilov, K.I. Hadjiivanov, Chem. Commun. 51 (2015) 5668–5671.
2. M.Y. Mihaylov, E.Z. Ivanova, H.A. Aleksandrov, P.St. Petkov, G.N. Vayssilov, K.I. Hadjiivanov, Appl. Catal. B 176–177 (2015) 107-119.

H_2S decomposition on bare and doped (0001) surface of Cr_2O_3: Doping changes the thermodynamic selectivity towards H_2O formation

John Carey, Michael Nolan

Tyndall national institute, University College Cork, Lee Maltings, Dyke Parade, Cork, Ireland

John.carey@tyndall.ie, Michael.nolan@tyndall.ie

Abstract:

Hydrogen sulfide (H_2S) is found in industrial flue gas streams, and its formation is caused by the combustion of complex fuels with organo-sulfur containing species. If this gas is not removed, its release into the atmosphere can cause environmental damage by forming acid rain (sulphuric acids) with atmospheric water. This can lead to health issues among people in urban areas by forming sulfur containing smog, and can also damage buildings and waterways. The removal of H_2S is therefore important to control the release of this deadly gas and to prevent the associated issues with its presence in the atmosphere.

Density functional theory is used to investigate the decomposition of H_2S on the (0001) surface of Cr_2O_3. The rate limiting step for the reaction process is the subsequent breakdown of HS to S + 2H, where the S adsorbate is found to favour Cr-S bond formation and the H atoms form surface hydroxyls. The H species diffuse to form H_2 gas, with the S atom remaining on the surface as Cr-S, with no indication of the formation of surface sulfoxides (SO_x) species. This suggests that Cr_2S_3 may form on the catalyst bed that may be removed by mechanical scrubbing. For many oxidation reactions on industrial catalyst beds, improving the reducibility of the surface promotes oxygenated product formation by improving the mobility of the lattice oxygen. The introduction of non-native dopant species can achieve this; however the effect this has on the breakdown of H_2S is of particular interest. Introducing these dopants on the surface is found to reduce the barrier for H_2S decomposition, resulting in spontaneous breakdown to HS + H. The rate limiting step of HS to S + 2H on the bare surface is found to increase with a larger energy requirement on the doped surfaces. As the presence of dopants increases the reducibility of the surface, the formation of H_2O is favoured over H_2 evolution which leaves behind surface oxygen vacancies. S atoms on the surface can diffuse and occupy these vacancies which leads to surface contamination, and introduction of another H_2S species forms H_2S-S complexes. This indicates that S-S chains can occur on doped surfaces, blocking active surface sites and hindering further surface reactions, which is important for industrial catalyst design.

We acknowledge funding from the European Commission 7th Framework program: BIOGO project (grant no: 604296) www.biogo.eu

XPS Characterization of Active Interfacial Copper Species in Ceria-Supported Copper Catalysts for Preferential Oxidation of CO

M. Monte[1], D. Costa,[2] J.C. Conesa[1], G. Munuera[3], **A. Martínez-Arias**[1]
[1] ICP-CSIC, 28049 Madrid, Spain. E-mail: amartinez@icp.csic.es
[2] Institut de Recherches Chimie-Paris, ChimieParistech, 75005 Paris, France.
[3] Departamento de Química Inorgánica. Universidad de Sevilla, 41092 Spain.

Catalysts combining copper and cerium oxides are an economically interesting alternative to noble metal catalysts for various processes involved during production-purification of hydrogen generated from hydrocarbons or biomass. In particular, they show promising characteristics for the preferential oxidation of CO (CO-PROX) required to achieve CO concentrations below about 100 ppm in order to minimize the poisoning of fuel cell electrodes. Active sites for such processes have been proposed to be located at the interface between the two component oxides [1]. However, direct information about such interface is not generally available due to the important difficulties for the isolation and characterization of such nanosized, generally amorphous, region. We explore this issue by near-ambient XPS spectroscopy (and Cu L_3 XANES) complemented with theoretical DFT analysis. Samples of copper oxide (at various loadings) dispersed on two different ceria supports (in the form of nanospheres –NS- and nanocubes –NC-, respectively), involving well differentiated situations in terms of copper dispersion and interfacial morphology, are employed. Direct evidence of reduced interfacial copper entities as well as significant details of the electronic properties of the dispersed partially reduced copper oxide entities are provided upon detailed analysis of the results obtained.

Details of the preparation and multitechnique (XRD, HREM, Raman, XPS, EPR, H_2-TPR, S_{BET}) characterization of the catalysts as well as their catalytic activity for CO-PROX can be found elsewhere [2,3]. The catalysts subjected to CO up to 300 ^{o}C or under model CO-PROX mixture (for which a physical mixture of the catalyst with a conducting inert material is used as an strategy to avoid charging effects during recording of the spectra) are examined by XPS in gas environment (100 Pa) obtained at the BESSY II synchrotron. Fig. 1 provides an example of the results obtained. New XPS Cu $2p_{3/2}$ (at 930.1 eV) and Auger $L_3M_{45}M_{45}$ signals (at ca. 913 eV) specific of interfacial Cu^+ entities are identified on the basis of theoretical analysis and consideration of respective amount and characteristics of the interfacial sites present in each sample [2,3]. The evolution of the chemical state of the various copper species as a function of the reduction temperature under CO or during treatment under CO-PROX mixture will be shown and discussed in the context of the catalytic properties of this type of systems.

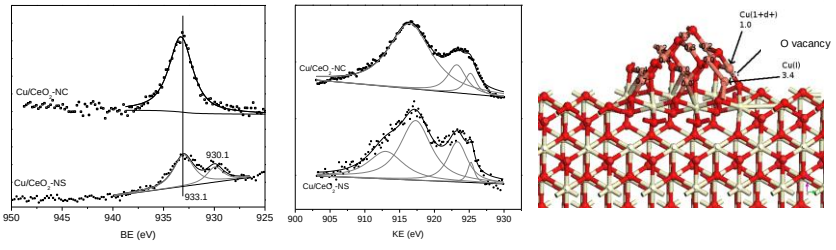

Figure 1. XPS Cu $2p_{3/2}$ (left) and Auger Cu $L_3M_{45}M_{45}$ (centre) spectra for the indicated samples under CO at 150 ^{o}C. Example of a model employed for the theroretical study with (111) exposed face of CeO_2 indicating the calculated core level shifts with respect to pure CuO (right).

[1] D. Gamarra et al. J. Am. Chem. Soc. **129**, 12064 (2007).
[2] D. Gamarra et al. Appl. Catal. B **130-131**, 224 (2013).
[3] M. Monte et al. Catal. Today **229**, 104 (2014).

spectra of ZrO_2/Pt in the reaction gases, switching from 0.1 mbar CH_4 (black) to 0.1 mbar CO_2 (red) at 400°C. In the Zr 3d region, a shift of 0.8 eV towards the lower binding energy side was observed, which can be induced by the change of oxidation state of Zr or the change of the ZrO_2 particle size. In the C 1s region the formed carbon species, that was present in CH_4 gas atmosphere, was completely removed by switching from CH_4 to CO_2 gas atmosphere. This is only possible when CO_2 reacts with the carbon on the surface to CO (CO_2 + C → 2 CO).
During methane dry reforming a shift of the Zr3d signal to 182.0 eV could be observed at temperatures above 400°C. At elevated reaction temperatures the surface stays free of carbon contaminations. Only below 150°C carbon and carbonate species could be observed. The Pt 4f signal stays at 71.0 eV during DRM.

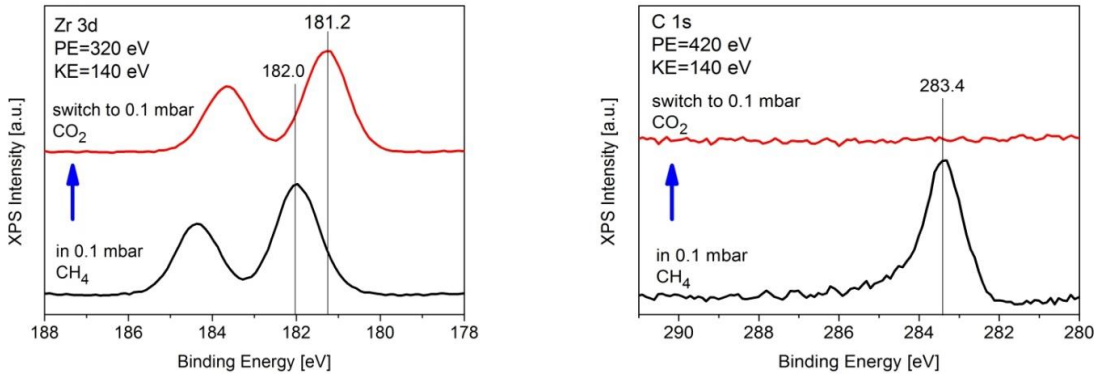

Figure 1: Zr 3d (left) and C 1s (right) in-situ XPS of ZrO_2/Pt in different reaction gases: switching from 0.1 mbar CH_4 (black) to 0.1 mbar CO_2 (red), spectra measured at 400°C in 0.1 mbar gas atmosphere.

Acknowledgement

The authors gratefully acknowledge BESSY II for providing beamtime at the ISISS beamline and BESSY staff for continuous support during beamtime. Also we want to thank MAXLAB for providing beamtime at the SPECIES beamline and for the support during beamtime. This work was supported by the Austrian Science Fund (FWF) through SFB “FOXSI” F4502 and through the European Community's Seventh Framework Programme (FP7/2007-2013) under grant agreement n.°312284

References

[1] N. Homs, J. Toyic, P. de la Piscina. *Acitivation of Carbon Dioxide. Chapter 1 Catalytic Processes for Activation of CO_2.*

[2] D. Pakhare, J. Spivey. *Chemical Society Reviews.* 43 (2014) 7813.

[3] H. Li, J.-I.J. Choi, W. Mayr-Schmoelzer, C. Weilach, C. Rameshan, F. Mittendorfer, J. Redinger, M. Schmid, G. Rupprechter, *Journal of Physical Chemistry C*. 119 (2015) 2462.

Poster presentation abstracts

A perfectly stoichiometric and flat CeO_2 (111) surface on a bulk-like ceria film

Clemens Barth,[1] Carine Laffon,[1] Reinhard Olbrich,[2] Alain Ranguis,[1] Ph. Parent[1] and M. Reichling[2]

1: Aix-Marseille University, CNRS, CINaM, Marseille, France
2: Fachbereich Physik, Universität Osnabrück, Barbarastr. 7, 49076 Osnabrück, Germany
Email: barth@cinam.univ-mrs.fr

To understand redox processes and related surface chemistry at the atomic scale, ultra-thin ceria films have been used as model systems in surface science and heterogeneous model catalysis. However, such studies are not suitable for understanding surface processes on thick ceria material as oxygen diffusion from the bulk may strongly influence the surface reaction state. Applications of ceria in catalysis, sensor technology as well as ceria catalysis model studies require materials with a well-defined surface and oxygen storage capacity.
Recently, a method for the growth of 150 to 250 nm thick fully oxidized ceria films on Si(111) by molecular beam epitaxy (MBE) has been proposed [1], and such films were suggested as an easy-to-prepare material to replace bulk ceria crystals that are most difficult to grow. In this contribution we show that a straightforward three step procedure in ultra-high vacuum (UHV) yields a fully oxidized CeO_2(111) surface with exceptionally wide, clean and atomically flat terraces [2]. This is substantiated by UHV noncontact atomic force microscopy (nc-AFM) and photoelectron spectroscopy (XPS) measurements. Our work demonstrates that even ceria surfaces that are exposed to the ambient air and transferred into the UHV can be cleaned and oxidized by this three step procedure.

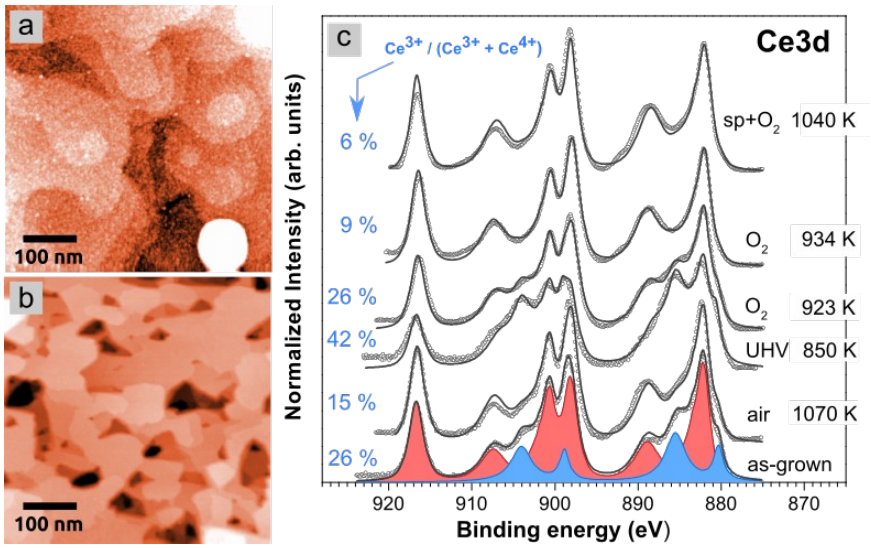

Figure: (a) The thick ceria film after annealing in air at 1100 K, imaged by nc-AFM afterwards in UHV. The granular structure on the terraces is due to hydroxyl and carbon species. (b) The same film after a sputtering with Ar^+ ions and annealing in O_2 at 1000 K inside the UHV chamber. (c) XPS Ce3d spectra taken after several preparation steps.

[1] G. Niu, M. H. Zoellner, T. Schroeder, A. Schaefer, J.-H. Jhang, V. Zielasek, M. Bäumer, H. Wilkens, J. Wollschläger, R. Olbrich, Ch. Lammers and M. Reichling, Phys. Chem. Chem. Phys. **17**, 4513 (2015).
[2] C. Barth, C. Laffon, R. Olbrich, A. Ranguis, Ph. Parent, M. Reichling, Sci. Rep. **6**, 21165, (2016).

Structure and composition of the MgAl2O4(110) surface

Igor Beinik[1], Thomas N. Jensen[1], Sergey Volkov[2], Andreas Stierle[2], Jeppe V. Lauritsen[1]

[1]Interdisciplinary Nanoscience Center (iNANO), Aarhus University, Denmark

[2]Fachbereich Physik, Universität Hamburg, Germany
jvang@inano.au.dk

Spinel (MgAl2O4) is an industrially important material that frequently plays a role of a support for metal nanoparticles in e.g. Ni/MgAl2O4 catalysts for steam reforming [1]. It is also the most abundant mineral in the group of the so-called normal spinels. Thus, it is often used as a prototypical material in model surface science studies [2,3]. Spinel is a wide band gap dielectric, which makes it difficult to investigate using the classical conductive probe surface science tools such as LEED or STM. Therefore, the exact structure of the spinel facets remains unfortunately largely unknown. This concerns in particular the structure of the MgAl2O4 surface that is expected to be a suitable substrate for the growth of s-Al2O3(110) films with g-Al2O3-like properties.

In the present study we investigate the structure of the MgAl2O4(110) polar facet and propose two possible models that are supported by our NC-AFM and SXRD experimental results. To investigate the structure of the MgAl2O4(110) surface, NC-AFM images have been recorded after cycles of sputtering and annealing in 1x10e-7 mbar of O2 at temperatures ranging from 800 to 1150 ˚C. Figure 1 demonstrates the MgAl2O4(110) surface after annealing at 1050 ˚C. The surface exposes large terraces with a width of approximately 100~nm and the reconstructed surface consists of parallel rows which are well visible in the NC-AFM image. The periodicity of the rows corresponds to a (3 × x) reconstructed surface. The surface reconstruction is possibly driven by the need to suppress the diverging electrostatic potential present on the bulk-terminated surfaces, and with this in mind the two structural models will be discussed.

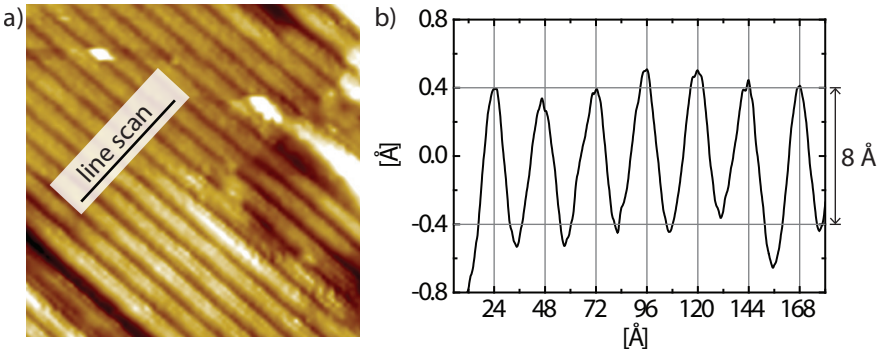

Figure 1. 15 nm × 15 nm NC-AFM image recorded after several cycles of sputtering and annealing at a temperature of 1050 ˚C revealing the row reconstruction.

[1] Sehested, J. Catalysis Today **111**, 103–110 (2006).
[2] Rasmussen, M. K. et al. Phys. Rev. Lett. **107**, 036102 (2011).
[3] Jensen, T. N. et al. Phys. Rev. Lett. **113**, 106103 (2014).

STM investigation on the surface structures of CeO_2 ultra-thin film

Hyun Jin Yang, Chi Ming Yim, Chi Lun Pang and Geoff Thornton

Department of Chemistry and London Centre for Nanotechnology, University College London, 20 Gordon Str., London WC1H 0AJ, UK

Among all metal oxide materials, cerium oxide is an emerging topic of interest in the field of heterogeneous catalysis for its role as a non-spectator support and active co-catalyst in the water-gas shift reaction. To understand the origin of such properties, atomic defects have been studied using scanning probe techniques on both single crystal and ultra-thin films on metals, successfully visualising the 1x1 surface structure of ceria. Here, we present a previously-unreported (√3x√3)R30° surface phase of ceria found on an ultra-thin film supported on Pt(111) identified using scanning tunnelling microscopy at 78 K (see Fig. 1) and low energy electron diffraction. Both the 1x1 and (√3x√3)R30° phases have hexagonal lattices with vacancies, but show different electronic structures as probed with empty-state imaging. We believe that the (√3x√3)R30° phase is restricted to the top layer(s), since the structure can be removed by exposure to electrons (~60-110 eV). The (√3x√3)R30° phase tends to dominate when a lower oxygen pressure is used during the oxidation (10^{-7} compared to 10^{-6} mbar) and for the same amount of Ce deposited, (√3x√3)R30° islands tend to be thicker.

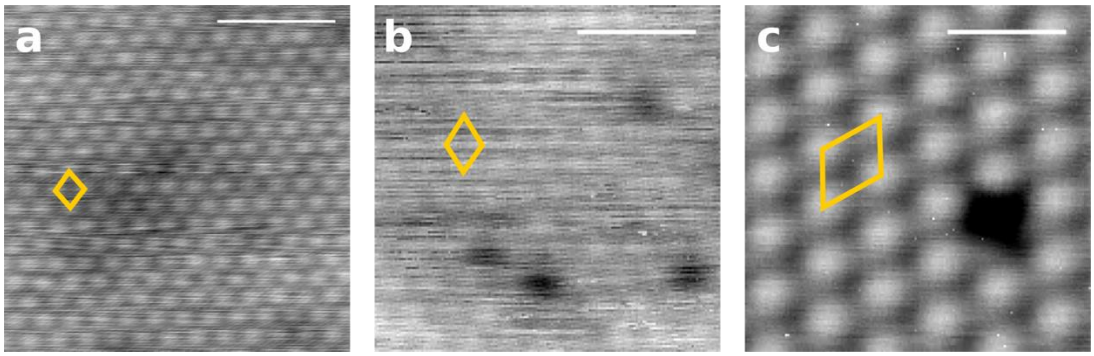

Figure 1 STM images of (a) clean Pt(111) substrate, (b) 1x1 surface of CeO_2/Pt(111), and (c) (√3x√3)R30° phase of CeO_2/Pt(111). All images are 3 nm x 3 nm.

Charge Transport at CeO_2 Interfaces: Electron Hopping and Oxygen Ion Migration

Javier Fdez. Sanz, José J. Plata and Antonio M. Márquez

Departamento de Química Física, Facultad de Química, Universidad de Sevilla, E-41012, Seville, Spain

The outstanding catalytic properties of cerium oxides, and, consequently, the broad use in heterogeneous catalysis rely on the easy $Ce^{3+} \leftrightarrow Ce^{4+}$ redox conversion, which involves not only electron hopping but also oxide ions diffusion across the network. In this work, electron polaron hopping is described according to the two-state model of Marcus as formulated for polaronic systems. The most important parameters required to describe the process, i.e. activation energy ΔG, reorganization energy λ, and the electronic coupling matrix element $V_{AB,}$ have been computed for bulk CeO_2 and (111), (100), and (110) surfaces using both periodic and cluster models.

Ion migration and charge redistribution in reduced CeO_2 (111) surfaces have been then analyzed by means of DFT+U calculations. A lowering in the activation energy for polaron hopping is observed, while the presence of Ce^{3+} modifies and increases the barrier for oxygen migration. These results suggest a correlation between electron mobility and oxygen ion transport.

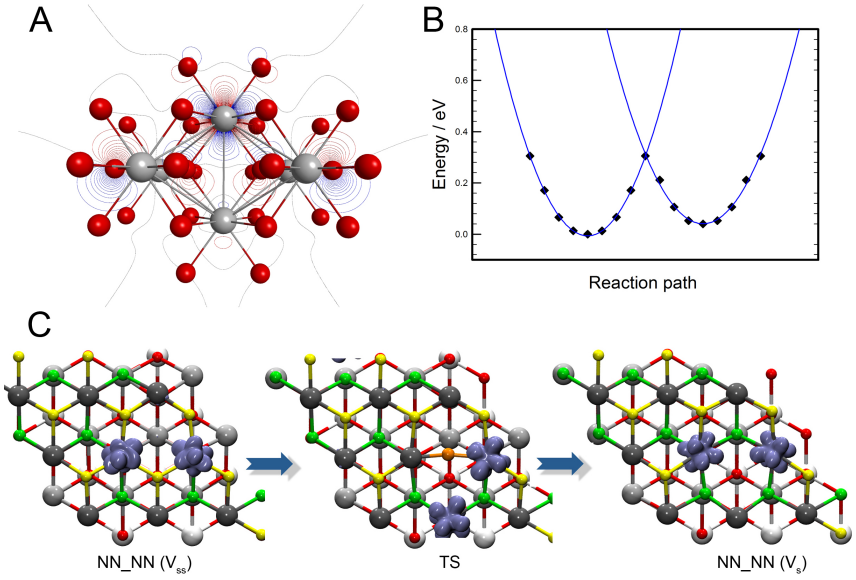

Figure. A) Localized electron density. B) Polaron hopping in presence of a vacancy. C) Reaction path of the (FM) spin density for oxygen migration from in defective CeO_2 (111) surface.

ReferenceS:

Plata, J.J.; Márquez, A.; Sanz J.F. *J. Phys. Chem. C* **2013**, *117*, 14502-14509; *J. Phys. Chem. C* **2013**, *117*, 25497−25503; *Chem. Mat.* **2014**, *26*, 3385–3390.

Photoactivity of Molecule-TiO_2 Clusters with Time-Dependent Density-Functional Theory

E. Luppi[1,2], I. Urdaneta[1,2], M. Calatayud[1,2,3*]

[1] Sorbonne Universités, UPMC Univ Paris 06, UMR 7616, Laboratoire de Chimie Théorique, F-75005, Paris, France
[2] CNRS, UMR 7616, Laboratoire de Chimie Théorique, F-75005, Paris, France
[3] Institut Universitaire de France, France
*e-mail: calatayu@lct.jussieu.fr

Abstract

The interaction of molecules with titanium oxide substrates may lead to substantial modifications of their optical properties, in particular a redshift of the absorption spectrum compared to bare titania. In the present paper we discuss the role of the interface between two molecules, catechol and dopamine, with gas-phase $(TiO_2)_N$ clusters (N=2,4,6). We studied, for the interface, the bidentate modes (the molecule bonded to two Ti sites via its two oxygen sites), which was the most energetically favorable, followed by the chelated modes (the molecule bonded to one Ti site via its two oxygen sites), and the monodentate mode (the molecule bonded to one Ti site via one oxygen site). The absorption spectra were calculated with Time-Dependent Functional-Theory with CAM-B3LYP for the description of charge-transfer excitations. We observe a red shift of the molecule/cluster systems with respect to the molecules and clusters alone. Moreover, the chelated mode was found to present bands at lower energies than the other modes, making it the most interesting mode to tune the absorption edge of these systems.

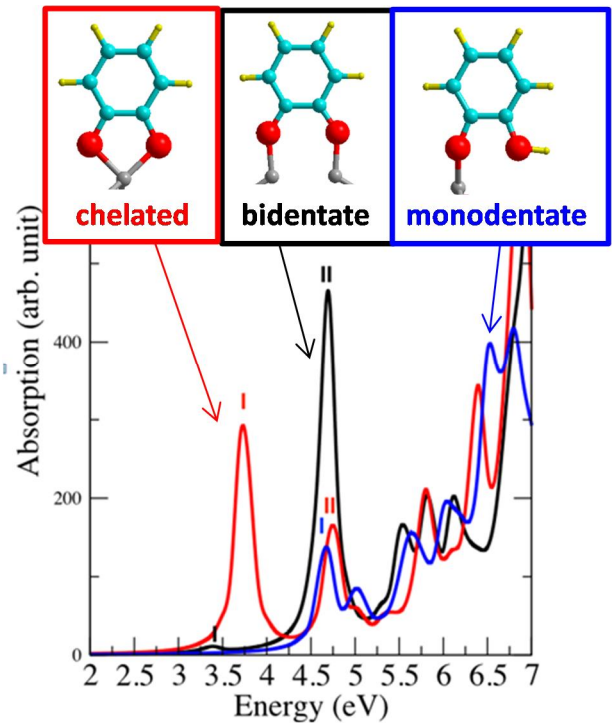

References

1. Luppi, E.; Urdaneta, I.; Calatayud, M.; Photoactivity of Molecule-TiO_2 Clusters with Time-Dependent Density-Functional Theory submitted
2. Urdaneta, I.; Keller, A.; Atabek, O.; Palma, J. L.; Finkelstein-Shapiro, D.; Tarakeshwar, P.; Mujica, V.; Calatayud, M. Dopamine Adsorption on TiO_2 Anatase Surfaces *J. Phys. Chem. C* **2014**, *118*, 20688-20693.
3. Urdaneta, I.; Pilme, J.; Keller, A.; Atabek, O.; Tarakeshwar, P.; Mujica, V.; Calatayud, M. Probing Raman Enhancement in a Dopamine-Ti_2O_4 Hybrid Using Stretched Molecular Geometries *J. Phys. Chem. A* **2014**, *118*, 1196-1202

Enhancing activity of the heterogeneous catalyst - multiple concepts with microscopic S/TEM insight

Paulina Indyka, Joanna Gryboś, Sylwia Gudyka, Andrzej Kotarba, Zbigniew Sojka
Faculty of Chemistry, Jagiellonian University, Ingardena 3, 30-060 Krakow, Poland
e-mail: paulina.indyka@uj.edu.pl

Recently, much effort was dedicated towards rational optimization of the catalyst loading, doping and spreading on supported systems with the aim of increasing the turnover rate/activity. The microscopic observations made in conjunction with the exploration of the catalysts properties can be used to understand their reactivity.

In the present study we examine the role of the structural-dependent reactivity of $ZnCo_2O_4$ nanoparticles in N_2O decomposition using combination of Scanning and Transmission Electron Microscopy (S/TEM) techniques (FEI Tecnai Osiris, 200kV). In particular glycerol-assisted dispersion of the spinel active phase at the nanoscale and the effect of the alumina polymorph on the reactivity of the alumina supported cobalt spinel catalyst were investigated in detail.

The size and the shape of the spinel nanocrystals dispersed on the Al_2O_3 support were retrieved by mean of High Angle Annular Dark Field imaging (HAADF) and image processing techniques involving gradient analysis and the edge detection. By combining the prior knowledge about the calculated Wulff shape of the spinel nanocrystals together with the information of the edge pattern and the thickness variations along the nanocrystal projection, it was possible to estimate the shape of the investigated nanocrystals by using a reverse Wulff construction. Owing to the constancy of the interfacial angles (Steno law), the inclinations of the malformed planes are the same as for the perfect crystals, so they were used for the assignment of the faceting. The analysis revealed prevailing abundance of the (111) and lowered abundance of the (100) facets ((111) - 73% and (100) - 27%, Fig b).

The shape retrieving method was also used for calculating the energy of adhesion of the spinel nanocrystals to alumina support (Wulff – Kaischew construction). The adhesion energy was equal to 0.61 $J \cdot m^{-2}$ and 0.27 $J \cdot m^{-2}$, when the nanocrystal adhered to the support surface via (100) and (111) facet, respectively. The intensity distribution of the Moiré pattern (Fig d) expressed in terms of the convolution of the transmission functions of the two crystals was used to determine a mutual orientation relationship of the spinel nanocrystals and the support.

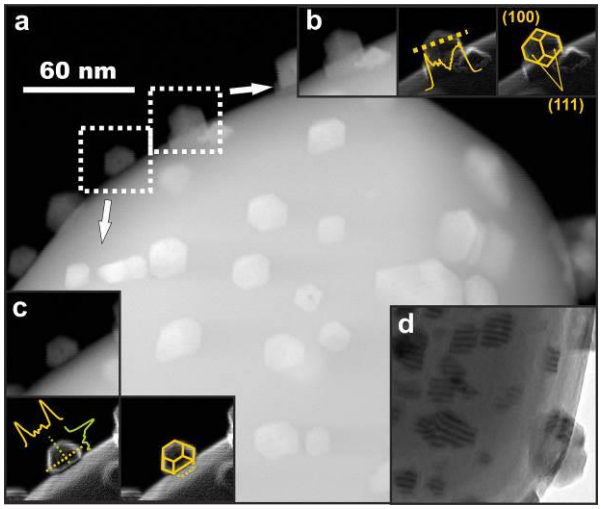

Fig. 1: (a) STEM-HAADF image of $ZnCo_2O_4$ nanocrystals dispersed on the Al_2O_3 support, (b-c) faceting determination showing general spinel nanocrystals morphology, (d) TEM image revealing Moiré pattern.

This work was supported by the National Centre for Research and Development through the research grant PBS-INNOKAT contract no. PBS2/A5/38/2013

Surface oxidation of the nanolayer CrN/(Cr,V)N coatings induced by nanosecond laser pulses

S. Petrović[1], B. Gaković[1], P.Panjan[2], J. Kovač,[2] V. Lazović[3], C. Ristoscu[4], I. Mihailescu[4]

(1) *Vinča Instiute of Nuclear Scinece, University of Belgrade, P.O.Box 522,11001 Belgrade, Serbia*

(2) *Jožef Stefan Institute, Jamova 39, 1000 Ljubljana, Slovenia*

(3) Institute of Physics Belgrade, University of Belgrade, Pregrevica 118, 11080 Belgrade, Serbia

(4) National Institute for Lasers, Plasma and Radiation Physics, POB MG-36, Magurele, Ilfov, Romania

Contact: S. Petrović (spetro@ivinca.rs)

Abstract. The oxidation behaviour and morphological modification of the nanolayer CrN/(Cr,V)N coatings were studied after laser processing in air ambient. Addition of vanadium to form CrVN coating has improved the tribological and lubricious properties with more or less the same hardness and toughness of CrN coating [1]. Usually, surface layers of contaminations or oxides effectively reduce the friction of ceramics. Laser processing without material removed is important for alloying, cladding, hardening etc., in which the purpose is to improve the surface properties by changing its chemical composition or/and structure [2,3]. The laser-induced surface oxidation depends on the material characteristics (composition, microstructure, surface state, and absorptivity), laser parameters (fluence, wavelength, pulse duration) and ambient conditions [4]. The surface structure, mechanical, corrosion and optical properties after laser processing of the material surfaces can be changed by formation of relatively thin oxide films.

The evolution of the surface composition and microstructure after laser irradiation at different number of accumulated pulses was systematically analysed depending on initial content of vanadium in the as-deposited coatings. Irradiation of CrN/(Cr,V)N coatings with different content of vanadium was carried out at fluence of 0.17 J cm^{-2} with different number of accumulated nanosecond pulses. The concentrations of metallic components were fairly homogeneous distributed through the sample, only at surface and in sub-surface region. The contents of Cr and V are reduced due to the surface oxidation in this region. The composition and thickness of formed oxide mixture Cr_2O_3 and V_2O_5 are conditioned by the number of applied laser pulses and the initial vanadium content. The oxidation process was prolonged in the depth of coating, where the nitrogen atoms are replaced by oxygen atoms. Oxygen atoms have penetrated the coating, wherein the concentration of oxygen on the surface of about 30% and gradually reduces to a different depth in the samples depending on vanadium content. Higher penetration depth is achieved for lower initial vanadium concentration in as-deposited coatings. The asymmetric progress of surface morphology involved the formation grain structures on peripheries and the appearance of cracks in form of the mosaic structure created of irregular closed shapes in the centre of the irradiated area. The special morphology of the laser-induced formation of mixture of Cr_2O_3 and V_2O_5 in the form of an ultra-thin oxide layer can improve coating's characteristics for their functional applications, especially as self-lubrication surfaces with the low wear rate.

REFERENCES

[1] L. Rapoport, A. Moshkovich, V. Perfilyev, I. Lapskera, et al., Surf. Coat. Technol. 238 (2014) 207–215.
[2] D. Baurle, *Laser Processing and Chemistry*, in Springer Verlag, Berlin (2000).
[3] G. Dumitru, B. Luscher, M. Krack, et al., Int. J. Refract. Met. Hard Mater. 23 (2005) 278- 286
[4] S. Petrović, D. Peruško, J. Kovač, Z. Siketić, et al, Mater. Chem. Phys.143 (2014) 530-535.

Kinetic Monte Carlo simulation of *de*N_2O on (001)Co_3O_4 – disentanglement of topological effects

Witold Piskorz, Filip Zasada, Zbigniew Sojka

Faculty of Chemistry, Jagiellonian University, Ingardena 3, 30-060 Kraków, Poland

The kMC simulation was carried out for the elementary step network of catalytic decomposition of N_2O over the (001) face of Co_3O_4, aiming at the disentanglement of the topological effects. The simulation was performed with selective exclusion (blocking) of the particular diffusion or recombination channels. The activation free energies were calculated based on the DFT GGA-PW91 level of theory, and the harmonic vibrational analysis. The NN–O bond cleavage products, O_{ads}, subsequently undergo two mechanisms of two-centre recombination towards $O_{2(gas)}$, either the Hinshelwood-Langmuir or the Elay-Rideal mechanisms. The O_{ads} can also be formed by readsorption of $O_{2(gas)}$. All conceivable modes of O_{ads} diffusion were calculated and implemented in kMC for all pairs of adjacent surface ions (satisfying periodic boundary conditions) or for all single ions, for two-centre and one-centre reaction steps, respectively.

The residual entropy in the adsorbed state in the OAT step was assessed from the fitting of the pre-exponential factor of $\Delta G^{\#}$ calculated from the kMC modelling to the experimental of the conversion (X) *vs*. temperature (T) relationship, holding for the CSR reactor: $X(T) = \frac{\tau e^{-\Delta G^{\#}}/RT}{1+\tau e^{-\Delta G^{\#}}/RT}$, where τ is the contact time. For the diffusion steps the entropic part is relatively low and is compensated to high extent. The $X(T)$ relationship was simulated for the blocking of the following sites (see Figure below): none (red line), Co^{Oct} (green), Co^{Tetr} (magenta), all O (orange), and for blocking of the following diffusion channels: O-Co^{Oct} (pale blue), and O-O (line very close to O-Co^{Oct}, therefore not shown). The experimental results are also shown (blue).

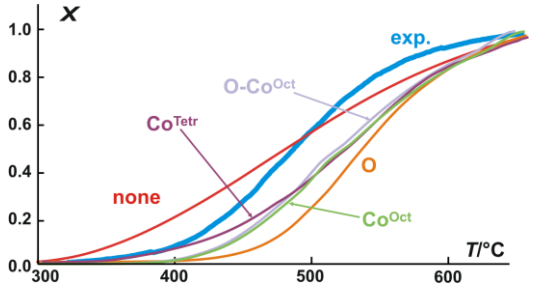

The T_{start} is in good agreement with experimental data when Co^{Tetr} are blocked (reproducing experimental conclusion[1]), whereas it is shifted too high when other sites/channels are blocked.

This work was supported by Polish National Science Center Grant DEC-2011/03/B/ST5/01564.

[1] F. Zasada, W. Piskorz, Z. Sojka *J. Phys. Chem. C* 2015, **119**, 19180−19191

Synthesis, characterization and catalytic application of KIT-5 mesoporous silica containing sulfur

A. Wawrzyńczak, S. Jarmolińska, K. Piasecka, I. Nowak
Adam Mickiewicz University in Poznań, Faculty of Chemistry, Poznań, Poland
agata.wawrzynczak@amu.edu.pl

Discovery of ordered mesoporous materials in early 1990's has initiated many studies on synthesis procedures for new materials with customizable structural and textural parameters, as well as potential applications in nanoscience, drug delivery, sensing, separation, adsorption and catalysis [e.g. 1]. Mesoporous materials, especially those of silica type, possess easily modifiable external and internal surfaces, where different functional groups can be introduced. Typically, functionalization of mesoporous silicas is accomplished by using different organosilanes. The resulting materials possess functional groups on the external, internal or both surfaces, depending on the applied synthesis procedure [2]. Thus, the aim of the presented studies was to develop the relatively straightforward synthesis procedures for obtaining silica-based acid catalysts with 3D interconnected cage-like mesoporous structure of KIT-5 type and modified with functional groups containing sulfur.

KIT-5 materials were synthesized in aqueous solution, using triblock co-polymer Pluronic F127 as a structure directing agent ($EO_{106}PO_{70}EO_{106}$), tetraethyl orthosilicate (TEOS) as silica precursor and 3-mercaptopropyltrimethoxysilane (MPTMS) as a source of functional groups. Two synthetic strategies were employed in order to achieve functionalization of mesoporous silica surface: (1) one-pot synthesis (co-condensation) and (2) post-synthesis modification (grafting). The molar ratio between TEOS and MPTMS was set to 0.0005 or 0.0010.

All synthesized samples were characterized by low-angle XRD and TEM method in order to confirm the structure typical for KIT-5 materials. Textural parameters were calculated on the basis of low-temperature N_2 sorption measurements, whereas the amount of sulfur introduced into the siliceous matrix was calculated by virtue of elemental analysis. TG and FT-IR measurements were applied in order to confirm the successful template removal. Catalytic activity tests were performed using Friedel-Crafts alkylation of anisole with benzyl alcohol.

All applied synthesis procedures led to silicas with 3D interconnected cage-like mesoporous structures, what was confirmed on the basis of low-angle XRD and TEM measurements. The resulting XRD patterns revealed reflexes typical for KIT-5 structure. According to new IUPAC recommendations [3], nitrogen sorption isotherms obtained for mesoporous KIT-5 silicas may be ascribed to a type IV(a) with a quite sharp capillary condensation step at higher p/p_0 values. A broad H2(a) hysteresis loops were also visible, indicating large uniformity of cage-like pores. Results of elemental analysis clearly point out that the employed synthesis methods allow to incorporate organic groups containing sulfur into KIT-5 materials. Preliminary catalytic test confirmed their potential as solid acid catalysts in the Friedel-Crafts alkylation.

National Science Centre is kindly acknowledged for financial support (project no: 2013/10/M/ST5/00652).

[1] E.M. Usai, M.F. Sini, D. Meloni, V. Solinas, A. Salis, Micropor. Mesopor. Mater. **179**, 54 (2013).
[2] T. Asefa, Z. Tao, Can. J. Chem. **90**, 1015 (2012).
[3] M. Thommes, K. Kaneko, A.V. Neimark, J.P. Olivier, F. Rodriguez-Reinoso, J. Rouquerol, K.S.W. Sing, Pure Appl. Chem. **87**, 1051 (2015).

Application of mesoporous materials in hydrogenation of citral using high-pressure reactor

Agnieszka Feliczak-Guzik, Paulina Dębek, Izabela Nowak
Adam Mickiewicz University, Poznań, PL61-614, Poland; agaguzik@o2.pl; nowakiza@amu.edu.pl

Citral, with a smell like lemon peel, occurs as trans and cis isomers (or as geranial (citral a) and neral (citral b), respectively). From this compound it is possible to obtain a large number of various ingredients. The hydrogenation of citral has been extensively studied due to the great interest for the reaction products. All derivatives of citral obtained in hydrogenation reactions are widely used in cosmetics, perfumery and as aroma compounds [1].

This work focuses on hydrogenation of citral using mesoporous material of SBA-12-type containing ruthenium. The main synthesis procedure of SBA-12-type mesoporous materials is based on the addition of the silicon alkoxide (TEOS) (Fluka, 99.9%) to a solution of commercially available non-ionic surfactant BRIJ-76, distilled water and hydrochloric acid (0.1 M, Fluka). The Ru-based SBA-12 catalysts with different Ru content (1-3 wt%) were prepared by the incipient wetness impregnation with ruthenium(III) chloride as the ruthenium precursor and SBA-12 as the support. After impregnation, the samples were dried at 338K for 1-24h and reduced in hydrogen at 523 K for 3.5 h (heating rate = 3º/min).

All of obtained materials were characterized by: X-ray diffraction (XRD), transition electron microscopy (TEM), scanning electron microscopy (SEM), N_2 physisorption, FTIR and UV-Vis spectroscopies. Hydrogenation of citral was carried out in the high-pressure reactor using acetonitrile and ethanol as solvents. The products of the reaction were identified by GC-Mass spectrometry (Varian 4000 mass spectrometer connected with a 30 × 0.25 mm VF-5MS capillary column) and quantitatively analyzed using a Varian GC 3900 gas chromatograph (GC).

Basing on XRD, TEM and N_2 sorption analyses, it can be determined that mesoporous materials containing ruthenium SBA-12-type were synthesized. These materials possessed BET surface areas of 690-1040 m^2/g, pore sizes of 4-6 nm width and pore volumes as large as 1.2 cm^3/g. Textural parameters showed that most of the synthesized materials have a relatively high internal surface area, whereas low external ones. The structural integrity with 3-D hexagonal packing was retained even after altering the concentration Ru from 1 to 3 wt%. Low-angle XRD profiles showed an intense (002) reflection along with resolved (112) and (300) reflections in the 2θ range of 1.5–3.5º.

In the hydrogenation of citral reaction, the influence of pressure, time of reaction, temperature, composition and structural/textural properties of the obtained materials on the conversion of citral to the desired products was determined. It was observed that the conversion of citral increased with temperature and pressure reaction alterations. The hydrogenation selectivity was depended on reaction temperature, i.e., at high temperature the selective hydrogenation of the C=O group was much more difficult in the presence of C=C bond. The product of the first hydrogenation step, citronellal, was isomerized to isopulegol on the acid sites and further hydrogenated to menthol at longer reaction times. The increase in the polarity of the solvent increases the catalytic activity, however the reaction pathway was modified. The hydrogenation of citral over these prepared Ru catalysts indicated that they can be also used as the catalysts for other hydrogenation reactions.

To summarize up – mesoporous materials SBA-12 type containing ruthenium have been synthesized. All of the obtained mesoporous molecular sieves were active in hydrogenation of citral.

References

[1] A. Corma, S. Iborra, A. Velty, *Chem Rev.*, **107**, 2411-2502 (**2007**).

Modeling interactions of transition metals with ceria nanoparticles: applications for fuel cell technologies

Alberto Figueroba[1], Konstantin M. Neyman[1,2]

[1] Dep. de Química Física and IQTCUB, Universitat de Barcelona, 08028 Barcelona, Spain
[2] Institució Catalana de Recerca i Estudis Avançats (ICREA), 08010 Barcelona, Spain
e-mail: afigue89@gmail.com

We present our density functional modeling results of the interactions of transition metals with ceria nanoparticles, which pave new ways for the design of more efficient catalytic materials for their application in fuel cell technologies. These studies have been motivated by discussions with several participants of the COST Action and performed jointly with the corresponding experimental and theoretical teams.
The topics discussed in the presentation are:

- Stability of atomically dispersed transition metal species at surfaces of nanostructured ceria for the development of single-atom catalysts [1].
- Reactivity of atomically dispersed Pt^{2+} species in fuel cell catalysts towards H_2 [2,3].
- Stability and reactivity of Pd-, Ni- and Pt-CeO_2 based catalysts [4].

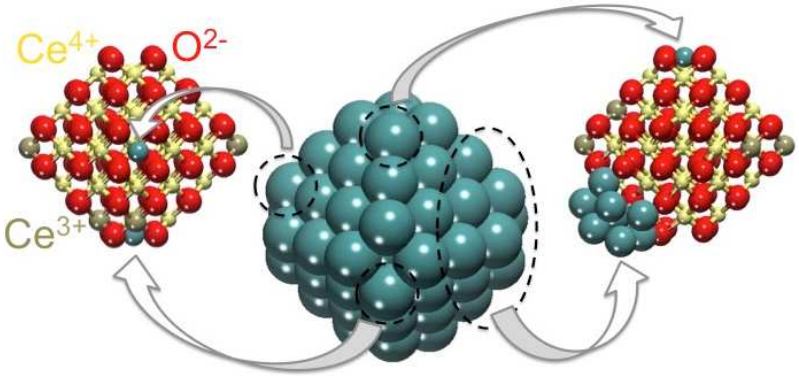

Figure. Surface oxygen sites of nanoparticulate ceria are able to anchor atoms of twelve different transition metals (turquois balls) strong enough to prevent their sintering [1].

References:

[1] A. Figueroba, G. Kovács, A. Bruix, K.M. Neyman, Towards stable single-atom catalysts: Strong binding of atomically dispersed transition metals on the surface of nanostructured ceria. Catal. Sci. Technol. **6** (2016), doi: 10.1039/c6cy00294c.

[2] R. Fiala, A. Figueroba, A. Bruix, M. Václavů, A. Rednyk, I. Khalakhan, M. Vorokhta, J. Lavková, V. Potin, I. Matolínová, F. Illas, K.M. Neyman, V. Matolín, High efficiency Pt^{2+}-CeO_x novel thin film catalyst as anode for proton exchange membrane fuel cells. Appl. Catal. B: Environ. (2016), doi: 10.1016/j.apcatb.2016.02.036.

[3] Y. Lykhach, A. Figueroba, M. Farnesi Camellone, A. Neitzel, T. Skála, F.R. Negreiros, M. Vorokhta, N. Tsud, K.C. Prince, S. Fabris, K.M. Neyman, V. Matolín, J. Libuda, Reactivity of atomically dispersed Pt^{2+} species towards H_2: Model Pt-CeO_2 fuel cell catalyst. Phys. Chem. Chem. Phys. **18** (2016), doi: 10.1039/c6cp00627b.

[4] A. Neitzel, A. Figueroba, Y. Lykhach, T. Skála, M. Vorokhta, N. Tsud, S. Mehl, K. Ševčíková, K. Prince, K.M. Neyman, V. Matolín, J. Libuda, Attomically dispersed Pd, Ni and Pt in ceria-based catalysts: Principal differences in stability and reactivity, *submitted*.

The effect of Pd and Ni on the structural properties and electrochemical performances of $La_{0.6}Sr_{0.4}Co_{1-x}Fe_{x-0.03}M_{0.03}O_{3-\delta}$ (x=0.2-0.8) perovskites

F. Puleo[1], A. Longo[1,2], S. Guo[1,3], V. La Parola[1], N. Yigit[4], G. Rupprechter[4], L.F. Liotta[1]

[1]Istituto per lo Studio di Materiali Nanostrutturati CNR-ISMN, Via Ugo La Malfa 153, 90146 Palermo, Italy.
[2]Netherlands Organization for Scientific Research (NWO), 6 rue Jules Horowitz, BP220, 38043 Grenoble CEDEX, France.
[3]Northwestern Polytechnical University, Xi'an 710072 PR China.
[4]Institute of Materials Chemistry, Technische Universität Wien, Getreidemarkt 9/BC, 1060 Vienna, Austria

E-mail: puleo@pa.ismn.cnr.it

Thanks to their mixed ionic/electronic conductivity and high catalytic activity for oxygen exchange reaction, $La_{1-x}Sr_xCo_{1-y}Fe_yO_{3-\delta}$ (LSCF) perovskites have received much attention as cathode materials for intermediate solid oxide fuel cells (IT-SOFCs) operating at relatively low-temperature, 600-800 °C. Lowering the operating temperature, however, decreases the electrode kinetics, in particular the oxygen reduction at the cathode.
It is widely accepted that the rate-limiting step of O_2 reduction process is the solid state diffusion of oxygen anions through the vacancies of the cathode lattice. LSCF oxides with metal substitution in B-site prepared by different methods, such as solid-state reaction or by impregnation of the perovskite with the metal dopant precursor, have been extensively investigated as new cathodes with enhanced oxygen reduction activity [1].The promotion of redox properties of $La_{0.6}Sr_{0.4}Co_{0.8}Fe_{0.2}O_{3-\delta}$ and of $La_{0.6}Sr_{0.4}Co_{0.2}Fe_{0.8}O_{3-\delta}$ by incorporation of Pd^{4+} into the B-site of the perovskite lattice, through one pot citrate synthesis, has been recently demonstrated by some of us [2]. The present work aims to get more insight into the B-site metal promotion by investigating the effect of two metals (Pd and Ni) and by using citrate-EDTA method which provides a good control of the microstructural properties. Perovskites with compositions $La_{0.6}Sr_{0.4}Co_{1-x}Fe_{x-0.03}M_{0.03}O_{3-\delta}$ (x=0.2-0.8) doped with Pd and Ni have been prepared and compared with the un-promoted $La_{0.6}Sr_{0.4}Co_{0.2}Fe_{0.8}O_{3-\delta}$ and $La_{0.6}Sr_{0.4}Co_{0.8}Fe_{0.2}O_{3-\delta}$ materials. Characterizations by XRD, EXAFS, TPR, XPS, TGA, CO FT-IR, CO-TPD, EIS techniques have been carried out.
EXAFS analyses show that Ni^{2+} is stabilized into the lattice of the perovskite or partially segregated as NiO as a function of the Fe content.
Addition of Pd and Ni to the LSCF perovskites influences in a different way surface and bulk properties.

Acknowledgements
S. Guo thanks COST Action CM 1104 (COST-STSM-ECOST-STSM-CM1104-270415-056579) and China Scholarship Council for financial support.

References

[1] S. Guo, H. Wu, F. Puleo, L.F. Liotta, Catalysts **5,** 366, (2015)
[2] F. Puleo, L. F. Liotta, V. La Parola, D. Banerjee, A. Martorana, A. Longo, Phys. Chem. Chem. Phys. **16**, 22677**,** (2014).

VOCs total oxidation over Au, Pd and Pd-Au catalysts supported on Y-doped ceria

G. Pantaleo, L. Ilieva[1], P. Petrova[1], L.F. Liotta, A.M. Venezia, Z. Kaszkur[2], R. Zanella[3], T. Tabakova[1]

Istituto per lo Studio di Materiali Nanostrutturati, CNR, I- 90146 Palermo, Italy
[1]Institute of Catalysis, Bulgarian Academy of Sciences, 1113 Sofia, Bulgaria
[2]Institute of Physical Chemistry, Polish Academy of Sciences, 01-224 Warsaw, Poland
[3]Universidad Nacional Autónoma de México, P. 04510 México D.F., Mexico
E-mail address of the corresponding author: giuseppe.pantaleo@ismn.cnr.it

The detoxification of volatile organic compounds (VOCs) remains one of the global environmental problems. Recently, considerable attention was paid to the complete oxidation of VOCs over nanosized gold catalysts. It is generally accepted that hydrocarbon oxidation reactions over Au catalysts on reducible supports take place through Mars–van Krevelen redox mechanism with active oxygen supplied by the support. The gold dispersion and the support features, in particular the redox properties, have been recognized as the key factors for high catalytic activity. It is known that the modification of ceria with proper metal dopants leads to a defective structure increasing the oxygen mobility in the ceria-based catalysts.
Benzene, a highly stable molecule, is a harmful air pollutant . Very recently (unpublished results) complete benzene oxidation (CBO) has been investigated over gold catalysts on Y-modified ceria supports. The effect of different dopant amounts and different preparation methods of the supports were studied. The best performance in CBO was established over gold catalyst supported on Y-doped ceria prepared by impregnation (IM) containing 1 wt.% Y_2O_3. Pd containing catalysts have also promising properties in the VOCs total oxidation. High complete oxidation activity was reported in the literature when Pd was loaded on already deposited Au particles. Based on our previous results, in the present study ceria supports with 1 wt.% Y_2O_3 dopant, prepared by IM or coprecipitation (CP) were chosen for the investigation of Au (3 wt.%), Pd (1 wt.%) and Pd-Au (1 wt.% of Pd over already prepared Au samples) for VOCs total oxidation. Benzene was chosen as a probe for aromatic and propene - for aliphatic hydrocarbons abatement. The catalysts were characterized by HRTEM/HAADF and TPR. XRD and XPS measurements are in progress. The average size of gold estimated by HRTEM did not differ substantially (2.6 nm on IM and 3.2 nm on CP support). It was difficult to measure PdO crystals by HRTEM due to the similar lattice distances of PdO and CeO_2. The TPR spectra of Au catalysts confirmed complete ceria surface layers reduction at around 150 ^oC. Very low temperature TPR peaks (below 100 ^oC) were registered with Pd samples, the calculated hydrogen consumption were in accord with PdO reduction and with partial ceria surface reduction. The test in CBO and complete propene oxidation (CPO) were performed after a pretreatment in air at 350^oC. The monometallic Pd catalysts demonstrated higher oxidation activity as compared to the corresponding Au catalysts in CBO as well as in CPO. The highest catalytic activity and good stability in both reactions were established over Pd-Au catalyst on Y-doped ceria support prepared by IM. The results of 100% propene total oxidation at 180 ^oC and especially the benzene combustion at temperature as low as 150 ^oC (see the figure) make this Pd-Au catalyst promising for practical application.

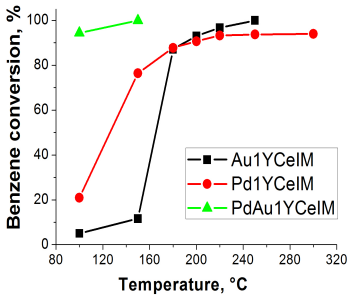

Acknowledgement: The support by the COST Action CM 1104 is gratefully acknowledged.

Gold catalysts on Y-modified ceria supports for complete benzene oxidation

L. Ilieva, P. Petrova, L.F. Liotta[1], S. Boghosian[2], V. Georgiev, J.W. Sobczak[3], W. Lisowski[3], Z. Kaszkur[3], G. Munteanu [4], T. Tabakova
Institute of Catalysis, Bulgarian Academy of Sciences, 1113 Sofia, Bulgaria
[1]Istituto per lo Studio di Materiali Nanostrutturati, CNR, I- 90146 Palermo, Italy
[2]Dept. of Chemical Engineering, University of Patras, and FORTH/ICE-HT Patras, Greece
[3]Institute of Physical Chemistry, Polish Academy of Sciences, 01-224 Warsaw, Poland
[4]Institute of Physical Chemistry, Romanian Academy, Bucharest 77208, Romania
E-mail address of the corresponding author: luilieva@ic.bas.bg

Catalytic total oxidation is considered as one of the most promising technologies for air pollutants abatement. The utilization of supported gold catalysts is suggested as promising because of their low temperature combustion activity. In relation to the generally accepted Mars–van Krevelen mechanism, a high activity is expected for gold on reducible oxide supports. In this regard ceria is an appropriate support of gold catalysts due to its ability to maintain a high gold dispersion and to take part in the oxidation reaction providing active oxygen species. The oxygen supplying by ceria could be increased by appropriate doping.
In the present study benzene was chosen as a stable probe molecule. Complete benzene oxidation (CBO) over Au catalysts supported on lightly Y-doped ceria supports (1, 2.5, 5 and 7.5 wt.% of Y_2O_3) was studied. Two series of mixed supports were synthesized by co-precipitation (CP) and by impregnation (IM). The gold catalysts (3 wt.% Au) were prepared by deposition-precipitation method and denoted as Au*x*YCeIM and Au*x*YCeCP (*x* = 1 to 7.5). The catalysts were characterized by XRD, XPS, Raman spectroscopy and TPR measurements. No substantial differences in the average size of gold and ceria particles in respect to the preparation method and Y-amount were found by XRD. The Raman spectroscopy results showed a progressive Y^{3+} incorporation into the CeO_2 cubic matrix with increasing Y-doping for the CP supports, while for the IM ones it is suggestive of Y_2O_3 segregation, probably in the form of some Y_2O_3 (evidenced by HRTEM). The catalytic tests in CBO were performed with special attention to the pretreatment conditions. The positive role of the higher temperature treatment in air was established (at 350^{o}C as compared to 200^{o}C) and it was related to CO_2 removal (QMS analysis). TPD experiments showed different O_2 evolution after absorption at 200^{o}C or 350^{o}C. A correlation between TPD and catalytic data was observed only for 7.5% doping, in this case revealing that oxygen supplying has to be a limiting step.
The highest activity after pretreatment at 350^{o}C is exhibited by Au1YCeIM (100% benzene conversion at 250^{o}C), while 100% conversion was not achieved even at 350^{o}C over other Y-containing catalysts. The best Au1YCeIM and Au1YCeCP with poor catalytic behavior were selected for further investigations. The XRD data showed that gold or ceria particles agglomeration during the CBO is not the reason for the different behavior The TPR results revealed even higher oxygen supplying in the case of CP support preparation. The presence of Au^0 and $Au^{\delta+}$ species in both fresh samples was registered by XPS. Only A^0 was observed in Au1YCeIM after using in CBO, while some $Au^{\delta+}$ still existed in the spent Au1YCeCP catalyst. In relation to the unresolved question about the role of the state of gold, these results revealed that the cationic gold cannot be supposed as important for high CBO activity. No signal due to carbon radicals was detected for either of the spent samples by EPR, thereby excluding coke formation as a reason for the different catalytic behavior. The catalytic performance (high oxidation activity) could be related to an enhanced activation of the stable benzene molecule in the case of Au1YCeIM catalyst.
Acknowledgement: The support by the COST Action CM 1104 is gratefully acknowledged.

First-principles microkinetic modeling of methane oxidation over PdO(101)

Maxime Van den Bossche[1], Henrik Grönbeck[1]
[1]Department of Applied Physics, Chalmers University of Technology, Göteborg, Sweden
E-mail: maxime.vandenbossche@chalmers.se

Transition metals for catalytic oxidation reactions often form oxides under environmental reaction conditions. One example is palladium, where the PdO(101) facet recently has been suggested to be the active phase for methane oxidation [1]. In this study [2], we have explored the mechanism for oxidation of methane to carbon dioxide and water over the PdO(101) surface.

This was done using a first-principles microkinetics approach, where the kinetic parameters are obtained by applying density functional and transition state theory. For the electronic structure part, the HSE06 functional was used to describe electronic exchange and correlation, as hybrid functionals were found to be significantly more accurate than gradient-corrected functionals such as PBE. The kinetic model was constructed on the basis of circa 80 elementary reactions. Due to the presence of strong attractive lateral interactions, spatial correlations between adsorbates needed to be taken into account beyond the mean-field approximation.

The results of the kinetic modeling confirm the common assumption that the first dissociation reaction is the main (though not sole) rate limiting step, where both energetic and entropic contributions create a large free energy barrier for this reaction. The resulting CH_3 species is converted to CO_2 through a series of surface intermediates such as CH_2, CH_2O, CHO and CO. Incorporation of oxygen into the molecule mainly occurs via a Mars – van Krevelen mechanism. The reduced oxide is then reoxidized by O_2 adsorption and dissociation. Another finding is that, at low temperatures and in the presence of water vapour, the process is hindered by adsorbed H_2O. This is in agreement with the negative reaction order in water pressure observed experimentally under such conditions.

[1] A. Hellman, et al., *J. Phys. Chem. Lett.* **2012**, 3, 678.
[2] M. Van den Bossche, H. Grönbeck, *J. Am. Chem. Soc*. **137**, 37 (2015).

Local Structure Correlation in Ln doped CeO_2 Nanoparticles: Roles of Ln Ionic Radius, Ln Concentration and Oxygen Vacancies

Mihaela Florea,[a] *Daniel Avram,*[b] *Bogdan Cojocaru,*[a] *Vasile Parvulescu,*[a] *Carmen Tiseanu*[b]

[a]University of Bucharest, Faculty of Chemistry, Department of Organic Chemistry, Biochemistry and Catalysis, 4–12 Regina Elisabeta Bvd., Bucharest, Romania

[b]National Institute for Laser, Plasma and Radiation Physics, P.O.Box MG-36, RO 76900, Magurele, Romania

Ceria has unique properties such as high mechanical strength, oxygen ion conductivity and oxygen storage capacity. It is well established that the generation and migration of oxygen vacancies plays a key role in all these applications. Undoped ceria has relatively small oxygen vacancy formation energy, due to the capability for cerium to change the oxidation state. Nevertheless, a significant increase of CeO_2 ionic conductivity is obtained by doping with aliovalent ions such as trivalent lanthanideions.

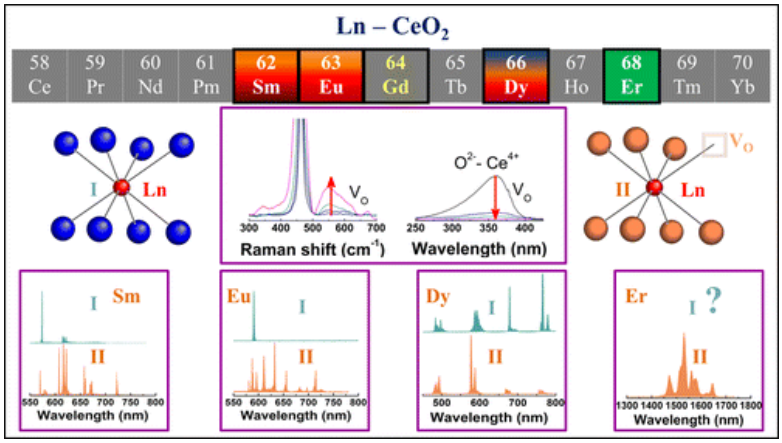

Figure 1. The fingerprint emission and excitation spectra and emission decays of Eu, Sm and Dy in CeO_2 (I and II refer to cubic and Ln - vacancy associate centers, respectively).

Herein, we present a first unified description of luminescence – structure – relationships in lanthanide doped CeO_2 nanoparticles. To achieve this goal, four lanthanides located to the left (Sm and Eu) and right side of Gd (Dy and Er) are investigated by use of an extensive set of luminescence measurements at room temperature down to 10K, seconded by X-ray diffraction, Raman and Fourier transform infrared spectroscopy and transmission electron microscopy. The effects of annealing temperature, defect and Ln concentration on the local oxygen environment surrounding each Ln center are investigated.

The main findings of this study can be summarized as follows: i) Ln situated to both left and right side to Gd in the Ln series, exhibit a two centers distribution: the Ln centers substitute for Ce4+ lattice sites, being characterized by narrow emission lines of 0.2 - 04 nm and mean lifetimes in the ~ ms range. The two Ln centers differentiate by the presence of zero (cubic Ln center) and one charge compensating oxygen vacancy in the nearest-neighbor oxygen shell (Ln - defect associate center). ii) The first example reported of Dy emission in an inversion symmetry is supposed to revisit the way this lanthanide is used as luminescence probe; iii) the relative contribution of the Ln centers to the overall emission depends on the Ln ionic radius: Sm exists predominantly as a cubic center while Er is found mostly as vacancy associate; iv) the local lattice distortion around Ln increases with the decrease of Ln ionic radius; iv) the sensitization of Ln emission via CeO_2 charge - transfer band is strongly affected by the subsequently induced oxygen vacancies and v) Zr co - doping of CeO_2 obstructs the formation of Ln – defect associates.

Role of Cu/Mn molar ratio and gold addition on the performance of alumina supported Cu-Mn catalysts for WGSR

T. Tabakova, I. Ivanov, E. Kolentsova[1], P. Petrova, A.M. Venezia[2], Y. Karakirova, G. Avdeev[3], L. Ilieva, K. Ivanov[1], V. Idakiev

Institute of Catalysis, Bulgarian Academy of Sciences, 1113 Sofia, Bulgaria
[1]Department of Chemistry, Agricultural University, 4000 Plovdiv, Bulgaria
[2]Institute for the Study of Nanostructured Materials (ISMN)-CNR, I- 90146 Palermo, Italy
[3]Institute of Physical Chemistry, Bulgarian Academy of Sciences, 1113 Sofia, Bulgaria
E-mail address of corresponding author: tabakova@ic.bas.bg

The Water-Gas Shift Reaction (WGSR) is a well established industrial process for hydrogen generation by conversion of CO with water. The need of high-purity hydrogen for fuel cell applications stimulates a great activity in the design of novel, highly active and stable WGS catalysts. Copper is often used as an active component in low-temperature (LT) WGS catalysts. Recently, we have reported that Cu-Mn spinel oxide demonstrated favorable characteristics and catalytic properties for WGSR [1]. Due to their good redox property, these mixed oxides play an important role in the activation of water. The aim of present study was to develop cost-effective and catalytically efficient formulations based on γ-Al_2O_3 modified with a superficial fraction of Cu–Mn mixed oxides. The effect of Cu/Mn molar ratio (2:1 or 1:5) and the role of Au addition on the structural and catalytic properties were examined.

The samples were prepared by the wet impregnation method. Commercial γ-Al_2O_3 was used as support. The impregnation with mixed solutions of copper and manganese nitrates (20 wt. % active phase) was performed at 80 ^{o}C for 12 hours. The samples were dried at 120 ^{o}C for 10 h and calcined at 450 ^{o}C for 4 hours. Au samples (2 wt. %) were synthesized by deposition-precipitation method.

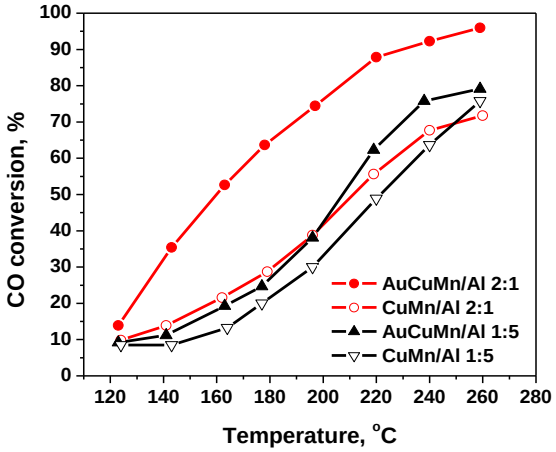

Fig. 1. WGS activity of the studied samples

Catalytic tests revealed that WGS activity is governed not only by the presence of Au, but also by the Cu-Mn molar ratio (Fig. 1). Higher activity was demonstrated by the sample with higher Cu content, i.e. that with ratio 2:1. Both gold-containing catalysts are more active than the corresponding supports. The highest catalytic activity among the studied catalysts was shown by the Au catalyst on support with Cu/Mn ratio 2:1. The characterization of as-prepared and used in WGSR samples by means of BET, XRD, HRTEM, XPS, EPR and TPR was performed in order to explain the relationship between structure, reduction behaviour and WGS activity.

Acknowledgement: The financial support by the Bulgarian National Science Fund (Project T 02/4) and COST Action CM 1104 is gratefully acknowledged.

[1] T. Tabakova et al., Appl. Catal. A, **451,** 184 (2013).

Rational design of alumina supported Au/doped ceria catalysts for preferential CO oxidation in H_2-rich gas mixtures

T. Tabakova, G. Pantaleo[1], L. Ilieva, P. Petrova, L.F. Liotta[1], Z. Kaszkur[2], J.W. Sobczak[2], W. Lisowski[2], A.M. Venezia[1]

Institute of Catalysis, Bulgarian Academy of Sciences, 1113 Sofia, Bulgaria
[1]Istituto per lo Studio di Materiali Nanostrutturati, CNR, I- 90146 Palermo, Italy
[2]Institute of Physical Chemistry, PAS, Kasprzaka 44/52, 01-224 Warsaw
E-mail address of corresponding author: tabakova@ic.bas.bg

The preferential CO oxidation (PROX) is one of the most effective methods for CO abatement from the H_2-rich gas mixtures utilized in fuel cell systems. Supported Au/ceria catalysts are promising candidates for PROX reaction due to their remarkably high CO oxidation activity at low temperature. Doping of ceria improves its reducibility, oxygen mobility and thermal stability. In a very recent study of Au/Y-doped ceria catalysts was examined the role of ceria modification with different amount Y_2O_3 by using impregnation (IM) and co-precipitation (CP) methods on the PROX activity and resistance towards deactivation caused by the presence of CO_2 and H_2O in the feed [1]. It was found that IM method contributed for improved tolerance to CO_2 because of the lower ceria surface basicity caused by the formation of nanosized Y_2O_3 phase over ceria grains.

The aim of present work was to combine the favorable features of gold-promoted Y-doped ceria and high surface area support (γ-Al_2O_3) in order to develop new catalytic formulations of improved efficiency and cost effectiveness. Special emphasis was given to the amount of active ceria phase and its impact on the catalytic behaviour.

Ceria modified alumina supports with 10, 20 and 30 wt% CeO_2 content were prepared by wet impregnation with aqueous solution of $Ce(NO_3)_3.6H_2O$ at room temperature for 2 h, evaporation under vacuum at 55 °C in a rotary evaporator until complete water removal, drying at 80 °C and calcination in air at 400 °C for 2 h. Further, the impregnation with 1 wt.% Y_2O_3 was carried out following the same procedure. The gold catalysts (3 wt.% Au) were prepared by deposition-precipitation method. The catalysts were characterized by means of XRD, XPS and TPR measurement. The activity in PROX was evaluated using 60% H_2+1% CO+1% O_2 (He as balance), WHSV- 60000 ml g^{-1} h^{-1}.

Gold catalyst on alumina with the lowest ceria amount exhibited the highest CO conversion. The following activity order in the temperature interval of interest for PROX reaction in fuel processors, i.e. 80-100 ^oC, was observed: Au10CeAl > Au20CeAl > Au30CeAl. The addition of small amount Y_2O_3 in the support composition improved the CO-PROX activity of all samples. The most favorable effect was observed on the performance of Au20CeAl, which attained the same activity as AuY10CeAl sample. The examination of the selectivity data allowed concluding that values are similar for all the samples (25-40%). The evaluation of the catalytic performance in the presence of CO_2 and water evidenced the promising behaviour of AuY20CeAl due to its resistance towards deactivation and long-term stability. The comparison with the performance of Au/CeO_2 catalyst indicated that differences in CO conversion and selectivity are less than 10 %. Additionally, the composition of this catalytic system, which is mostly composed of alumina (80%), is advantageous in case of practical applications because of its economic viability. This study provides some guidelines for design of multicomponent catalytic system in order to achieve the best performance at reasonable price.

Acknowledgement: The support by the COST Action CM 1104 is gratefully acknowledged.

[1] L. Ilieva et al., Appl. Catal. B, **188**, 154 (2016).

Water oxidation with holes: What we learn from *operando* studies

Artur Braun[a], Yelin Hu[a,b], Debajeet K. Bora [a], Florent Boudoire [a,c],
Jinghua Guo[d], Michael Grätzel [c], Edwin C. Constable [b]

[a] *Laboratory for High Performance Ceramics, Empa. Swiss Federal Laboratories for Materials Science and Technology, CH - 8600, Dubendorf, Switzerland.*
[b] *Department of Chemistry, University of Basel, CH - 4056 Basel, Switzerland.*
[c] *Laboratory for Photonics and Interfaces, Ecole Polytechnique Federale de Lausanne, CH - 1015 Lausanne, Switzerland*
[d] *Advanced Light Source, Lawrence Berkeley National Laboratory, Berkeley CA 94720, California*

artur.braun@alumni.ethz.ch

Photogenerated electron holes are the key players in photoelectrochemical water oxidation. They provide the basis for direct solar fuel production in photoelectrochemical cells. The physics and the chemistry underlying the processes relevant for the water oxidation are probably the most complex known in physical chemistry. Therefore it is not surprising that the science of solar water splitting rests still on some speculative elements. Thanks to considerable progress in synchrotron radiation instrumentation, x-rays and electrons as fundamental probes for chemical and physical processes can now be used in complex electrocatalytic and photoelectrochemical experiments during actual device operation (1). The results of these studies which were impossible until very recently are indeed spectacular. We show (2-5) how we can assess with x-ray based ligand and valence band NEXAFS and AP-XPS spectroscopy the density of hole states in photoelectrodes as a function of electrochemical parameters and at the same time find quantitative information on the surface intermediates formed prior to, during and after water splitting. We are able to resolve the interaction of the photoelectrode with the electrolyte down to the Fe3d and O2p orbitals with bias parameterized energetic and spatial depth resolution, including the charge carrier accumulation layer, the electrode surface and the Helmholtz layer. The x-ray electronic structure data are in full alignment with the charge carrier dynamics probed with electroanalytical methods. Noteworthy is that we could verify and confirm a historically speculated second electron hole, which corresponds to a transition into the charge transfer band, which precedes the water splitting and coincides with the formation of a hydroxyl intermediate. Latter disappears when water oxidation sets on.

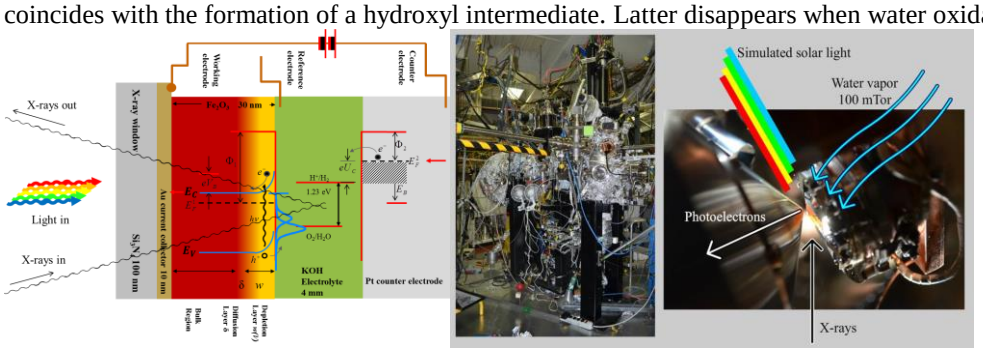

References

(1) D. K. Bora et al. Between Photocatalysis and Photosynthesis: Synchrotron spectroscopy methods on molecules and materials for solar hydrogen generation, J. Electron Spectr. Rel. Phenom. 2013, 190 A, 93-105.
(2) A Braun et al. The electronic, chemical and electrocatalytic processes and intermediates on iron oxide surfaces during photoelectrochemical water splitting, Catal. Today (2015) http://dx.doi.org/10.1016/j.cattod.2015.07.024
(3) A. Braun et al. Direct observation of two electron holes in hematite during photo-electrochemical water splitting, J. Phys. Chem. C 2012, 116 (23) 16870-16875.
(4) A. Braun et al. Iron resonant photoemission spectroscopy on anodized hematite points to electron hole doping during anodization, invited for Special Issue: Electrochemistry and Energy in ChemPhysChem 2012, 13(12), 2937-2944.
(5) D.K. Bora et al. Evolution of an oxygen NEXAFS transition in the upper Hubbard band in α-Fe2O3 upon electrochemical oxidation, J. Phys. Chem. C, 2011, 115 (13), 5619–5625.

Nucleation and Growth of Anatase TiO_2 (001) on the $SrTiO_3$ (001) Surface

Y. Gao[a], S.U. Rahman[b] and M.R. Castell[c]

[a] Department of Materials, University of Oxford, Parks Road, Oxford, OX1 3PH, U.K.
E-mail: yakun.gao@materials.ox.ac.uk
Tel: +44 - 1865 - 273 746
[b] Department of Physics, Comsats Institute of Information Technology, Islamabad 44000, Pakistan.
[c] Department of Materials, University of Oxford, Parks Road, Oxford, OX1 3PH, U.K.

Nanostructured TiO_2 is a widely used material for catalysis applications. The anatase phase is more catalytically active under ultraviolet irradiation for photocatalytic applications than the rutile polymorph. However, anatase TiO_2 is generally only found in small crystal sizes, but is not thermodynamically stable for large crystals. To be able to study the surface of anatase an epitaxial growth method can be applied to grow anatase (001) onto the $SrTiO_3$ (001) surface. The lattice of anatase is only 3.1% smaller than that of $SrTiO_3$. This method allows the production of high quality and large anatase (001) films which are stable at temperatures up to 600 °C.

Scanning tunneling microscopy reveals that following certain surface processing steps a class of TiO_x nanostructures are formed on the $SrTiO_3$ (001) surface. $SrTiO_3$ single crystals doped with 0.5wt% Nb (n-type) were used in these experiments. The sample surfaces were prepared by Ar^+ ion sputtering and ultra-high vacuum (UHV) annealing in the temperature range 850 – 900 °C. Annealing samples at different temperatures and for different lengths of time results in a different degree of TiO_x segregation to the $SrTiO_3$ (001) surface. The excessive TiO_x on the sample surfaces form different types of epitaxial TiO_x-rich nanostructures. These nanostructures can be classified as parallel packed nanolines (dilines, metadilines, trilines and tetralines) or small dot features. Upon extensive UHV annealing leading to significant TiO_x surface enrichment, the TiO_2 (001) anatase phase starts to nucleate on the nanostructured $SrTiO_3$ (001) surfaces. This occurs after several annealing cycles at temperatures around 880-900 °C. The growth of anatase TiO_2 (001) can be further enhanced through the evaporation of Ti onto the nanostructured $SrTiO_3$ (001) surface followed by an annealing step at 750 – 900 °C. Anatase TiO_2 (001) epitaxially grown on $SrTiO_3$ (001) surfaces can have large surface areas of (1×4) reconstructions. These surfaces are ideally suited for the study of metal nanoparticle (e.g. Pd) growth.

Defects in ZnO nano-smoke: a combined structural and spectroscopic study

M. Zhang,[1,2] S. Suman[1], F. Aversang,[2] G. Costentin[2] and S. Stankic,[1,*]

[1]*CNRS – Institut des Nanosciences de Paris, UPMC – Université Paris 06, Paris, 75252 cedex 05, France*

[2] *CNRS – Laboratoire de Réactivité de Surface, UPMC – Université Paris 06, Paris, 75252 cedex 05, France*

** Author to whom correspondence should be addressed. Electronic mail: stankic@insp.upmc.fr*

A number of synthesis approaches, a wide variety of morphologies and the unique electronic and optical properties exhibited by nanostructured ZnO have made them a potential agent for application in many fields. This metal oxide encompasses an amazing spectrum of applications (UV-light-emitting diodes (LEDs), sensors, catalysis, biomedical science etc.) competing, thus, to be one of the most promising compounds among other functional materials [1]. With a direct band gap of 3.4 eV, ZnO reveals absorption in the near UV range (<360 nm) and luminescence emission in the visible ranging from green to red light. High exciton-binding energy (60 meV) allows efficient excitonic emission even at room temperature. The presence of very rich defect chemistry [2, 3] – with Zn interstitials and oxygen vacancies known to be the predominant ionic defect types – complicates, however, the advances necessary for ZnO to become a front-runner in the context of new applications. Only to precise which defect dominates in native, undoped ZnO is still a matter of great controversy.

Our goal is to map spectroscopic fingerprints of ZnO which correlate defects with conditions of synthesis and processing. We employ metal combustion, the solvent free synthesis along with the annealing treatments which allow us to not only obtain pure and high crystal quality nanoparticles but also to tune the type and concentration of defects in the final ZnO nanopowder. TEM and XRD analysis have been used to determine the morphology and structure whereas for the purpose of optical and paramagnetic species characterization, Diffuse Reflectance, Raman, Photoluminescence (PL) and Electron Paramagnetic Resonance (EPR) spectroscopy have been performed. In this contribution, we will show that there exists a straightforward correlation between Zn-interstitials, defects which have been found to dominate under non-equilibrium conditions of the employed synthesis technique, and the PL emission (2.92 eV), Raman shift

(600 cm^{-1}) and EPR signal (g~1.956). In a similar way, spectroscopic features attributed to oxygen related defects (V_{ox} and/ or O_i) were found to be observable in function of synthesis, processing and measurement conditions.

[1] Lukas Schmidt-Mende and Judith L. MacManus-Driscoll, *Materials Today*, 10 (**2007**).

[2] Anderson Janotti and Chris G. Van de Walle, *Physical Review* B 76 (**2007**).

[3] M. D. McCluskey and S. J. Jokela, *J. Appl. Phys*. 106 (**2009**).